Deciphering the role of mitogen-activated protein kinases in host cell death induced by *Mycobacterium tuberculosis*

Inaugural-Dissertation

zur

Erlangung des Doktorgrades

der Mathematisch-Naturwissenschaftlichen Fakultät

der Universität zu Köln

vorgelegt von

Jessica Gräb

aus Jammu

Köln 2020

Berichterstatter:	Prof. Dr. Hamid Kashkar
	Prof. Dr. Karin Schnetz
Tag der mündlichen Prüfung:	23.06.2020

Content

1. Abbreviations

°C	Degree Celsius
ΔΨm	Mitochondrial membrane potential
7H9c	7H9 complete medium
ADC	Albumin dextrose catalase
AIM	Absent in melanoma
AKT	Protein kinase B
ANT	Adenosine translocase
ASC	Apoptosis-associated speck-like protein
ASK	Apoptosis signal-regulating kinase
ATP	Adenosine triphosphate
BCA	Bicinchoninic acid
Bcl-2	B cell lymphoma 2
BMDM	Bone marrow-derived macrophage
BSA	Bovine serum albumin
Ca^{2+}	Calcium
CARD	Caspase activation and recruitment domain
Casp	Caspase
CCCP	Carbonylcyanid-m-chlorophenylhydrazon
CCL	Chemokine (C-C motif) ligand
CD	Cluster of differentiation
cDNA	Complementary DNA
CFP-10	Culture filtrate protein of 10 kDa
CFU	Colony-forming unit
CHAPS	3-[(3-cholamidopropyl)dimethylammonio]-1-propanesulfonate
CsA	Cyclosporine A
CXCL	Chemokine (C-X-C motif) ligand 1
CypD	Cyclophlin D
CytoC	Cytochrome C
DAMP	Danger-associated molecular pattern
DAPI	4’,6-Diamidin-2-phenylindol
DC	Dendritic cell
DISC	Death-inducing signaling complex
DMEM	Dulbecco’s modified eagle’s medium
DMSO	Dimethyl sulfoxide
DNA	Deoxyribonucleic acid
EDTA	Ethylenediaminetetraacetic acid
ELISA	Enzyme-linked immunosorbent assay
EMB	Ethambutol
ER	Endoplasmic reticulum
ERK	Extracellular signal-regulated kinase
ERS	ER stress
ETC	Electron transport chain
FBS	Fetal bovine serum
FCS	Fetal calf serum
FSA	Fibroblast survival assay
g	Acceleration of gravity
GAPDH	Glyceraldehyde 3-phosphate dehydrogenase
Gpx	Glutathione peroxidase

GSDMD	Gasdermin D
GSH	Glutathione
h	Hours
HBSS	Hank's balanced salt solution
HDT	Host-directed therapy
HEPES	4-(2-hydroxyethyl) -1-piperazineethanesulfonic acid
HIV	Human immunodeficiency virus
HMBS	Hydroxymethylbilane synthase
HMGB1	High-Mobility-Group-Protein B1
HRP	Horseradish peroxidase
IFN	Interferon
IL	Interleukin
IMM	Inner mitochondrial membrane
INH	Isoniazid
iNOS	Inducible nitric oxide synthase
IRAK	Interleukin receptor-associated kinase
JNK	c-Jun N-terminal kinase
KD	Knockdown
kDA	Kilo Dalton
KI	Knockin
KO	Knockout
LDH	Lactate dehydrogenase
LPS	Lipopolysaccharide
LTA4H	Leukotriene A4 hydrolase
LTBI	Latent tuberculosis infection
M-CSF	Macrophage colony-stimulating factor
Mϕ	Macrophage
MACS	Magnetic activated cell sorting
ManLAM	Mannose-capped lipoarabinomannan
MAP	Mitogen-activated protein
MAP2K	MAP kinase kinase
MAPK	MAP kinase
MDR-TB	Multi-drug resistant TB
MEM	Minimum Essential Medium
min	Minutes
MKP-1	Mitogen-Activated Protein Kinase Phosphatase 1
MLKL	Mixed lineage kinase domain-like pseudokinase
MOI	Multiplicity of infection
MOMP	Mitochondrial outer-membrane permeabilization
MOPS	3-(N-morpholino)propanesulfonic acid
MPT	Mitochondrial permeability transition
mPTP	Mitochondrial permeability transition pore
mRNA	Messenger RNA
Mtb	*Mycobacterium tuberculosis*
mTOR	Mammalian target of rapamycin
MW	Molecular weight
MyD88	Myeloid differentiation primary response 88
NDH	NADH-hydrogenase
NK cell	Natural killer cell
NLR	NOD-like receptor
NOD	Nucleotide oligomerization domain

OD	Optical density
OMM	Outer mitochondrial membrane
OXPHOS	Oxidative phosphorylation
PAMP	Pathogen-associated molecular patterns
PBMC	Peripheral blood mononuclear cells
PBS	Phosphate buffered saline
PCR	Polymerase chain reaction
PDE2	Prostaglandin E2
PDIM	Phthiocerol dimycocerosate
PFA	Paraformaldehyde
PGL	Phenolic glycolipid
pH	*potenia Hydrogenii*, negative decadic logarithm of the H_3O^+ concentration
PRR	Pattern recognition receptors
PZA	Pyrazinamide
RD1	Region of difference 1
RIF	Rifampicin
RIPA	Radio immunoprecipitation assay
RIPK	Receptor-interacting protein kinase
RNA	Ribonucleic acid
ROS	Reactive oxygen species
rpm	Revolutions per minute
RPMI	Roswell Park Memorial Institute
s	Seconds
SDS	Sodium dodecyl sulfate
T7SS	Type VII secretion system
TB	Tuberculosis
TBS	Tris-buffered saline
TBST	TBS Tween 20
TCA	Tricarboxylic acid
TDM	Trehalose di-mycolate
TIR	Toll/interleukin receptor
TLR	Toll- like receptor
TMM	Trehalose mono-mycolate
TMRM	Tetramethylrhodamine
TNF	Tumor necrosis factor
TNFR	TNF receptor
TNT	Tuberculosis necrotizing toxin
TRADD	TNFR-associated death domain
TRAIL	TNF-related apoptosis-inducing ligand
TRIF	TIR-domain containing the adapter-inducing interferon
VDAC	Voltage-dependent anion channel
w/o	Without
WT	Wild type
VDAC	Voltage-dependent anion channel
XDR-TB	Extensively-drug resistant TB

2. Introduction

2.1 Tuberculosis

Tuberculosis (TB) is an airborne disease which is spread through the inhalation of droplets containing *Mycobacterium tuberculosis* (*Mtb*). According to the WHO Global Tuberculosis Report approximately 1.7 billion people are infected with *Mtb* and 1.5 million people died in 2018 (WHO, 2019). Hence, *Mtb* is the major killer among infectious agents and the ninth cause of death worldwide. TB can infect most organs within the body, including the bones, the central nervous system, the lymph nodes and the genitourinary tract. However, the most common form of active TB is pulmonary TB (Kaufmann, 2001).

Following inhalation of the bacteria, *Mtb* migrates through the respiratory tract to settle in the host alveoli. The bacteria are engulfed by alveolar macrophages (Mϕ) and restrained within the phagosome in a process called phagocytosis (Mack et al., 2009). However, phagocytosis of *Mtb* by Mϕ does not lead to complete clearance of the bacteria. Therefore, Mϕ recruit other immune cells through the secretion of pro-inflammatory cytokines and chemokines, like tumor necrosis factor (TNF), to the site of infection to induce a local immune response (Russell, 2007). Potentially, novel recruited immune cells represent a new host for *Mtb*. Subsequently, a secondary immune response is triggered in the lymph nodes to recruit and activate T cells, resulting in the formation of granuloma. Granuloma consist of Mϕ, B cells, T cells and fibroblasts surrounding the infected Mϕ (**Fig. 1**). Hence, the bacteria are contained within the granuloma, preventing dissemination of the disease. Simultaneously though the bacteria cannot be eliminated by the immune system of the host (Russell, 2007). This homeostasis can exist for decades until an immunosuppressive condition, such as an infection with the human immunodeficiency virus (HIV), causes an immune imbalance and a reactivation of the disease. Therefore, the role of the granuloma is either protective by containing the bacteria or detrimental by allowing the survival of the bacteria and persistence of infection (Russell, 2007).

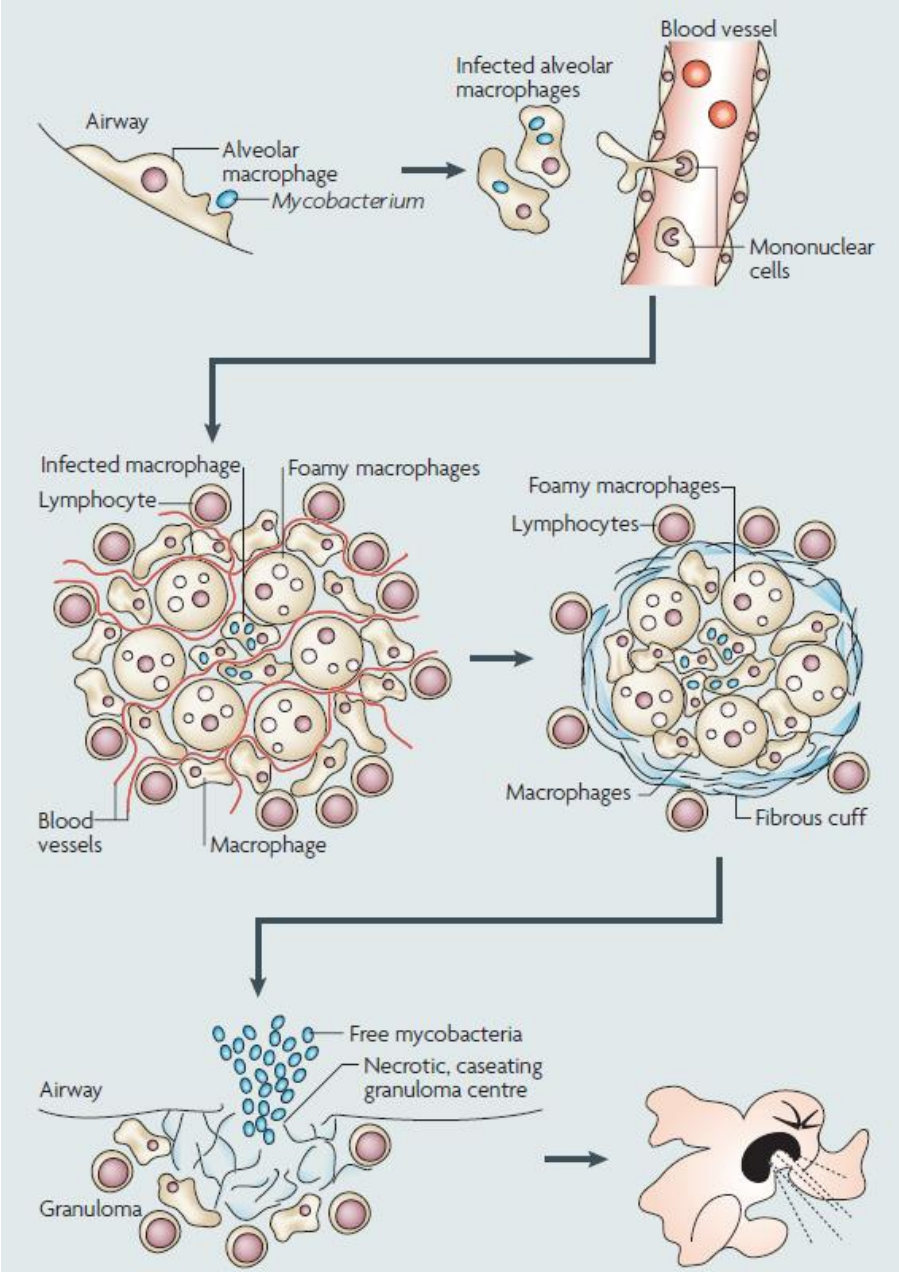

Figure 1. Pathology of *Mycobacterium tuberculosis* (*Mtb*) infection. Inhalation of droplets containing *Mtb* leads to phagocytosis by alveolar macrophages (Mϕ) and induction of a local immune response. The recruitment of other immune cells, such as lymphocytes, results in the formation of granuloma. These consist of infected Mϕ surrounded by mononuclear cells and lymphocytes as well as a fibrous cuff of extracellular matrix structures. At later stages of infection, a fibrous sheath is built while the amount of blood vessels is reduced, creating a hypoxic environment in which the infection is contained. Immunosuppressive conditions can reactivate the disease leading to caseating granulomas and the release of the bacteria (Russell, 2007).

A latent, asymptomatic infection (LTBI) is developed in approximately 90% of infected people, while only 10% develop an active primary TB. Thus, a TB infection has three possible outcomes. An active disease (primary TB), an asymptomatic LTBI or a

reactivation of a LTBI and progression to an active form of the disease even months to years after infection (post-primary TB) (Kaufmann, 2001). The treatment period for drug-susceptible TB strains lasts 6 months in most cases and results in cure of the disease in up to 95% of the cases. During the first two months, four first-line drugs, namely rifampicin (RIF), isoniazid (INH), pyrazinamide (PZA) and ethambutol (EMB), are administered to the patients, followed by four months of RIF and INH (Yew et al., 2011). A major problem in recent years has been the spread of multi-drug resistant (MDR-) and extensively-drug resistant (XDR-) TB strains. These MDR-strains are resistant to the first-line antibiotics RIF and INH. Approximately 484,000 cases of MDR-TB were reported in 2018 and about 6.2% of them were caused by XDR-TB strains, which are in addition resistant to most second-line antibiotics. Therefore, the WHO declared TB a public health crisis (WHO, 2019).

2.2 *Mycobacterium tuberculosis*

Mycobacterium tuberculosis (*Mtb*), the causative agent of TB, is an aerobic, rod shaped, acid fast bacterium. *Mtb* belongs to a complex of mycobacterial species which causes TB in mammals. These include *M. bovis* and *M. caprae* (cattle), as well as *M. microti* (voles) and *M. pinnipedii* (pinnipeds). Other mycobacteria include *Mycobacterium leprae*, the causative agent of leprosy (Herdman and Steele, 2004). In addition there is large number of ubiquitous so called non-tuberculous mycobacteria (NTM) which may cause disease primarily in the immunocompromised patient population (Porvaznik et al., 2017).

Mycobacteria have a unique cell wall, which consists of a peptidoglycan layer, arabinogalactan and mycolic acid (**Fig. 2**). The thick peptidoglycan layer resembles that of Gram-positive bacteria and the waxy outer layer resembles that of Gram-negative bacteria. The peptidoglycan layer outside of the cytoplasmic membrane is covalently bound by phosphodiester bonds to the arabinogalactan layer, while the mycolic acids are attached between the arabinogalactan and trehalose, forming mono- or di-mycolate (TMM, TDM). Finally, the cell envelope is surrounded by a polysaccharide-rich capsule-like structure (Alderwick et al., 2015).

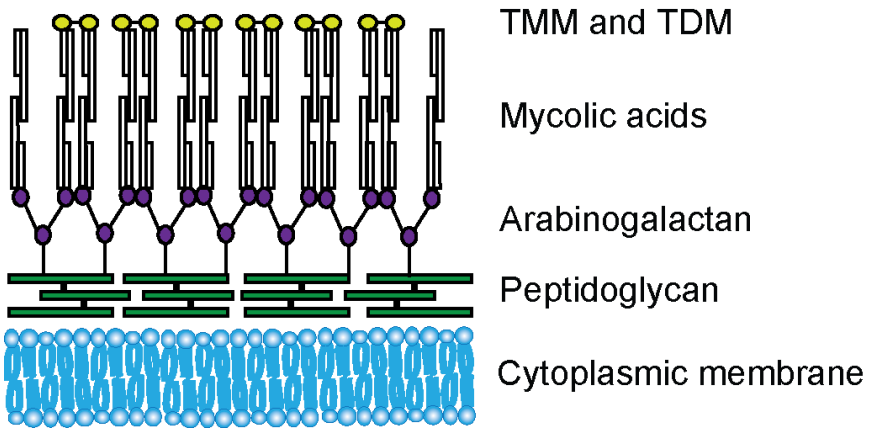

Figure 2. Mycobacterial cell wall. Schematic of the mycobacterial cell wall, containing peptidoglycan, arabinogalactan and mycolic acids.

It has been reported that components of the mycobacterial cell wall are involved in the manipulation of the host immune response and the formation of granuloma. The lipoarabinomannan and the arabinomannan are released inside the infected cells by a passive, undirected process. These bacterial lipids are taken up by uninfected immune cells, allowing mycobacteria to influence host cells even beyond the actively infected cells (Beatty et al., 2000). Hence, the cell wall of mycobacteria is a major virulence factor. Furthermore, the cell wall is also important in intrinsic antibiotic resistance. For instance, the peptidoglycan layer covered by arabinogalactan is hydrophilic and thereby prevents the transport of hydrophobic molecules. Similarly, the mycolic acids, which are long chain fatty acids, build a waxy layer to limit the transport of hydrophilic molecules, such as the tetracycline antibiotics (Brennan and Nikaido, 1995). The manipulation of genes involved in cell wall synthesis by transposon mutagenesis has resulted in increased antibiotic sensitivity of *Mtb* (Gao et al., 2003). In addition to these passive resistance mechanisms, *Mtb* also possesses specialized mechanisms to actively neutralize antibiotics (Nguyen, 2016). One mechanism is the modification of the drug targets by a modulation in the methylation pattern of ribosomal ribonucleic acid (RNA), resulting in resistance to cyclic peptide antibiotics (Maus et al., 2005). Another mechanism is the enzymatic degradation of antibiotics, such as β-lactam antibiotics, which are hydrolyzed by β-lactamases (Chambers et al., 1995). Finally, mycobacteria use efflux pumps to actively expel antibiotics. *Rv1473* is such an efflux pump encoding gene that is induced by the transcription regulator WhiB7 upon exposure to macrolides and tetracyclines (Duan et al., 2019).

These mechanisms as well as a robust cell wall and a slow replication rate of approximately 20 hours are essential for persistence of mycobacteria inside the host cell (Nguyen, 2016).

2.2.1 ESX-1 secretion system

Mycobacteria further evade and subvert the host immune system through the secretion of virulence factors via secretion systems. In mycobacteria five type VII secretion systems (T7SS; ESX-1 to ESX-5) have been identified (Shah and Briken, 2016). The first T7SS discovered, was the ESX-1 system, which is encoded by a genetic locus called region of difference 1 (RD1). This locus is deleted in the TB live vaccine strain *M. bovis* BCG resulting in attenuation of the bacterium (Pym et al., 2002). The ESX-1 system is a multi-component translocation system consisting of transmembrane proteins, adenosine triphosphate (ATP)ases and accessory proteins. ESX-1 secreted proteins have been shown to be important for host-cell invasion, prevention of phagosome maturation and intracellular replication (Wong, 2017). One of the most essential ESX-1 substrates is the heterodimeric complex comprised of a 6 kDa protein EsxA (ESAT-6) and a culture filtrate protein of 10 kDa (CFP-10). Both proteins are responsible for induction of host cell death and subsequently dissemination of *Mtb* (Wong, 2017).

2.2.2 Immune response to *Mtb* infection

The host responds with both the innate and the adaptive immune system to TB infection. The bacterium is recognized by the immune cells via the expression of pathogen-associated molecular patterns (PAMP), such as lipoproteins and glycolipids, on the bacterial surface. These antigens are bound by pattern recognition receptors (PRR) (Ferraris et al., 2018). The most important PRR in *Mtb* infection are the Toll- like receptor (TLR) 2 and TLR4, which recognize different components of the bacterial cell wall, as well as the nucleotide oligomerization domain (NOD)-like receptors (NLR) 1 and 2, which are cytoplasmic PRR (Ferraris et al., 2018). Upon recognition of a PAMP, TLR2 activates the myeloid differentiation primary response 88 (MyD88) and interleukin-1 receptor-associated kinase (IRAK) pathway, resulting in the release of pro-inflammatory cytokines. These pro-inflammatory cytokines (TNF) and chemokines (CXCL9,10 and CCL2,3,4,5) recruit Mϕ and lymphocytes to kill the bacteria by phagocytosis and the production of reactive nitrogen intermediates (Ferraris et al., 2018).

TLR4 can also trigger the toll/interleukin receptor (TIR)-domain containing the adapter-inducing interferon-β (TRIF) pathway, leading to the secretion of interferon (IFN)-β, while NOD receptors mainly induce inflammation by activating mitogen-activated protein (MAP) kinase (MAPK) pathways (Shaw et al., 2008). MAPK are a family of serine/ threonine kinases, consisting of the extracellular signal-regulated kinase (ERK), the c-Jun NH2-terminal kinase (JNK) and p38 MAPK. MAPK are activated by dual phosphorylation of threonine and tyrosine residues by MAPK kinases (MAP2K) and are deactivated by MAPK phosphatases (MKP). Phosphorylation of these kinases is triggered in response to growth stimuli and environmental stresses, such as UV irradiation and inflammation (Johnson and Lapadat, 2002). p38 MAPK has four isoforms, p38α, p38β, p38γ and p38δ, which differ in their expression patterns and their specific substrates (Cuenda and Rousseau, 2007). The two main activators of p38 MAPK are the MAP2K MKK3 and MKK6. Downstream of the signaling cascade, p38 MAPK regulates the expression of many cytokines, such as TNF and interleukins (IL), as well as the expression of intracellular enzymes, like inducible nitric oxide synthase (iNOS), which are important in inflammation and host cell death (Zarubin and Han, 2005). p38 MAPK is postulated to play a role in the immune response against *Mtb* (Aguilo et al., 2013). However, the exact role in host defense and manipulation of host signaling pathways by *Mtb* is not well described so far.

2.3 *Mtb* and its host cell

Unlike many other bacteria *Mtb* is highly dependent on the human host for survival, growth and spread. Therefore, a host-pathogen adaptation was essential for the survival of *Mtb.* The bacterium exploits, evades and modulates the immune system to persist inside the host (Cambier et al., 2014).

After reaching the alveolar spaces in the lung, *Mtb* uses phthiocerol dimycocerosate (PDIM) on its surface to evade recognition by PRR. Simultaneously, the bacterium expresses phenolic glycolipid (PGL) to trigger CCL2 expression in Mϕ for further recruitment of additional Mϕ that can be infected (Cambier et al., 2014).

Moreover, *Mtb* is highly adapted to survive inside Mϕ by preventing phagosome acidification and phagolysosomal fusion (Deretic et al., 2006). Phagocytosis, a form of endocytosis, is an important mechanism of the innate immunity. Under normal conditions, the pathogen is engulfed by the phagosome, which subsequently fuses with the lysosome to form the phagolysosome. The phagolysosome is acidified to pH 5.2 and enzymes are activated to degrade bacteria. However, *Mtb* is able to interfere with

this process. The cell wall component mannose-capped lipoarabinomannan (ManLAM) inhibits phagolysosomal fusion, possibly via the secretion of EsxA, and allows *Mtb* to reside in non-acidified endosomes (Cambier et al., 2014). Similarly, *Mtb* uses proteins secreted through the ESX-1 secretion system, such as EsxA, to permeabilize the phagosomal membrane, which enables *Mtb* to be released out into the cytosol (Wallis and Hafner, 2015). Furthermore, EsxA is involved in the inhibition of autophagy, a process that normally leads to bacterial killing (Romagnoli et al., 2012). Nevertheless, prior activation of the Mϕ can overcome the interference of *Mtb*, resulting in phagosome acidification and death of the bacteria (Schaible et al., 1998). At later stages of infection, the adaptive immune system is induced to help to control the disease. However, *Mtb* also has mechanisms to evade adaptive immunity. For instance, the bacterium delays the priming and activation of T cells by reducing the migration of dendritic cells (DC) to the lymph nodes, as well as limits the responsiveness of Mϕ to IFN-γ secreted by T cells at the site of inflammation (Pagan and Ramakrishnan, 2014). IFN-γ signaling is also responsible for intracellular tryptophan starvation, which restricts bacterial growth. *Mtb* responds with production of its own tryptophan and thereby is not dependent on the host (Zhang et al., 2013). Taken together, these mechanisms enable *Mtb* to survive inside the Mϕ and the granuloma.

2.4 Apoptosis, programmed host cell death

In order to escape the granuloma, the bacterium is depended to induce host cell death. TB-infected Mϕ die either by apoptosis or necrosis. Apoptosis is an immunologically silent process, which results in the uptake of dead cells by other immune phagocytes (Ramakrishnan, 2012). In general, the two pathways of apoptosis, the intrinsic and the extrinsic pathway, induce the activation of effector cysteine proteases (caspases) leading to the degradation of cellular organelles and fragmentation of deoxyribonucleic acid (DNA). The extrinsic or death receptor pathway, is activated in response to extracellular stimuli recognized by TLR or the TNF receptor superfamily. After recognizing a ligand the receptors recruit caspase 8 to form the death-inducing signaling complex (DISC) and to complete apoptosis (Elmore, 2007). Subsequently, the components of the apoptotic cell are engulfed by apoptotic bodies and phagocytosed by other Mϕ (**Fig. 3**). Therefore, these Mϕ represent new potential hosts for *Mtb*, allowing the bacterium to avoid extracellular host defenses and to spread via cell-to cell spread (Hotchkiss and Nicholson, 2006).

Most intracellular pathogens, including *Mtb*, have developed strategies to modulate host cell death to their own benefit. The role of apoptosis in *Mtb* infection has been a matter of debate for years. Evidence for both, the inhibition (Divangahi et al., 2009) or activation (Aporta et al., 2012) of apoptosis has been provided. It has been shown that *Mtb* may trigger apoptosis through the secretion of EsxA. EsxA induces an intracellular increase of reactive oxygen species (ROS) and calcium (Ca^{2+}) to promote the activation of endoplasmic reticulum (ER)-stress-associated pathways. These pathways are regulated by apoptosis signal-regulating kinase 1 (ASK1) and p38 MAPK and result in intrinsic apoptosis (Davis and Ramakrishnan, 2009). The phosphorylation of p38 MAPK leads to the activation of pro-apoptotic B-cell lymphoma 2 (Bcl-2) family proteins, such as Bim and Bcl-2 associated X protein (Bax). The proteins of the Bcl-2 family are essential for maintaining the mitochondrial function and integrity. Upon phosphorylation of Bim or the tumor-suppressor protein p53, the expression of pro-apoptotic proteins is promoted, while anti-apoptotic proteins are repressed, resulting in the accumulation of pro-apoptotic proteins at the mitochondria (Marchenko and Moll, 2014; Perfettini et al., 2005). Subsequently, intrinsic apoptosis induces mitochondrial outer-membrane permeabilization (MOMP) leading to the release of cytochrome c (CytoC), the activation of the initiator caspase 9 and finally the activation of the effector caspases 3,6 and 7 (Elmore, 2007).

In contrast, it has been shown that *Mtb* encodes anti-apoptotic genes, like *nuoG*, which expresses the NuoG subunit of NDH-1, a type I NADH-hydrogenase. NDH-1 inhibits phagosomal ROS and TNF secretion and thereby abrogates apoptosis (Miller et al., 2010). In addition, recently published data show that only attenuated *Mtb* strains promote apoptosis and that virulent *Mtb* strains favor necrotic cell death, making *Mtb* an ideal model organism to study the effects of different cell death pathways (Gräb et al., 2019; Zhao et al., 2017).

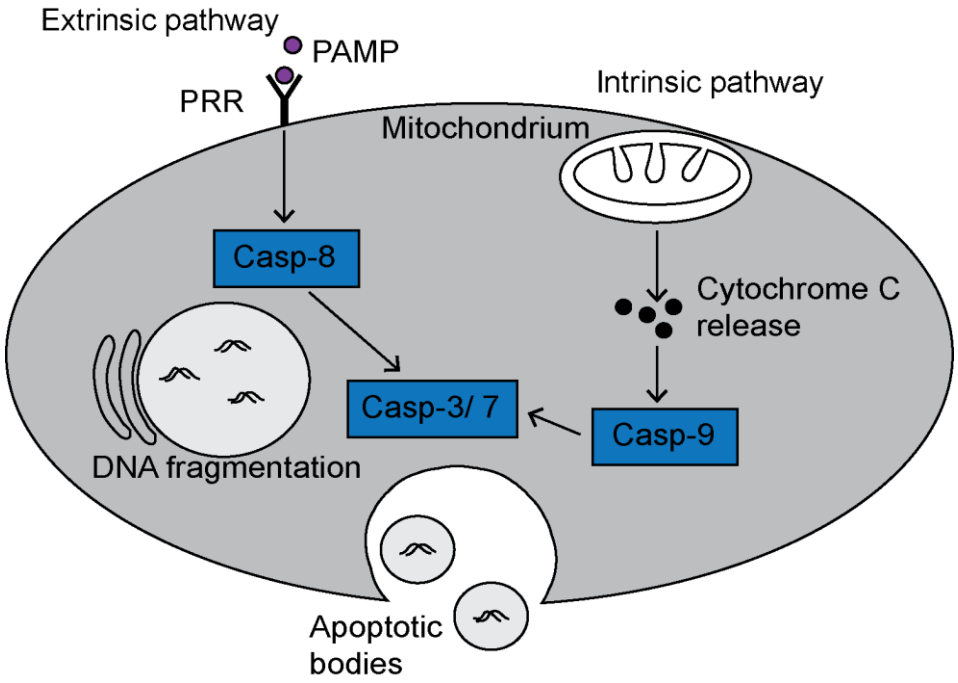

Figure 3. Pathways of apoptosis. Extrinsic apoptosis is triggered by pathogen-associated molecular patterns (PAMP) on the bacterial surface, which are recognized by pattern recognition receptors (PRR). Subsequently, caspase (Casp-) 8 is recruited to activate Casp-3 and 7 to complete apoptosis. Intrinsic apoptosis is mediated by cytochrome c (CytoC) released after mitochondrial outer membrane permeabilization (MOMP). CytoC recruits Casp-3 and 7 via Casp-9. Finally, the apoptotic cell is engulfed by apoptotic bodies and phagocytosed by Mϕ.

2.5 Necrosis

Necrosis was first described as an accidental form of cell death in response to environmental insults, clearly separating necrosis from the regulated and programmed apoptosis. Cells undergoing necrosis are characterized by a swollen morphology and random degradation of DNA, resulting in the release of cellular contents into the surrounding tissues (**Fig. 4**). Therefore, necrosis is considered a highly pro-inflammatory and energy independent form of cell death (D'Arcy, 2019). Unlike apoptosis, no distinct markers have been identified in necrotic cells, leading to the assumption that necrosis is an unstoppable and undruggable process (Ying and Padanilam, 2016). However, in recent years many advances have been made in the research field of cell death, challenging the perception of necrosis. By now, programmed forms of necrosis have been identified, such as necroptosis, pyroptosis and ferroptosis (Abe and Morrell, 2016; Shimada et al., 2016). These types of cell death demonstrate that regulated cell death is not restricted to apoptosis and that the different cell death pathways are interconnected. Furthermore, regulated necrosis may

present new opportunities to pharmacologically intervene with necrotic cell death (Conrad et al., 2016).

Mtb promotes necrosis by impeding the synthesis of prostaglandin E2 (PGE2) and thereby influences the plasma membrane repair mechanisms. These are especially important for the repair of lysosomal membranes, which rupture during necrosis (Divangahi et al., 2009). Lysosomes contain around 80 hydrolases that upon release into the cytoplasm inhibit energy metabolism in the cytoplasm and reduce ATP production and oxidative phosphorylation of the mitochondria (Ferri and Kroemer, 2001). Thus, virulent *Mtb* delays host cell death at an early stage of infection to hide from the host immune system and promotes cell death at later stages to escape from the confines of the Mϕ into the residing tissues and start a cycle of re-infection (Russell, 2007).

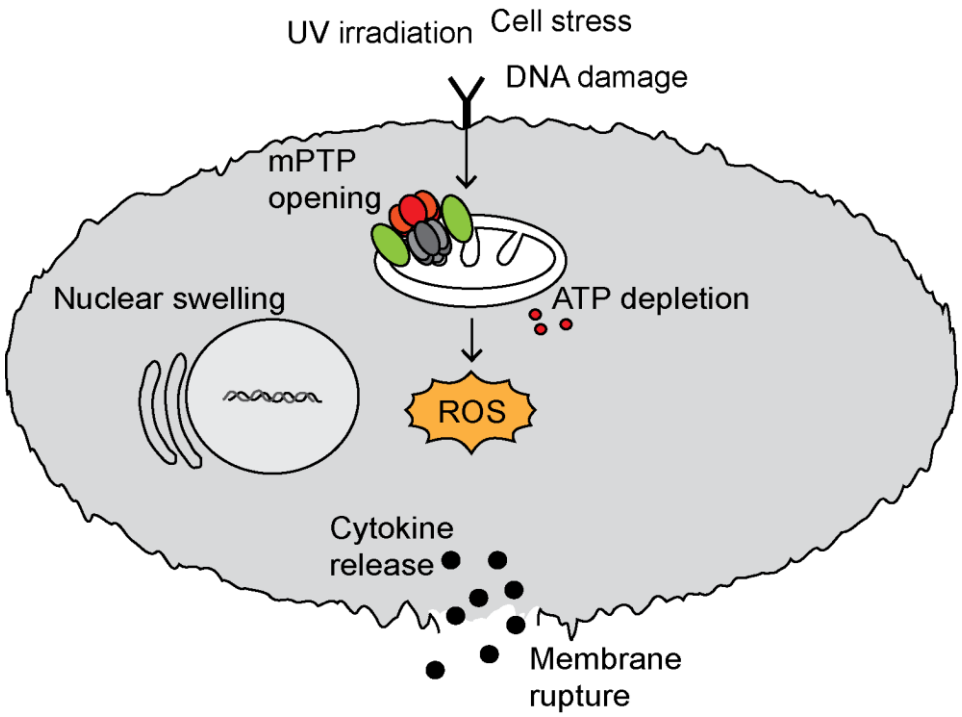

Figure 4. Necrosis. Environmental stress leads to opening of the mitochondrial permeability pore (mPTP) and the release of mitochondrial reactive oxygen species (ROS), as well as the depletion of adenosine triphosphate (ATP). Necrotic cell death is accompanied by nuclear swelling and rupture of the cell membrane resulting in the release of all cellular content into residing tissues.

2.5.1 Necroptosis

Until recently necrosis was only described as an unregulated form of cell death. By now, other forms of cell death have been described, which are regulated but have characteristics of necrosis. One such form is called necroptosis. Necroptosis is

mediated either by TNF receptor 1 (TNFR1) or by TNF-related apoptosis-inducing ligand (TRAIL) and Fas receptors. Afterwards, the receptor-interacting protein kinase (RIPK)1 and RIPK3 are activated. TNFR1 recruits RIPK1 to the TNFR-associated death domain (TRADD) to build complex I (**Fig. 5**). De-ubiquitination of RIPK1 normally activates caspase 8 and subsequently apoptosis. However, if caspase 8 is inhibited, RIPK1 and RIPK3 are phosphorylated and trigger the formation of the necrosome. The phosphorylated RIPK3 recruits and phosphorylates the mixed lineage kinase domain-like pseudokinase (MLKL). This kinase oligomerizes and migrates to the cell membrane where it binds to cardiolipin and phosphatidylinositol lipids, resulting in membrane permeabilization (Vandenabeele et al., 2010).

The role of necroptosis in *Mtb*-mediated host cell death is still a matter of debate. While proof for the induction (Roca and Ramakrishnan, 2013; Zhao et al., 2017) of necroptosis has been provided, others have demonstrated that *Mtb*-induced host cell death is independent of MLKL activation (Gräb et al., 2019; Stutz et al., 2018). However, the different findings regarding the role of necroptosis in *Mtb*-mediated host cell death are potentially influenced from cell-type-specific differences, such as the origin of the cells and their maintenance of molecular pathways in culture, and therefore need to be further investigated (Stutz et al., 2018).

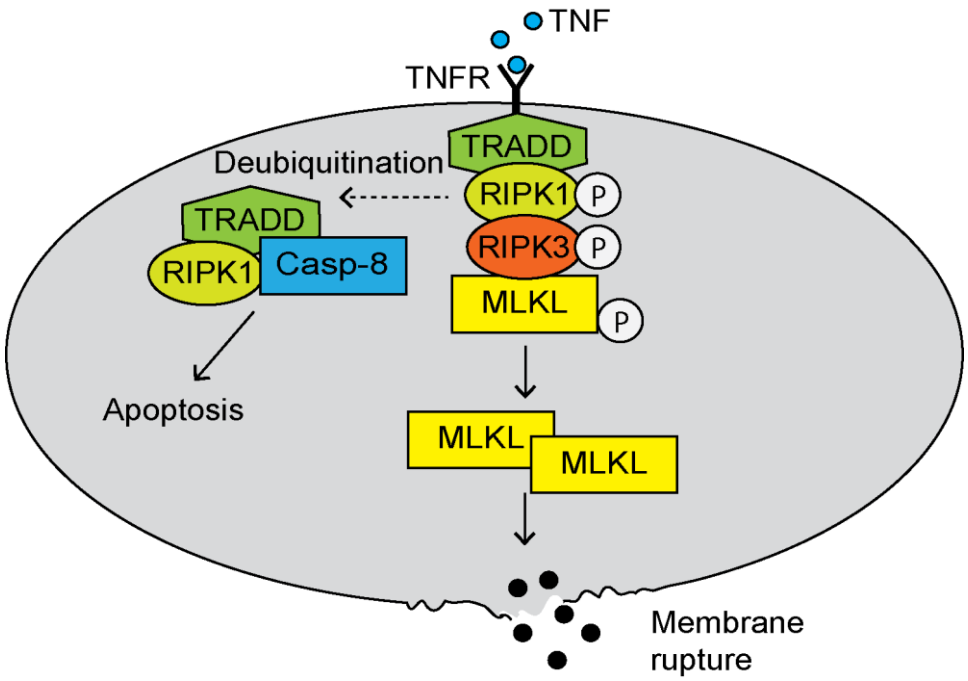

Figure 5. Necroptosis. Recognition of tumor necrosis factor (TNF) by the TNF receptor (TNFR) leads to the assembly of the necrosome. The necrosome consists of the TNFR-associated death domain (TRADD), the receptor-interacting protein kinase (RIPK)1 and 3 and the mixed lineage kinase domain-like pseudokinase (MLKL). Oligomerized MLKL migrates to

the cell membrane and leads to membrane permeabilization. Deubiquitination of RIPK1 activates caspase 8 and triggers apoptosis.

2.5.2 Pyroptosis

Pyroptosis is a caspase-dependent and pro-inflammatory form of cell death. This form of cell death is characterized by swelling of the cells, formation of pores on membranes and finally the release of pro-inflammatory cytokines, such as IL-1β and IL-18 (Abe and Morrell, 2016). The canonical pathway is triggered by PAMP or danger-associated molecular patterns (DAMP), like increasing levels of ROS or bacterial peptidoglycan, which result in the activation of inflammasomes. Inflammasomes consist of a PRR, the adapter protein apoptosis-associated speck-like protein (ASC), the caspase activation and recruitment domain (CARD) of ASC and pro-caspase 1. Following caspase 1 activation, gasdermin D (GSDMD) cleavage results in membrane pore formation and finally, in the release of cytokines from the pyroptotic cell (**Fig. 6**). Recruitment of other immune cells to the site of inflammation is also a characteristic of pyroptosis (Liu et al., 2016).

The role of pyroptosis in *Mtb* infection is still under investigation. Although it has been proven that mice deficient for IL-1β and IL-18 cytokine production are more susceptible to the infection. Therefore, the activation of inflammasomes in response to endoplasmic reticulum stress (ERS) might play an important role in *Mtb* infection (Wawrocki and Druszczynska, 2017).

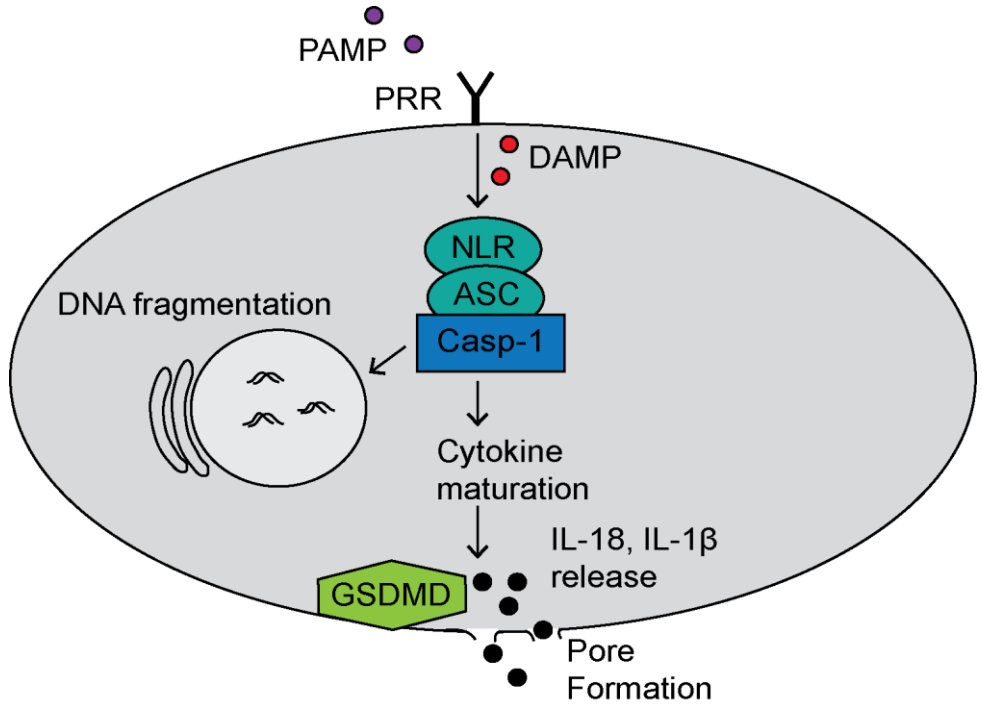

Figure 6. Canonical pathway of pyroptosis. Recognition of danger-associated molecular patterns (DAMP) or PAMP activate the inflammasome, which consists of PRR, adapter protein

apoptosis-associated speck-like protein (ASC) and caspase 1 (Casp-1). The inflammasome activates gasdermin D (GSDMD) resulting in membrane pores and the release of the pro-inflammatory cytokines interleukin (IL)-1β and IL-18.

2.5.3 Ferroptosis

Ferroptosis is a regulated form of necrosis that is induced by an overload of iron. Iron is essential in the Fenton reaction, which leads to the production of ROS in antibacterial immune reactions. Under normal conditions, the toxic lipid peroxides generated by an interaction between Fenton reaction-mediated hydrogen peroxides and membrane lipids would be degraded by glutathione peroxidase-4 (Gpx4). However, a dysfunction of Gpx4 causes an accumulation of lipid peroxides and results in membrane disruption. Gpx4 is a lipid repair enzyme that reduces lipid peroxides through glutathione (GSH) oxidation. Therefore, ferroptosis is characterized by reduced Gpx4 activity and GSH levels, as well as increased iron and lipid peroxide levels (Stockwell et al., 2017). Ferroptosis can be inhibited by lipid peroxidation inhibitors, such as ferrostatin-1.

The role of ferroptosis in *Mtb*-mediated host cell death is not well described. Iron is an important bioactive metal for bacterial growth. Limited iron levels reduce the growth of most pathogens (Schaible et al., 2002). *Mtb* infection induces heme oxygenase-1, an enzyme responsible for the degradation of heme to free iron, to increase the production of iron and thus the growth of the bacteria (Shiloh et al., 2008).

2.5.4 Necrotic cell death and mitochondria

Another form of regulated necrosis is mitochondrial-driven necrotic cell death. The permeabilization of the inner mitochondrial membrane (IMM) causes mitochondrial permeability transition (MPT). The opening of the mitochondrial permeability transition pore (mPTP) disrupts the mitochondrial membrane potential (ΔΨm) by an influx of ions and finally results in a loss of mitochondrial integrity. By now, the only identified regulator of the mPTP is the mitochondrial protein cyclophilin D (CypD). It has been shown that virulent *Mtb* induces MPT in a CypD-dependent manner (Gräb et al., 2019; Zhao et al., 2017).

2.6 Aim

The emergence and prevalence of drug resistant *Mtb* strains remains a public health crisis and has intensified research efforts to develop alternative therapeutic approaches, including host-directed therapies (HDT) to assist antibiotic treatment. As a pathogen, *Mtb* is highly adapted to humans as a host and continuously evades and

exploits the human immune system. Therefore, *Mtb* strongly influences gene expression and signaling pathways of the host cell using different virulence factors. A major mechanism of pathogenesis in a TB infection is the induction of host cell death. However, the type of cell death triggered by *Mtb* and its role during the infection is still a matter of debate. Further knowledge of the host-pathogen interaction could thereby provide new targets for therapies. These targets include the promotion of phagolysosomal fusion, or the inhibition of the pro-inflammatory pathways triggered by *Mtb*. Several drugs can be re-purposed for adjunct immunotherapies in TB treatment. The promotion of phagolysosomal fusion has been reported to be enhanced by metformin, a type 2 diabetes drug (Oglesby et al., 2019), while the tyrosine kinase inhibitor imatinib has been shown to reduce the bacterial load in *Mtb*-infected patients (Napier et al., 2011). Another potential drug for a HDT are the immunosuppressive corticosteroids, which reduce the mortality of TB meningitis patients (Schutz et al., 2018). So far, host cell death induced by *Mtb* has not been exploited as a target for HDT.

Thus, the aim of this thesis is to investigate the role of different host cell death pathways induced by virulent *Mtb* and to find potential candidates for therapeutic interventions.

3. Materials

3.1 Equipment

Table 1. Equipment

Equipment	Manufacturer
Centrifuge Z 446	Hermle Labortechnik
CKX41 inverted microscope	Olympus
CO2 Incubator with SafeCell	Sanyo
Cytation 3 Cell Imaging Multi-Mode Reader	Biotek
Curix 60	AGFA
GENESYS™ 20VIS spectrophotometer	Thermo Fisher Scientific
Heraeus™ Fresco™ 21 centrifuge	Thermo Fisher Scientific
Hidex Sense multimodal microplate reader	Hidex
IX81 inverted microscope	Olympus
Class II biological safety cabinet Golden Line	Kojair
Light Cycler	Roche
LC Carousel Centrifuge 2.0	Roche
MACS Multistand	Miltenyi Biotec
MACSxpress Separator	Miltenyi Biotec
MACSmix™ Tube Rotator	Miltenyi Biotec
MidiMACS Separator	Miltenyi Biotec
MultiskanTM FC Microplate Photometer	Thermo Fisher Scientific
MyCyclerTM thermal cycler system	Bio-Rad
NanoDrop spectrophotometer	Thermo Fisher Scientific
OctoMACS^{TM} Separator	Miltenyi Biotec
ScanLaf Mars Pro class 2 safety cabinet	LaboGene
Thermomixer Eppendorf comfort	Thermo Fisher Scientific
Trans-Blot® Turbo™ Transfer System	Bio-Rad
Water bath SW22	Julabo GmbH
Vortexing device	Scientific Industries, Inc.

3.2 Chemicals

Table 2. Chemicals and solutions

Chemicals and solutions	Manufacturer
Acetoxime	Sigma-Aldrich
Adalimumab	InvivoGen
BI-653048	Boehringer Ingelheim
BMS-582949	Selleckchem
Bromopyruvic acid	Sigma-Aldrich
CHAPS	Thermo Fisher Scientific
Cyclosporin A	Cayman Chemicals
DAPI	Invitrogen
Dexamethasone acetate	Sigma-Aldrich
Dimethyl sulfoxide	Sigma-Aldrich
Doramapimod	Axon Medchem
Etanercept	Sigma-Aldrich
Etoposid	Cayman Chemicals
Fetal bovine serum	PAN-Biotech
Fetal calf serum	Biowest
Ficoll-Paque	GE Healthcare
HBSS	Merck
HEPES	Biochrom
Losmapimod	Abcam
M-CSF	Miltenyi Biotec
MCC950	Sigma-Aldrich
Methyljasmonate	Sigma-Aldrich
MitoSOX™ Red	Invitrogen
Mitotempo	Sigma-Aldrich
Necrostatin-1	Cayman Chemicals
Necrostatin-5	Cayman Chemicals
Pamapimod	Selleckchem
PBS	Invitrogen
PFA	Carl Roth
Pifithrin α	Sigma-Aldrich

PrestoBlue™ Cell Viability Reagent	Thermo Fisher Scientific
Puromycin dihydrochloride	Carl Roth
Resazurin sodium salt	Sigma-Aldrich
Rifampicin	AppliChem
Ru-360	Sigma-Aldrich
SDS	Sigma-Aldrich
Staurosporine	Sigma-Aldrich
Tacrolimus (FK506)	Cayman Chemicals
Thalidomide	Sigma-Aldrich
TMRM	Sigma-Aldrich
Triton X	Sigma-Aldrich
Trypan blue	Invitrogen
Z-VAD-FMK	Selleckchem

3.3 Consumables

Table 3. Consumables

Consumables	**Manufacturer**
Adhesive gas permeable seal	Thermo Fisher Scientific
Bottle-top-filter 0.2 µm	Thermo Fisher Scientific
CellBIND microplate (96-well)	Corning
Cell scraper	Corning
Cell strainer	Corning
Conical centrifuge tube (15 and 50 ml)	Greiner Bio-One
Cryo vial	Greiner Bio-One
LS and MS columns for MACS	Miltenyi Biotec
Microcentrifuge tube (1.5 and 2 ml)	Eppendorf
Microtiter plate (6- and 96-well)	TPP
SealPlate® sealing films	Excel Scientific
Sterile filter storage bottle	Thermo Fisher Scientific
Tissue culture dish and flask	TPP
Adhesive gas permeable plate seals	Thermo Fisher Scientific
Transfer pipette (5, 10 and 25 ml)	Sarstedt

3.4 Media and buffer

7H9 complete medium (7H9c)	Middlebrook 7H9 Broth Base
	10% albumin dextrose catalase (ADC)
	0.05% Tween 80
	0.2% glycerol
7H10 complete medium	Middlebrook 7H10 Agar Base
	10% ADC
	0.5% glycerol
DMEM/ FBS	DMEM
	10% FBS
MACS buffer	PBS
	2% FBS
	2 mM EDTA
MEM complete medium (MEMc)	MEM with GlutaMAXTM
	10% FBS
	1% sodium pyruvate
	1% non-essential amino acids
RPMI 1640/ FBS	RPMI 1640 with L-glutamine
	10% FBS
RPMI 1640/ FBS/ M-CSF	RPMI 1640 with L-glutamine
	10% FBS
	50 ng/ ml M-CSF
VLE-RPMI 1640 complete medium	VLE- RPMI 1640
(RPMIc)	10% FCS
	10 mM HEPES
	2 mM L-glutamine
	1 mM sodium pyruvate
	10 µg/ ml penicillin/ streptomycin
	15% M-CSF
TBST	10 mM Tris
	150 mM NaCl
	1% Tween 20

3.5 Kits and reagents

Table 4. Commercial kits and reagents

Kit	Manufacturer
20X LumiGLO® Reagent and 20X Peroxide	Cell Signaling Technology
Caspase-Glo® 3/7 Assay	Promega
CellTiter-Glo® 2.0 Assay	Promega
CD14 MicroBeads, human	Miltenyi Biotec
Fluo-4 NW Calcium Assay Kit	Thermo Fisher Scientific
Halt™ Protease and Phosphatase Inhibitor Cocktail	Thermo Fisher Scientific
HMGB1 ELISA	IBL International GmbH
Light Cycler Fast Start DNA MasterPLUS SYBR Green	Roche
Mitochondria Isolation Kit for Mammalian Cells	Thermo Fisher Scientific
Pierce™ BCA Protein Assay	Thermo Fisher Scientific
Pierce™ LDH Cytotoxicity Assay	Thermo Fisher Scientific
PrestoBlue™ Cell Viability Reagent	Thermo Fisher Scientific
RIPA lysis and extraction buffer	Thermo Fisher Scientific
RNeasy Mini Kit	Qiagen
SuperScript III First-Strand Synthesis SuperMix	Thermo Fisher Scientific
Trans-Blot® Turbo™ RTA Mini PVDF Transfer Kit	Bio-Rad

3.6 Primer

Table 5. Primers for quantitative real-time polymerase chain reaction (PCR)

Target gene	Forward primer (5'- 3')	Reverse primer (5'- 3')
GAPDH	GGTATCGTGGAAGGACT	GGGTGTCGCTGTTGAA
HMBS	TGCACGATCCCGAGAC	CGTGGAATGTTACGAGC
Hexokinase II	TCTAAGCGGTTCCGCA	AGAAGGGTCATACCTGG
MKP-1	GGAATCTGGGTGCAGT	CTGGTAGTGACCCTCAA
p38 MAPK	GCCCGAACGATACCAG	CTGAAACGGTCTCGACA

3.7 Antibodies

Table 6. Western blot antibodies

Target protein	Manufacturer
β-Actin	Cell Signaling Technology
Caspase 3	Cell Signaling Technology
Cleaved caspase 3	Cell Signaling Technology
Cyclophilin D	Abcam
ERK	Cell Signaling Technology
Hexokinase II	Cell Signaling Technology
JNK	Cell Signaling Technology
p38 MAPK	Cell Signaling Technology
Phosphor ERK	Cell Signaling Technology
Phosphor JNK	Cell Signaling Technology
Phosphor p38 MAPK	Cell Signaling Technology
VDAC-1	Cell Signaling Technology

3.8 Cell lines

Table 7. Cell lines

Cell line	Provider
J774A.1: mouse Mϕ	ATCC - LGC Standards
J774.2: mouse Mϕ	Sigma-Aldrich
MRC-5: human lung fibroblast	Coriell Institute for Medical Research
p38 MAPK knockdown J774A.1	Christian Pallasch, University of Cologne
p53 knockdown J774A.1	Christian Pallasch, University of Cologne

3.9 Primary mouse cells

Cells from various knockout mice (MLKL$^{-/-}$, TNFR1$^{-/-}$) or knockin mice (Bcl-2) were a kind gift of Hamid Kashkar and Manolis Pasparakis (University of Cologne, Cologne, Germany).

3.10 Bacteria

Mycobacterium tuberculosis Erdman

3.11 Software

Table 8. Software

Software	Provider
Adobe creative suit 5	Adobe
cellSens Standard	Olympus
Fiji, ImageJ 1.46h	Wayne Rasband
Gen3 Software	BioTek
GraphPad Prism 5.04	GraphPad Software
Office 365 Personal	Microsoft

4. Methods

4.1 Cell biology methods

4.1.1 Culturing of cell lines

All cell lines were grown in tissue culture flasks at 37 °C with 5% CO_2. For frozen cell stocks, the cells were resuspended in medium containing 5% DMSO and 95% FBS and stored in cryo-vials at -150 °C.

4.1.1.1 J774A.1 and J774.2 macrophages

J774A.1 Mϕ and J774.2 Mϕ were grown in DMEM supplemented with 10% FBS. Both cell lines were passaged twice a week at a ratio of 1:4.

4.1.1.2 MRC-5 fibroblasts

MRC-5 human lung fibroblasts were cultured in MEMc medium. Cells were sub-cultured when reaching 100% confluency. After culturing the cells for 10 days, the cells were passaged by seeding 1.5 x 10^6 cells per culture flask.

4.1.2 Isolation of single cell suspensions

Single cell suspensions were gained from human peripheral blood and mouse bone-marrow as follows. Primary cells were cultured at 37 °C with 5% CO_2.

4.1.2.1 Isolation of peripheral blood mononuclear cells

Blood samples were obtained from healthy volunteers as well as patients with active TB before therapy was initiated. The study was approved by the University of Cologne Ethics Committee (18-079). Patients as well as healthy volunteers participated after giving written informed consent

Human peripheral blood mononuclear cells (PBMC) were isolated from venous blood using density centrifugation. Briefly, blood was diluted with RPMI supplemented with 10% FBS at a ratio of 1:1 and layered over Ficoll-Paque. After centrifugation (540 x g, 20 min), the interphase, containing lymphocytes (B cells, T cells and NK cells), monocytes and dendritic cells (DC), was collected and centrifuged (650 x g, 10 min). PBMC were washed three times with RPMI supplemented with 10% FBS (300 x g, 10 min). Following Ficoll-Paque separation of PBMC from granulocytes and erythrocytes, the number of PBMC was determined using the hemacytometer as described in 4.2.3. Monocytes were isolated by magnetic separation of $CD14^+$ cells from unlabelled cells.

Therefore, CD14 micro beads were added to gain a defined number of monocytes from the PBMC population. $CD14^+$ monocytes were counted and seeded in RPMI medium supplemented with 10% FBS and 50 ng/ml human macrophage colony-stimulating factor (M-CSF) at a density of 1 x 10^5 cells per well in 96-well plates. Following differentiation of monocytes into Mϕ, the growth medium was changed to RPMI supplemented with 10% FBS.

4.1.2.2 Isolation of bone marrow-derived macrophages from mice

Bone marrow-derived Mϕ (BMDM) were isolated from C57BL/6 mice by expelling the bone marrow from femurs and tibia with RPMI by needle. Following centrifugation (400 x g, 10 min) cells were plated in dishes and incubated at 37 °C and 5% CO_2. BMDM were differentiated in RPMIc for 7 days with fresh medium being added after 5 days. Cells were seeded at a density of 8 x 10^4 cells per well in 96-well plates.

4.1.3 Determination of cell numbers

The cell suspensions were diluted with Trypan blue and the numbers of cells were counted using a hemocytometer. The total number of cells was determined by multiplying the number of living cells with the volume of the cell suspension, the dilution factor, and the volume expansion factor of the hemocytometer (10^4).

4.1.4 Survival Assay

4.1.4.1 Fibroblast survival assay

MRC-5 lung fibroblasts were analyzed using the fibroblast survival assay (FSA). Therefore, compounds were pre-plated into 96-well plates at different concentrations. MRC-5 fibroblasts were harvested and seeded at a density of 2 x 10^4 cells per well and could adhere for 2 h. Afterwards, cells were infected with multiplicities of infection (MOI of 10) for three days. Cell survival was analyzed by measuring the fluorescence signal of PrestoBlue™ (10% final concentration) in a Cytation 3 Cell Imaging Multi-Mode Reader.

4.1.4.2 Macrophage survival assay

Survival of Mϕ was assessed using fluorescence microscopy. Primary cells were plated as mentioned beforehand (4.1.2) and J774A.1 and J774.2 Mϕ were plated at a density of 2 x 10^4 cells per well in 96-well plates containing different compounds. Following 2 h of pre-treatment, J774 and BMDM were infected with *Mtb* Erdman with

a MOI of 3 and human Mϕ were infected with a MOI of 1. After 48 h, cells were washed several times with PBS, fixed with 4% PFA and stained with DAPI.

4.1.5 Fluorescence microscopy

Images were acquired on an IX81 inverted microscope using cellSens standard software and the number of surviving cells was determined using Fiji processing software to count the number of stained nuclei. *Mtb*-infected cells were fixed with 4% PFA prior to microscopy.

4.1.5.1 Measurement of mitochondrial membrane potential

J774.2 Mϕ were seeded at a density of 2 x 10^4 per well in a 96-well plate and infected with *Mtb* Erdman (MOI 5) for 24 h and 48 h, respectively. Cells were washed several times with PBS before adding Tetramethylrhodamine-methyl ester (TMRM) at a final concentration of 100 nM. Cells were incubated at 37 °C in 5% CO_2 for 30 minutes and washed with PBS. For microscopy, cells were covered with PBS. The accumulation of TMRM in the mitochondrial matrix represents a stable mitochondrial membrane potential, while a loss of membrane potential results in a release of TMRM from mitochondria.

4.1.6 Isolation of mitochondria

Mitochondria were isolated from infected MRC-5 lung fibroblasts or J774.2 Mϕ using the Mitochondria Isolation Kit for Cultured Cells (Thermo Fisher Scientific). After 5 h and 24 h of infection, cells were washed twice with PBS and detached from the culture flask with a cell scraper. Mitochondria of 1 x 10^7 cells were isolated using the reagent-based method. Separation of the mitochondrial and the cytosolic fraction of samples was achieved by centrifugation (12 000 x g, 15 min, 4 °C). Thereafter, the mitochondria were lysed with 2% CHAPS in TBS (25 mM Tris, 150 mM NaCl, pH 7.2), containing Halt™ Protease and Phosphatase Inhibitor Cocktail. Both fractions were stored at -80 °C and the purity of the mitochondrial fraction was analyzed by Western blotting.

4.2 Molecular biology methods

4.2.1 Culture conditions of *Mycobacterium tuberculosis*

Mtb was grown in Middlebrook 7H9 broth or 7H10 agar plates. Freezer stocks were thawed and grown in 7H9c medium at 37 °C and 100 rpm until reaching an optical density of 1 at a wavelength of 560 nm (OD_{560}). Cells were infected with washed logarithmic-phase *Mtb* at varying MOI.

4.2.2 Determination of colony-forming units

The colony-forming unit (CFU) of *Mtb*-infected J774.2 Mϕ was determined 5 days post infection. 5 x 10^3 cells were seeded in 96-well plates, pretreated with different compounds for 2 h, and infected with *Mtb* Erdman (MOI 2) for 24 h. The CFU of *Mtb*-infected BMDM was also analyzed 5 days post infection. Therefore, 8 x 10^4 BMDM were seeded in 96-well plates and infected with Mtb Erdman (MOI 1) for 5h. Subsequently, cells were washed twice with PBS to remove unphagocytosed bacteria and fresh medium containing the different compounds was added. Plates were incubated at 37 °C in 5% CO_2 for 5 days and the cells were lysed with 0.1% SDS. Viable bacteria were grown in serial dilutions on 7H10 agar plates and colonies were counted after 10 to 14 days of incubation at 37 °C.

4.2.3 Lactate dehydrogenase release assay

The release of lactate dehydrogenase (LDH) was measured utilizing the Pierce™ LDH Cytotoxicity Assay Kit conducted according to the manufacturer's recommendations. Therefore, MRC-5 lung fibroblasts or J774.2 Mϕ were harvested, seeded in a 96-well plate (2 x 10^4 cells per well) containing different compounds. After 2 h of pre-treatment, cells were infected with *Mtb* Erdman at a MOI of 10 and 5, respectively. Following 24 h, 48 h and 72 h of infection, the release of LDH into the supernatant was detected by measuring the reduction of tetrazolium salt to a red formazan product in a BioTek Cytation™ 3 Cell Imaging Multi-Mode Reader.

4.2.4 Caspase activity assay

The activity of caspase 3 and caspase 7 was measured with the Caspase-Glo® 3/7 Assay according to the manufacturer's instructions. Compounds were pre-plated into white-walled 96-well plates, before MRC-5 or J774.2 Mϕ were seeded at a density of 2 x 10^4 cells per well. Following adherence of the cells, MRC-5 lung fibroblasts (MOI 10) and J774.2 Mϕ (MOI 5) were infected with *Mtb* Erdman. Infected cells were incubated up to 48 h at 37 °C in 5% CO_2. The Caspase-Glo® Reagent was added to the wells 24 h and 48 h post infection and luminescence was measured in a BioTek™ Cytation™ 3 Cell Imaging Multi-Mode Reader.

4.2.5 Adenosine triphosphate assay

The CellTiter-Glo® 2.0 Assay was conducted according to the manufacturer's recommendations to measure the level of intracellular ATP. Harvested MRC-5 lung fibroblasts and J774.2 Mϕ were seeded in white-walled 96-well plates at a density of 2

x 10^4 cells per well and pretreated for 2 h with different compounds. Afterwards, MRC-5 fibroblasts (MOI 10) and J774.2 Mϕ (MOI 5) were infected with *Mtb* Erdman and the amount of ATP was quantified by adding the CellTiter-Glo® 2.0 reagent 24 h and 48 h post infection. The luminescent signal was measured in a BioTek Cytation™ 3 Cell Imaging Multi-Mode Reader.

4.2.6 Quantification of calcium

Intracellular calcium concentration was determined using the Fluo-4 NW Calcium Assay Kit according to the manufacturer's instructions. Cells were plated at a density of 2 x 10^4 cells per well in black-walled 96-well plates and pre-treatment of the given compound was applied 2 h prior to infection with *Mtb* Erdman at varying MOI for up to 24 h. Cells were washed once with HBSS and incubated with Fluo-4 NW for 30 min at 37 °C. Fluo-4 NW (Ex/ Em 488 nm/ 530 nm) was immediately detected following incubation using a BioTek Cytation™ 3 Cell Imaging Multi-Mode Reader. Calcium was quantified by calculating the ratio of the ion-bound (Ex 340 nm) and ion-free indicators (Ex 380 nm).

4.2.7 Quantification of reactive oxygen species

ROS production in the mitochondria was detected by MitoSOX Red, a superoxide indicator. Cells were plated at a density of 2 x 10^4 cells per well in black-walled 96-well plates and pre-treatment of the given compound was applied 2 h prior to infection with *Mtb* Erdman at varying MOI for up to 24 h. Rotenone (50 µM), an inhibitor of the complex I of the electron transport chain, was used as a positive control. The medium was removed, and cells were washed with HBSS. Afterwards, cells were incubated with MitoSOX Red (5 µM in HBSS) at 37 °C for 15 min. Following incubation, cells were washed three times with HBSS and fluorescence was detected in a BioTek Cytation™ 3 Cell Imaging Multi-Mode Reader. Cell-specific fluorescence was calculated by subtracting the fluorescence of cell-free wells containing HBSS.

4.2.8 Isolation of RNA

RNA was isolated from whole cell lysates. Therefore, 1 x 10^6 MRC-5 lung fibroblasts or J774.2 Mϕ were seeded in a 6-well plate and infected with *Mtb* Erdman at a MOI of 10 and 5, respectively. Following 5 h and 24 h of infection, cells were washed twice with PBS and lysed with RLT buffer containing β-mercaptoethanol. Total RNA was isolated with the RNeasy Mini Kit according to the manufacturer's instructions and

quantification of RNA was done using a NanoDrop spectrophotometer. All samples had A260/ A280 ratios of 1.90 to 2.10.

4.2.9 Synthesis of cDNA

Following isolation of total RNA, first-strand cDNA was synthesized with the SuperScript III First-Strand Synthesis SuperMix for qRT-PCR. Reaction mix, containing random hexamers, oligo(dT) and magnesium chloride, as well as enzyme mix, containing M-MLV RT and a recombinant ribonuclease inhibitor (RNaseOUT™), was added to the RNA. The samples were first incubated at room temperature for 10 min prior to cDNA synthesis conducted at 50 °C for 30 min. The reaction of the reverse transcriptase was stopped by heating the samples for 5 min at 85 °C. Finally, *Escherichia coli* RNase H was added, and the cDNA was incubated for 20 min at 37 °C. The cDNA was transferred into 1.5 ml tubes and stored at -20 °C until further use.

4.2.10 Quantitative real-time PCR

Quantitative real-time PCR was conducted to compare the relative amount of the expression of different genes. Therefore, the Light Cycler Fast Start DNA MasterPLUS SYBR Green Kit was used. SYBR Green is a DNA binding fluorescent probe, which integrates itself into double stranded DNA, causing a fluorescent signal. The fluorescent signal generated during each cycle is proportional to the amount of generated PCR product. The relative quantification was done by comparative Cp method. Hence, the Cp values of each sample were normalized against the Cp values of the house-keeping genes glyceraldehyde 3-phosphate dehydrogenase (GAPDH) or hydroxymethylbilane synthase (HMBS). Additionally, a melting curve analysis was performed to eliminate non-specific amplification.

4.3 Biochemical methods

4.3.1 Enzyme-linked immunosorbent assay

The HMGB1 ELISA kit (IBL International) was utilized to measure the release of the protein HMGB1. 1 x 10^6 MRC-5 lung fibroblasts were seeded in a 6-well plate and allowed to adhere overnight. The following day cells were infected with *Mtb* Erdman (MOI 10) and incubated for 48 h at 37 °C in 5% CO_2 prior to collecting the supernatant. The samples were processed according to the manufacturer's protocol. Briefly, the samples were transferred into a 96-well plate pre-coated with polyclonal anti-HMGB1 and incubated for 24 h at 37 °C. Thereafter, HMGB1 conjugated to peroxidase was

added to the samples, the plate was incubated for 2 h at 25 °C, and TMB substrate solution was used for detection. The absorbance was measured and analyzed using the Multiskan™ FC Microplate Photometer with internal software.

4.3.2 Immunoblot analysis

For immunoblot analysis whole cell lysates were gained from MRC-5 lung fibroblasts or J774.2 Mø. 1 x 10^6 cells were seeded in 10 cm culture dishes and allowed to adhere for at least 24 h. Prior to infection with *Mtb* Erdman cells were pretreated with different compounds for 2 h. Whole cell lysates were obtained 5 h, 24 h and 48 h post infection from MRC-5 lung fibroblasts and 5 h, 24 h and 30 h post infection from J774.2 Mø using RIPA lysis and extraction buffer containing Halt™ Protease and Phosphatase Inhibitor Cocktail. The samples were detached from the culture flask with a cell scraper and incubated on ice for 20 min. Subsequently, the samples were centrifuged (12000 x g, 10 min, 4°C) and the supernatant containing the proteins was stored at -80 °C until further use. The protein concentration was measured with the Pierce™ BCA Protein Assay Kit and equal amounts of protein (15–20 µg) were loaded onto a SDS-polyacrylamide gel and separated by gel electrophoresis. Afterwards, the proteins were transferred to a PVDF membrane using the Trans-Blot® Turbo™ Transfer System. The membrane was blocked with 5% dried milk or 5% BSA in TBST buffer and was incubated with primary antibodies at 4 °C overnight. The following day, the membranes were washed three times for 5 minutes with TBST and incubated for 1 h at room temperature with the corresponding secondary, horseradish peroxidase-conjugated, antibody. Visualization of the transferred proteins was achieved with the 20X LumiGLO® Reagent, and X-ray films were processed in a Curix 60.

4.4 Statistical analysis

Data are displayed as mean ± standard error of the mean (SEM). The data were analyzed with the Graphpad Prism version 5 software program. The unpaired t-test was used to compare two matched groups and the One-Way analysis of variance (ANOVA) with Bonferroni posttests was used to compare more than two groups. Differences with the following *p* values $p < 0,05$ (*), $p < 0,01$ (**) and $p < 0,001$ (***) were defined as statistically significant.

5. Results

5.1 Inhibition of *Mtb*-induced cell death by corticosteroids

Infection of Mϕ with *Mtb* leads to the phagocytosis of the bacterium and ultimately to host cell death by the secretion of virulence factors through the ESX-1 secretion system of *Mtb*. Death of the Mϕ allows the spread of the bacteria and causes tissue damage and hyperinflammation (Bold and Ernst, 2009). Therefore, host cell death is a major mechanism of *Mtb* pathogenesis and a potential drug target for *Mtb* treatment. In recent years, efforts in finding a suitable compound that abrogates mycobacterial cytotoxicity and promotes host cell survival have increased. Especially, the re-purpose of already approved drugs that are pharmacologically active has become of high interest (Tsenova and Singhal, 2020).

I performed a high-throughput screen of Food and Drug Administration (FDA)-approved drugs to find a compound that inhibits host cell death. For that purpose, MRC-5 human lung fibroblasts were infected with wild type *Mtb* and host cell survival was monitored by fluorescence, in a FSA. Interestingly, corticosteroids were potent hit compounds and nearly as effective in promoting host cell survival as the antibiotic rifampicin, which was used as a positive control (**Fig. 7A**). The most efficient compound was the corticosteroid dexamethasone with a half maximal inhibitory concentration (IC_{50}) of 15 nanomolar (**Fig. 7B**). Additionally, cell death was reduced in primary human Mϕ (**Fig. 7C**) isolated from blood and in the mouse Mϕ cell line J774.2 (**Fig. 7D**). These data illustrate that dexamethasone is highly effective in reducing mycobacterial cytotoxicity independent of different phagocytes.

However, corticosteroids have many off-target and adverse effects, such as diabetes mellitus (Blackburn et al., 2002) or corticosteroid-induced lipodystrophy (Hasselgren et al., 2010). Thus, I wanted to decipher the pathway that dexamethasone induces to promote host cell survival to find a suitable alternative for the treatment of TB patients.

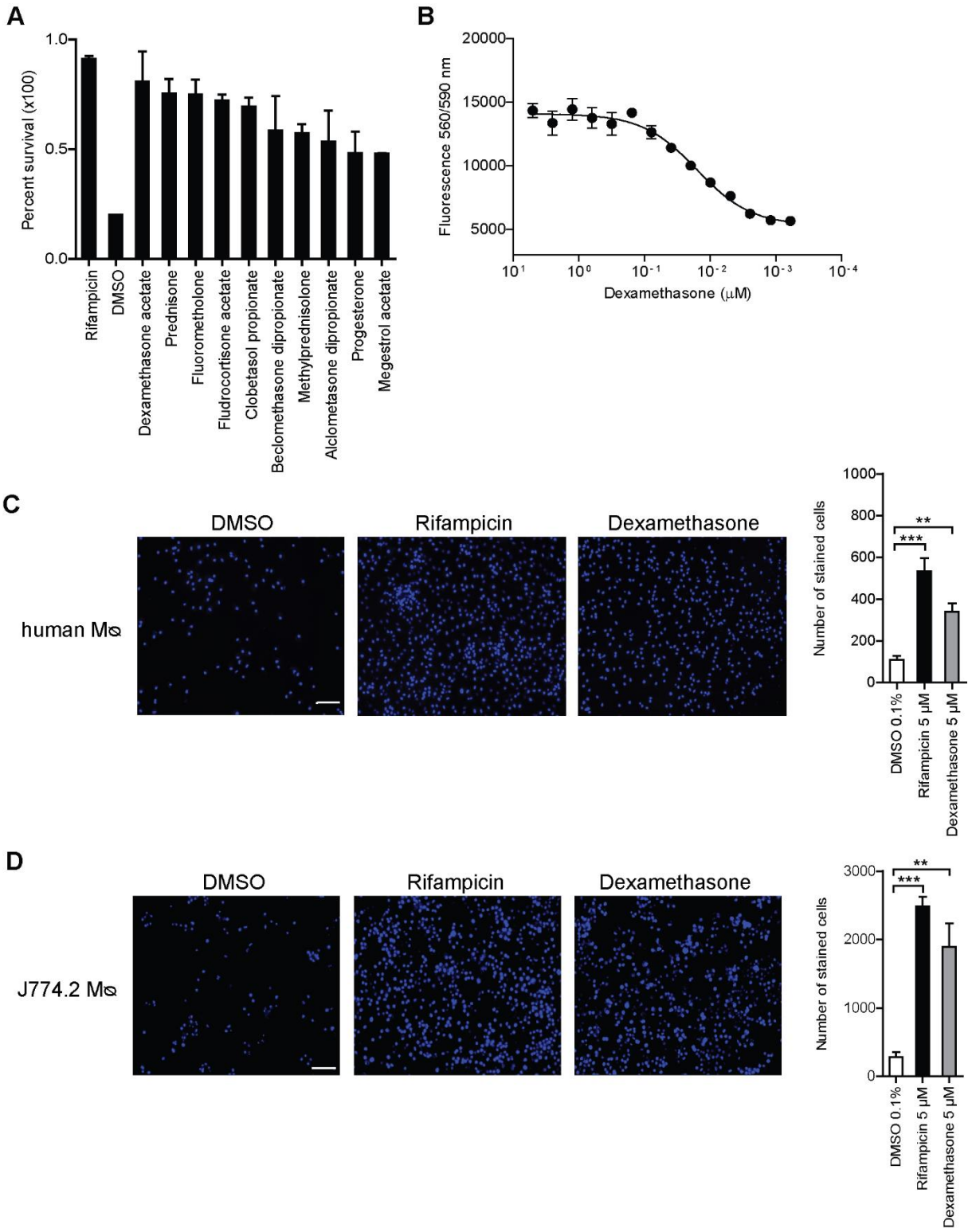

Figure 7. Corticosteroids reduce cytotoxicity in *Mtb*-infected cells. Protective effect of corticosteroids (10 µM; **A**) and dose-response curve of dexamethasone (**B**) in MRC-5 lung fibroblasts infected with wild type *Mtb* Erdman with a multiplicity of infection (MOI) of 10. Host cell survival was measured by PrestoBlue™. The data is derived from a high-throughput screen using duplicate assay plates. Representative fluorescent microscopy images and survival of *Mtb*-infected primary human Mϕ (MOI 1; **C**) and J774.2 Mϕ (MOI 5; **D**) treated with dexamethasone (5 µM), rifampicin (5 µM) or DMSO (0.1% or 0.5%). Nuclei were stained with 4',6-diamidino-2-phenylindole (DAPI) 48 h post infection (scale bar: 100 µm). Data from one experiment with duplicates are shown in **A** and **B**; data were pooled from three (**C**) or two (**D**)

independent experiments with multiple replicates. Results are expressed as the mean ± SEM. Statistical analysis were performed by One-Way ANOVA (**, p≤ 0.01; ***, p≤ 0.001).

5.2 Activation of p38 MAPK initiates host cell death

Corticosteroids have been used in the clinic to treat TB meningitis and it has been shown that dexamethasone reduces the mortality rate of such TB-patients (Schutz et al., 2018). However, not much is known about the exact mechanism, which is responsible for the protective effect in TB patients. So far, only the MAPK phosphatase 1 (MKP-1; DUSP1) has emerged as a key regulator for corticosteroid-dependent effects (Abraham et al., 2006). Hence, I hypothesize that the inhibition of MKP-1 should reverse the protective effect of dexamethasone in *Mtb*-infected cells.

In order to validate this hypothesis, MRC-5 lung fibroblasts were co-treated with dexamethasone and the MKP-1 inhibitor (E/Z)-Bcl. While (E/Z)-Bcl had no cytotoxic effects on MRC-5 fibroblasts, the inhibitor fully diminished the protective effect of dexamethasone (**Fig. 8A**). Similarly, the co-treatment of MRC-5 fibroblasts with dexamethasone and the glucocorticoid receptor (GR) inhibitor Ru-486 lead to increased host cell death (**Fig. 8A**). In addition, the treatment of human Mϕ with the non-steroidal GR agonist BI653048 lead to increased survival of the Mϕ (**Fig. 8B**). These findings suggest that dexamethasone protects the cells from cell death by activation of the GR and upregulation of MKP-1. The upregulation of MKP-1 in *Mtb*-infected MRC-5 fibroblasts was confirmed by qRT-PCR indicated by a significant increase upon treatment (**Fig. 8C**).

MKP-1 is a known regulator of MAPK and can inactivate the kinases p38 MAPK, ERK and JNK (Abraham et al., 2006). Therefore, the activation of all three kinases was analyzed by detecting their corresponding phosphorylated forms via Western blot. Upon infection of J774.2 Mϕ with *Mtb*, p38 MAPK was phosphorylated at different time points (**Fig. 8D**). Treatment of the cells with dexamethasone prevented the phosphorylation of p38 MAPK 24 h and 30 h after infection.

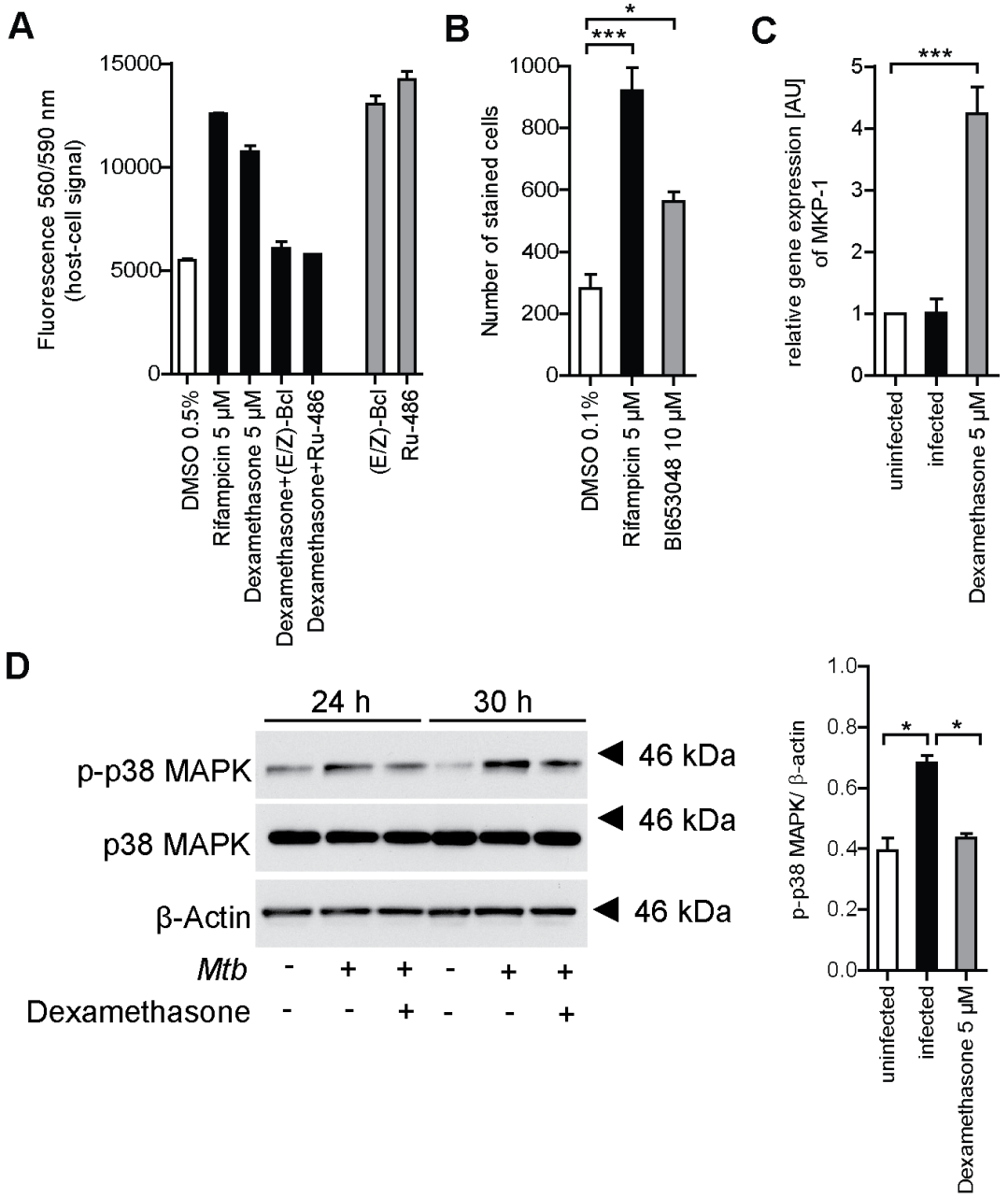

Figure 8. The cytoprotective effect of dexamethasone is mediated by mitogen-activated protein kinase (MAPK) phosphatase (MKP)-1 activation. Inhibition of the glucocorticoid receptor (GR) by Ru-486 or inhibition of MKP-1 by (E/Z)-Bcl hydrochloride (**A**) reduces the protective effect of dexamethasone (5 µM) on *Mtb*-infected MRC-5 lung fibroblast (MOI 10) survival. Viable fibroblasts were quantified 72 h post infection using the fibroblast survival assay (FSA). Treatment of *Mtb*-infected human Mϕ (MOI 1) with the GR agonist BI653048 (10 µM) lead to increased cell survival. Mϕ were stained with DAPI and the number of surviving cells was assessed 48 h post infection (**B**). Dexamethasone (5 µM) treatment increases MKP-1 expression in infected MRC-5 lung fibroblasts 5 h after infection. Relative expression of MKP-1 was measured by quantitative real-time (qRT-)PCR (**C**). Infection of J774.2 Mϕ with *Mtb* (MOI 5) leads to p38 MAPK phosphorylation. Whole cell lysates were obtained at indicated time points after infection and subjected to Western blot analysis. β-Actin was used as a loading control (**D**). Data from one experiment with multiple replicates (**A**, **B**), data pooled from four individual experiments (**C**) or data from three individual experiments (**D**) are shown as mean ± SEM. Analysis was done using One-Way ANOVA (*, p≤ 0.05; ***, p≤ 0.001).

In addition, the phosphorylation of JNK and ERK was investigated in *Mtb*-infected J774.2 Mϕ in the presence or absence of dexamethasone. No significant difference in the phosphorylation status of JNK (**Fig. 9A**) or ERK (**Fig. 9B**) could be observed at 5 h or 24 h post infection compared to the uninfected cells. Though dexamethasone treatment of *Mtb*-infected J774.2 Mϕ lead to a slight reduction of phosphorylation for both kinases 24 h post infection. Thus, p38 MAPK was identified as the sole target of corticosteroid treatment in *Mtb*-infected phagocytes.

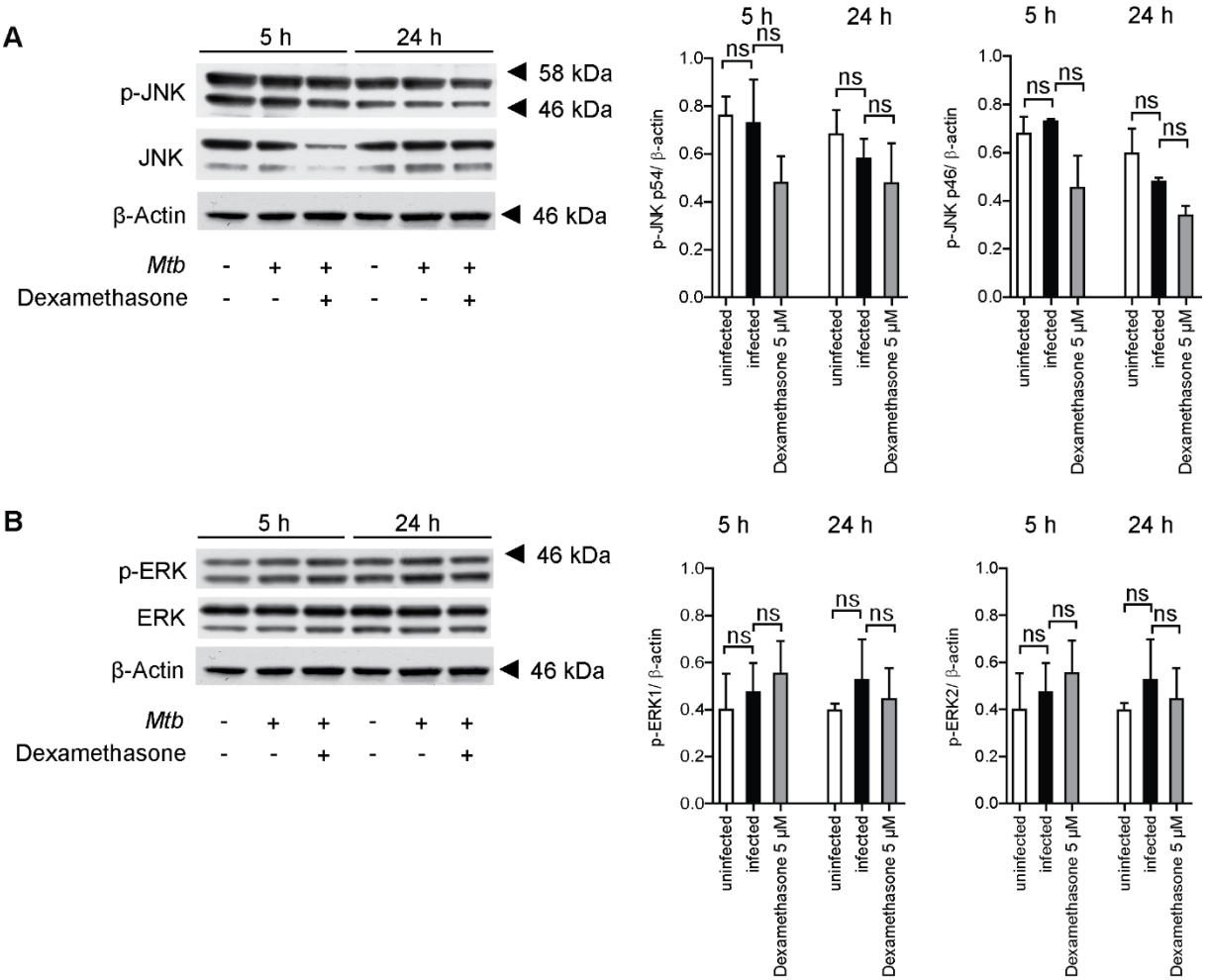

Figure 9. Infection with *Mtb* does not lead to phosphorylation of c-Jun N-terminal kinase (JNK) or extracellular signal-regulated kinase (ERK). Infection of J774.2 Mϕ with *Mtb* (MOI 5) does not induce JNK (**A**) or ERK (**B**) activation. Whole cell lysates were obtained at indicated timepoints from J774.2 Mϕ in the presence or absence of 5 µM dexamethasone and equal amounts of protein were subjected to Western blot analysis to determine the levels of phosphorylated and total JNK and ERK. β-Actin was used as a loading control. Data from two independent experiments (**A**, **B**) are shown as mean ± SEM. Analysis was done using One-Way ANOVA (ns, not significant).

Subsequently, different p38 MAPK inhibitors were tested for their cytoprotective effect in *Mtb*-infected cells to determine whether direct p38 MAPK inhibition is as protective as corticosteroid treatment. These inhibitors include doramapimod (BIRB796) and BMS-582949. The inhibitor doramapimod was as efficient in promoting host cell survival as dexamethasone in *Mtb*-infected human Mϕ (**Fig. 10A**). However, BMS-582949 was not able to prevent host cell death (data not shown). To decipher the divergent data regarding different p38 MAPK inhibitors, the phosphorylation status of p38 MAPK was quantified. While doramapimod fully suppressed p38 MAPK phosphorylation 24 and 48 h after infection, BMS-582949 did not achieve the same effect (**Fig. 10B**). Hence, doramapimod was used as an exclusive p38 MAPK inhibitor in the following experiments. To further verify the role of p38 MAPK in TB infection, p38 MAPK expression was knocked down in J774A.1 Mϕ (p38KD) with selective small interfering RNA (siRNA; **Fig. 10C**). The downregulation of p38 MAPK lead to increased J774A.1 Mϕ survival (**Fig. 10D**). Although, both dexamethasone and doramapimod are potent inhibitors of host cell death, they have no impact on the intracellular bacterial load in J774.2 Mϕ (**Fig. 10E**). These data show that dexamethasone and doramapimod only impact on the host cell and not on the bacterium. In summary, both compounds mediate host cell survival by the inhibition of p38 MAPK activation.

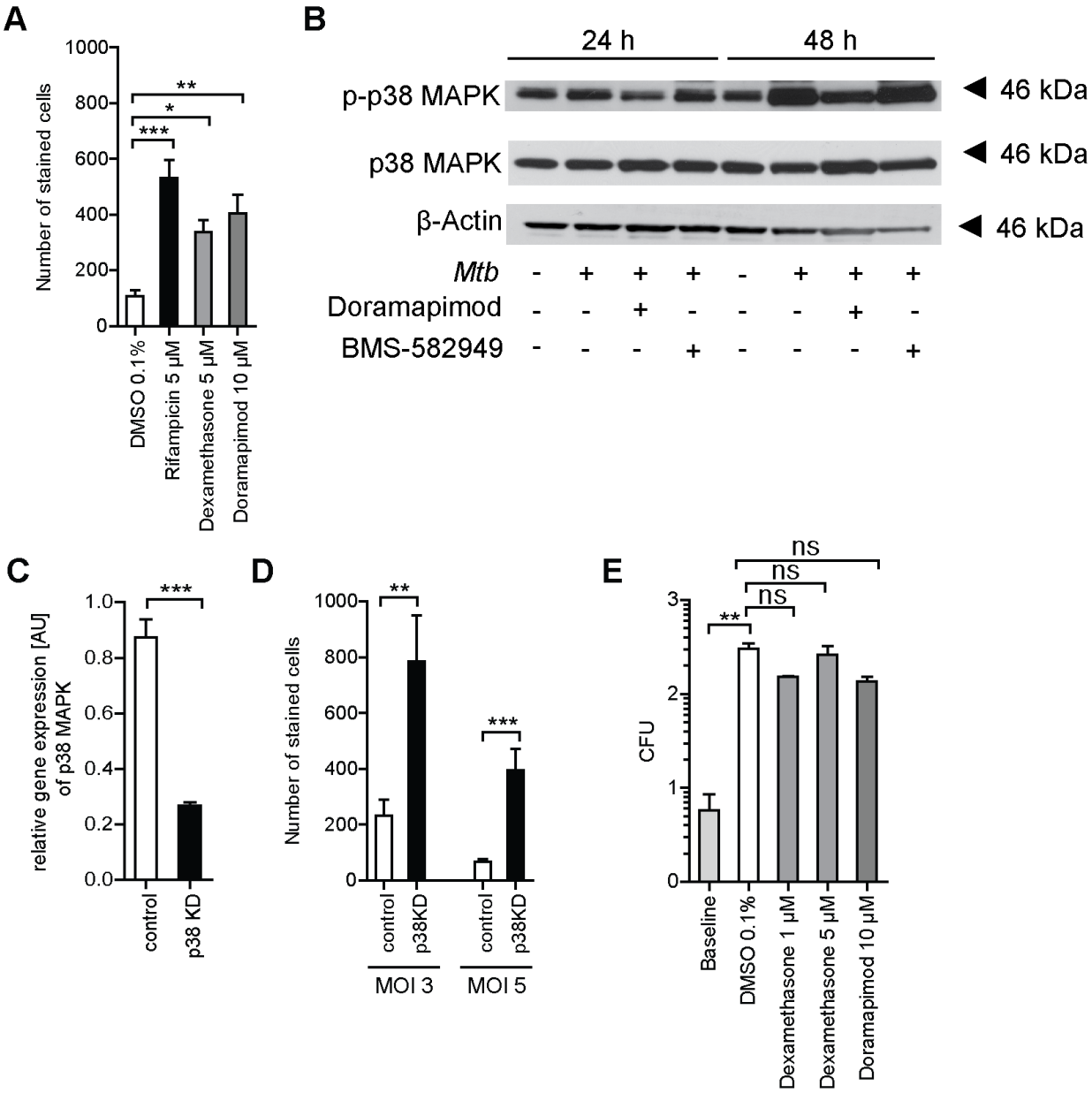

Figure 10. Inhibition of p38 MAPK by doramapimod increases host cell survival. Cytoprotective effect of the p38 MAPK inhibitor doramapimod (10 µM) in *Mtb*-infected human Mϕ (MOI 1). Mϕ were stained with DAPI and the number of living cells was determined 48 h post infection (**A**). Phosphorylation status of p38 MAPK was detected by Western blot in MRC-5 lung fibroblasts infected with *Mtb* (MOI 10) and treated with the p38 MAPK inhibitors BMS-582949 (10 µM) or doramapimod (**B**). Expression of p38 MAPK in J774A.1 Mϕ and J774A.1 p38 MAPK knockdown (KD) Mϕ analyzed by qRT-PCR (**C**). Survival of *Mtb*-infected p38 MAPK KD J774A.1 Mϕ (MOI 3 and 5) 48 h after infection (**D**). Dexamethasone or doramapimod treatment has no effect on intracellular bacterial burden. Determination of the colony-forming units (CFU) of *Mtb*-infected J774.2 Mϕ treated with dexamethasone (1 or 5 µM) or doramapimod (**E**). Data from three independent experiments with multiple replicates are shown (**A**, **D**); representative data of two experiments are shown in **B** and **E**; data from one experiment with multiple replicates are shown in **C**. Data are expressed as mean ± SEM. Analysis was done using One-Way ANOVA (ns, not significant; *, p≤ 0.05; **, p≤ 0.01; ***, p≤ 0.001).

5.3 Apoptosis in *Mtb*-mediated host cell death

p38 MAPK plays a crucial role in different forms of cell death (Gräb and Rybniker, 2019). To decipher the pathway induced by *Mtb*, several cell death pathways were dissected. One of the major forms of cell death p38 MAPK has been associated with is apoptosis (Aguilo et al., 2014).

First, the activation of caspase 3, one of the executioner caspases, was analyzed by detecting the cleaved form of caspase 3 by Western blot. The infection of J774.2 Mϕ with *Mtb* triggered a slight proteolytic cleavage of caspase 3 at several time points, which was inhibited upon dexamethasone treatment (**Fig. 11A**). This could be confirmed in a more sensitive caspase 3 and 7 activity assay in *Mtb*-infected MRC-5 lung fibroblasts, using a luminescent probe (**Fig. 11B**). Though, not significant, dexamethasone and doramapimod were able to reduce caspase activation. Therefore, I assume that *Mtb* potentially triggers apoptosis in phagocytes. To confirm this, cells were treated with the pan-caspase inhibitor Z-VAD-FMK, which fully abrogates caspase activation (**Fig. 11B**). In contrast, neither MRC-5 lung fibroblasts (**Fig. 11C**) nor human Mϕ (**Fig. 11D**) were protected from *Mtb*-induced host cell death upon Z-VAD-FMK treatment. These data indicate that although apoptosis might be activated in TB-infected cells, it is a secondary event, rather than the major form of cell death induced upon *Mtb* infection.

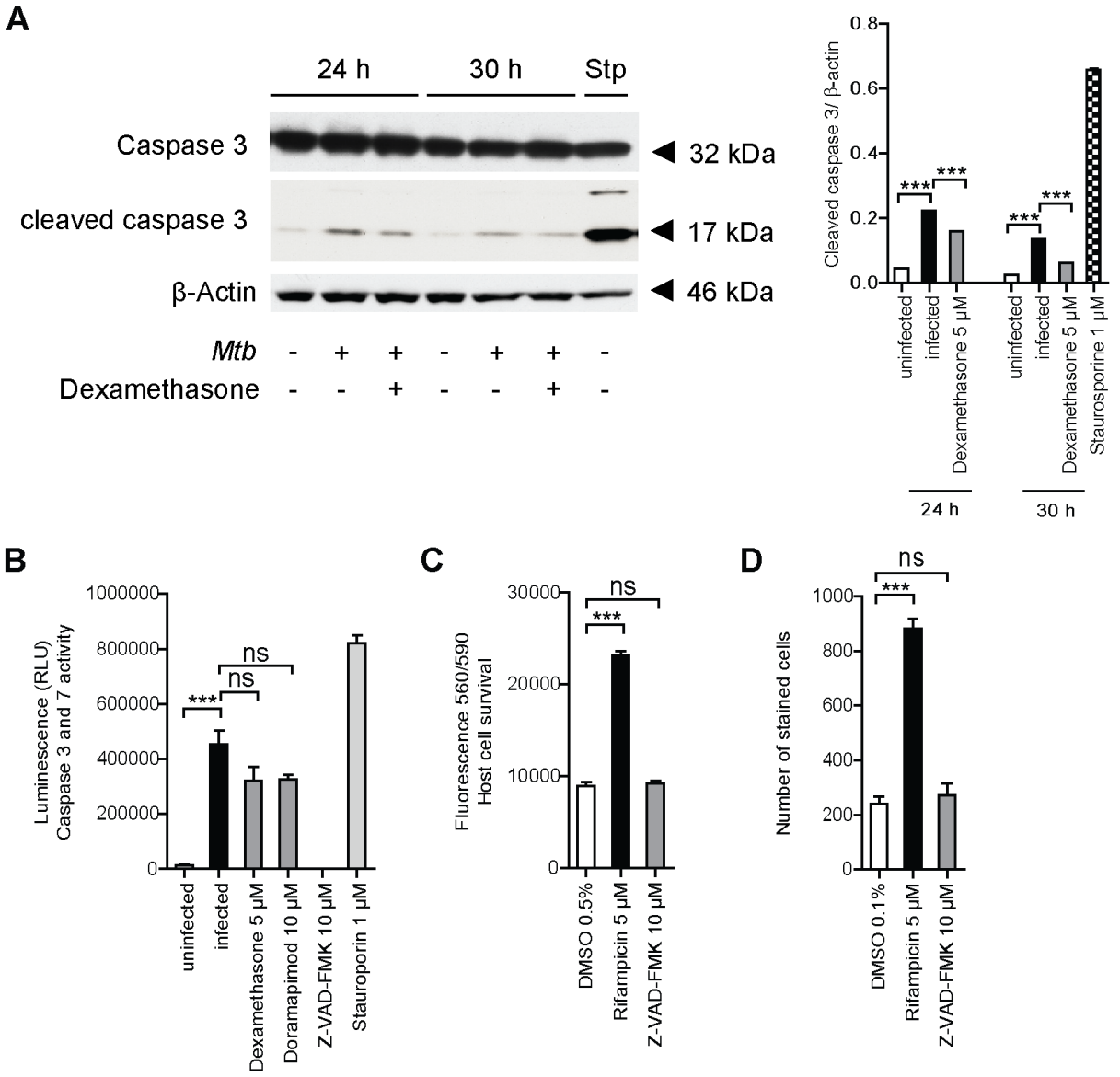

Figure 11. *Mtb*-induced host cell death is independent of caspase 3 and 7 activation. Western blot analysis of cleaved caspase 3 in *Mtb*-infected J774.2 Mϕ (MOI 5) in the presence or absence of dexamethasone (5 µM). β-Actin was used as a loading control and staurosporine (1 µM) as a positive control (**A**).Caspase 3 and 7 activity was assessed in *Mtb*-infected MRC-5 lung fibroblasts (MOI 10) treated with dexamethasone (5 µM), doramapimod (10 µM) or the pan-caspase inhibitor Z-VAD-FMK (10 µM) 48 h post infection using a luminescent probe. Uninfected and staurosporine (1 µM) treated cells were used as controls (**B**). Effect of caspase 3 and 7 inhibition by Z-VAD-FMK on survival of infected MRC-5 lung fibroblasts (**C**) and human Mϕ (**D**). Viable fibroblasts were detected using Prestoblue™ and Mϕ were quantified by DAPI staining. Representative data from at least two experiments with multiple replicates are shown. Results are expressed as mean ± SEM. Analysis was done using One-Way ANOVA (ns, not significant; ***, p≤ 0.001).

5.4 Induction of necrosis in *Mtb*-infected cells

5.4.1 *Mtb* infection triggers the secretion of necrotic markers

Based on my results indicating that apoptosis is not the major cell death pathway, I want to further dissect other potential pathways involved in TB-mediated host cell death. In recent years, it has been suggested that virulent *Mtb* strains rather induce necrotic host cell death. Necrosis is accompanied by hyperinflammation and allows the cell to cell spread as well as a dissemination of the disease (Zhao et al., 2017). There are several markers to detect necrosis of infected cells, including LDH and HMGB1. Following *Mtb* infection of MRC-5 lung fibroblasts (**Fig. 12A**) and human Mϕ (**Fig. 12B**) large amounts of LDH were found in the supernatant of the infected cells compared to rifampicin treated controls. Moreover, infected MRC-5 fibroblasts showed enhanced secretion of the chromatin protein HMGB1 (**Fig. 12C**). The treatment of *Mtb*-infected cells with doramapimod (**Fig. 12**) or dexamethasone (**Fig. 12C**) blocked the release of both LDH and HMGB1 and thereby links p38 MAPK activation to necrotic cell death.

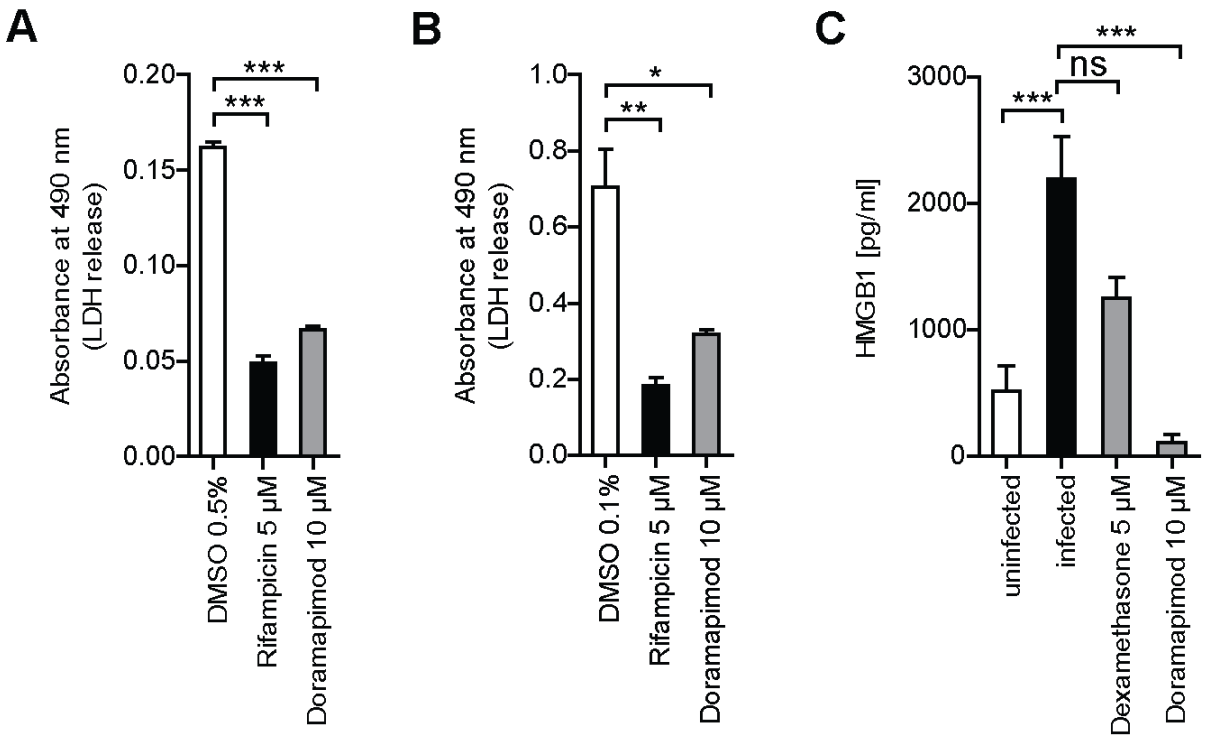

Figure 12. *Mtb* promotes necrotic host cell death. Quantification of lactate dehydrogenase (LDH) in the supernatant of MRC-5 lung fibroblasts (**A**) 72 h post infection and human Mϕ 48 h post infection in the presence or absence of doramapimod (10 µM; **B**). Dexamethasone (5 µM) and doramapimod (10 µM) reduce the release of the necrosis marker High-Mobility-Group-Protein B1 (HMGB1) in *Mtb*-infected MRC-5 lung fibroblasts measured by enzyme-linked immunosorbent assay (ELISA; **C**). Representative data from two experiments with multiple replicates are shown in **A** and **B**. Data pooled from eight independent experiments are shown

in **C**. Results are expressed as mean ± SEM and analysis was done using One-Way ANOVA (ns, not significant; *, p≤ 0.05; **, p≤ 0.01; ***, p≤ 0.001).

5.4.2 Necroptosis is not relevant in TB infection

Necrosis is mainly known as an uncontrolled form of cell death. However, regulated necrosis has become of high interest in recent years, in particular necroptosis. Necroptosis is a TNF-mediated cell death pathway, which results in the formation of the necrosome, a complex consisting of TNFR, RIPK1, RIPK3 and MLKL (Vandenabeele et al., 2010). The role of necroptosis in connection to TB-induced host cell death will be evaluated since TNF is a major player in *Mtb* pathogenesis and corticosteroids inhibit the release of the pro-inflammatory cytokine. Therefore, RIPK1, TNF and TNRF were chemically inhibited in *Mtb*-infected human MΦ. Neither the inhibition of RIPK1 by necrostatin-1 or necrostatin-5 (Nec-1 and Nec-5) nor the inhibition of TNF by thalidomide, etanercept or adalimumab was cytoprotective (**Fig. 13A**). Additionally, the knockout (KO) of MLKL (**Fig. 13B**) or TNFR1 (**Fig. 13C**) failed to promote host cell survival in mouse BMDM. Necroptosis can only take place if caspase 8 is inhibited (Vandenabeele et al., 2010). To create a pro-necroptotic environment, human MΦ were treated with the pan-caspase inhibitor Z-VAD-FMK in addition to Nec-1. However, the co-treatment failed to prevent *Mtb*-induced host cell death. Collectively, the data show that corticosteroid treatment and p38 MAPK inhibition is independent of necroptosis.

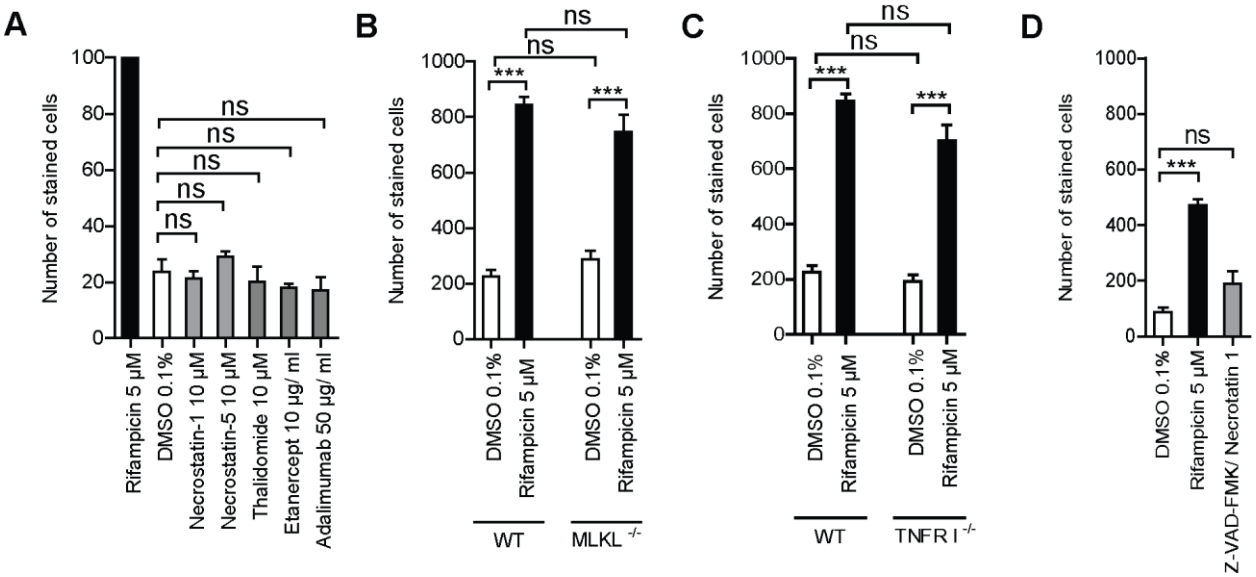

Figure 13. *Mtb* triggers receptor-interacting serine/threonine-protein kinase 1 (RIPK1) independent necrotic cell death. Effect of necrostatin (Nec; 10 µM), etanercept (10 µg/ ml), adalimumab (50 µg/ ml) and thalidomide (10 µM) in *Mtb*-infected human Mϕ (MOI 1). Cell survival was quantified by DAPI staining 48 h after infection. The control rifampicin was set to 100 percent (**A**). Bone marrow-derived Mϕ (BMDM) from WT and MLKL$^{-/-}$ (**B**) or TNFR$^{-/-}$ (**C**) mice were infected with *Mtb* (MOI 10) and cell survival was assessed 48 h after infection using DAPI staining. *Mtb*-infected human Mϕ (MOI 1) were treated with Z-VAD-FMK (10 µM) and Nec-1 (10 µM) and viable cells were detected 48 h post infection using DAPI staining (**D**). Data from at least two experiments with multiple replicates are shown. Results are expressed as mean ± SEM. Analysis was done using One-Way ANOVA (ns, not significant; ***, p≤ 0.001).

5.5 Opening of the mitochondrial permeability transition pore results in host cell death

After excluding necroptosis as a mechanism of *Mtb*-induced and p38 MAPK-mediated host cell death, alternative pathways of cell death were analyzed. The original high-throughput screen of FDA-approved drugs also identified the CypD and calcineurin inhibitor cyclosporin A (CsA) as a potent hit compound. Intriguingly, CypD is a regulator of the mPTP (Vanden Berghe et al., 2014). The mPTP plays a key role in mitochondria-driven necrosis and mitochondrial damage (Zhao et al., 2017). Thus, the role of the mPTP in *Mtb*-induced host cell death was studied in more detail.

Treatment of *Mtb*-infected MRC-5 fibroblasts with CsA was as cytoprotective as the treatment with dexamethasone or doramapimod. Since CsA is an inhibitor of CypD and calcineurin, a specific calcineurin inhibitor (FK-506) was also used, to determine which effect is responsible for host cell survival. FK-506 treatment had no effect on MRC-5 fibroblasts infected with *Mtb*, thereby indicating that MPT is necessary for *Mtb*-driven host cell death (**Fig. 14A**). Opening of the mPTP disrupts the ΔΨm and subsequently leads to a loss of mitochondrial function and integrity (Biasutto et al., 2016). A change in the ΔΨm can be detected with TMRM, a reporter-dye only visible in cells with intact mitochondrial membranes. The dye accumulated in uninfected human Mϕ, while it was nearly invisible in *Mtb*-infected Mϕ (**Fig. 14B**). Furthermore, the mPTP regulator CypD was analyzed by immunoblots. Treatment of *Mtb*-infected MRC-5 lung fibroblasts with CsA lead to an accumulation of CypD in the cytosol and a decrease in mitochondrial CypD (**Fig. 14C**). Since dexamethasone and doramapimod prevent necrotic host cell death, it was assumed that they also decrease mitochondrial CypD levels. However, both compounds had no effect on CypD expression, suggesting that they have a mechanism independent of CsA (**Fig. 14C**). Furthermore, a significant decrease in intracellular ATP was observed after *Mtb* infection in J774.2 Mϕ (**Fig. 14D**) and MRC-

5 lung fibroblasts (**Fig. 14E**), which could be reversed with dexamethasone or doramapimod treatment. Hence, the data show that *Mtb* triggers host cell necrosis by opening of the mPTP and disrupting the ΔΨm, resulting in a loss of intracellular ATP.

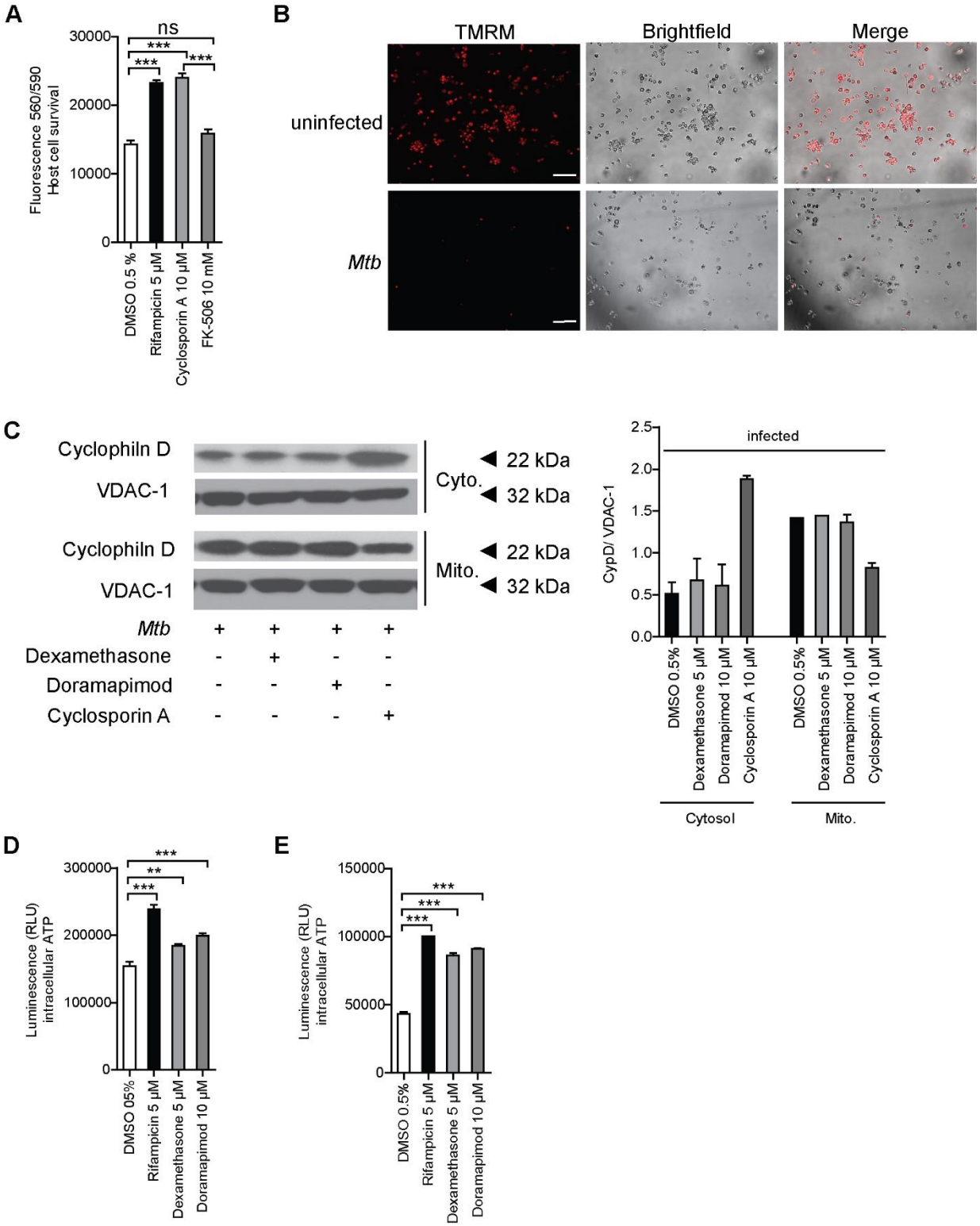

Figure 14. p38 MAPK dependent necrosis opens the mitochondrial permeability transition pore (mPTP). Cytoprotective effect of cyclosporin A (CsA; 10 µM) in *Mtb*-infected MRC-5 lung fibroblasts (MOI 10). Viability was determined 72 h after infection using the FSA

(**A**). Mitochondrial membrane potential was quantified using tetramethylrhodamine-methyl ester (TMRM) staining in *Mtb*-infected human Mϕ (MOI 1) 48 h post infection (scale bar: 100 µm; **B**). Western blot analysis of cytosolic and mitochondrial cyclophilin D (CypD) 5 h after *Mtb* infection in MRC-5 lung fibroblasts (MOI 10), treated with dexamethasone (5 µM), doramapimod (10 µM) or CsA (10 µM). Voltage-dependent anion-selective channel 1 (VDAC-1) was used as a loading control (**C**). Intracellular ATP levels in *Mtb*-infected J774.2 Mϕ (**D**) and MRC-5 lung fibroblasts (**E**) 24 h and 48 h after infection, respectively. Cells were treated with dexamethasone (5 µM) or doramapimod (10 µM). Data from at least two experiments with multiple replicates are shown in **A**, **D** and **E**. Representative data from 2 experiments are shown in **B** and **C**. Results are expressed as mean ± SEM and experiments were analyzed using One-Way ANOVA (ns, not significant; **, p≤ 0.01; ***, p≤ 0.001).

5.5.1 Mitochondrial damage is crucial for *Mtb*-induced host cell death

Opening of the mPTP is a result of mitochondrial damage and leads to a high influx of ions, which alters the ΔΨm and results in decreased ATP production and oxidative phosphorylation. Two indicators of mitochondrial damage are mitochondrial ROS and mitochondrial Ca^{2+} accumulation (Zorov et al., 2014). ROS are generated by the respiratory electron transport chain (ETC) in the mitochondria during energy production and can diffuse into the cytosol. Several intracellular bacteria, such as *Listeria monocytogenes*, are able to induce ROS production in the mitochondria (Stavru et al., 2011; West et al., 2011). ROS production in the mitochondrial matrix can be quantified by MitoSOX Red (Mukhopadhyay et al., 2007). Infection of MRC-5 lung fibroblasts with *Mtb* triggered ROS production in mitochondria (**Fig. 15A**). While scavenging of mitochondrial ROS by MitoTEMPO, a mitochondrial matrix-targeting form of the superoxide scavenger TEMPO, lead to reduced ROS generation (**Fig. 15A**) and increased host cell survival in *Mtb*-infected human Mϕ (**Fig. 15B**). Notably, treatment of MRC-5 lung fibroblasts with dexamethasone, doramapimod or CsA also decreased ROS production after *Mtb* infection (**Fig. 15A**).

Another indicator of mitochondrial damage is Ca^{2+}, which has specific binding sites in the IMM. Accumulation of Ca^{2+} in the mitochondria is mediated by the mitochondrial calcium uniporter (MCU), a transmembrane protein that allows the migration of Ca^{2+} from the cytosol into the mitochondria. The MCU complex consists of the MCU, the mitochondrial calcium uptake 1 (MICU1) and MICU2 (Tajeddine, 2016). The MCU can be specifically blocked by Ru-360, a dinuclear ruthenium ammine complex and analog of ruthenium red, which prevents the mitochondrial uptake of Ca^{2+}. *Mtb* infection of J774.2 Mϕ lead to increased Ca^{2+} levels and the treatment with Ru-360 reversed this effect (**Fig. 15C**). To study whether inhibition of the MCU influences host cell survival,

human Mϕ were treated with Ru-360 and cell survival was assessed 48 h post *Mtb* infection. The inhibition of the MCU was cytoprotective (**Fig. 15D**). Interestingly, the simultaneous inhibition of mitochondrial ROS and Ca^{2+} was even more protective than the monotreatment with MitoTEMPO or Ru-360. Thus, the infection with *Mtb* causes mitochondrial damage inside the host cell and results in increased mitochondrial ROS generation and mitochondrial Ca^{2+} uptake.

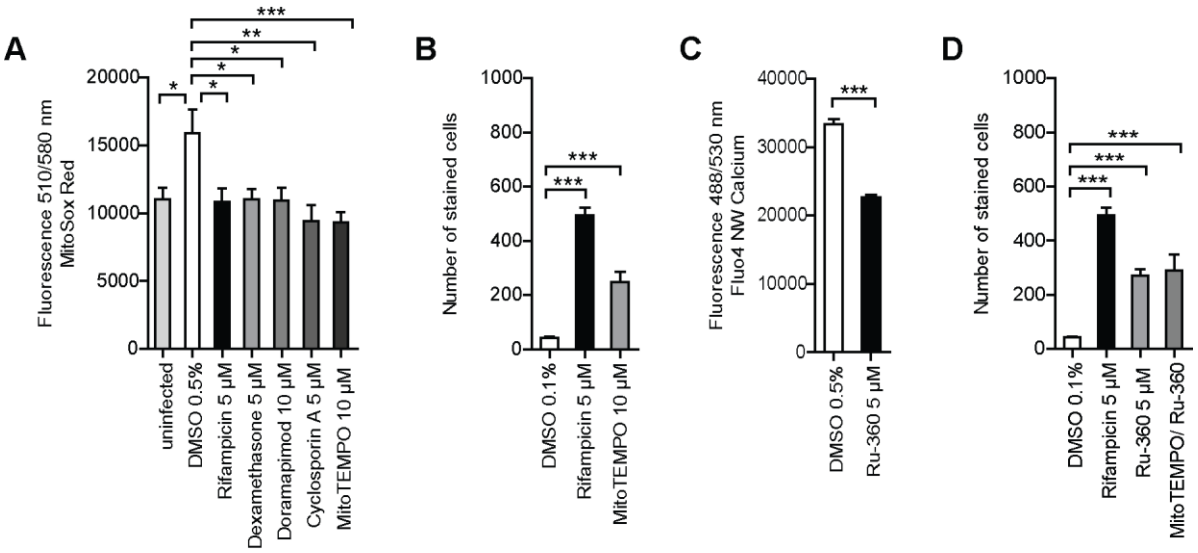

Figure 15. Infection with *Mtb* increases the release of mitochondrial reactive oxygen species (ROS). Mitochondrial ROS was quantified in *Mtb*-infected MRC-5 lung fibroblasts (MOI 10) using MitoSOX Red 24 h after infection (**A**). Viability of *Mtb*-infected human Mϕ (MOI 1) in the presence or absence of MitoTEMPO (10 µM). Mϕ were stained with DAPI and the number of surviving cells was determined 48 h post infection (**B**). Intracellular calcium (Ca^{2+}) concentrations were measured 24 h after infection with *Mtb* (MOI 5) in J774.2 Mϕ in the presence or absence of Ru-360 (**C**). Protective effect of the mitochondrial calcium uniporter (MCU) inhibitor Ru-360 in human Mϕ infected with *Mtb*. Viability was assessed 48 h after infection using DAPI staining (**D**). Representative data from two experiments with multiple replicates are shown. Results are expressed as mean ± SEM. Analysis was done using One-Way ANOVA (A, B, D) or unpaired t test (C) (*, p≤ 0.05; **, p≤ 0.01; ***, p≤ 0.001).

5.5.2 Hexokinase II and p53 are potential regulators of the mPTP

One of the potential regulators of mPTP opening is the OMM bound enzyme hexokinase II (HKII), an antagonist of ROS-induced mPTP opening. Although HKII is not directly involved in mPTP regulation, the accumulation of HKII at the mitochondria can prevent mPTP opening (Biasutto et al., 2016). Early in the infection, HKII was up-regulated in *Mtb*-infected J774.2 Mϕ compared to uninfected cells (**Fig. 16A**). However, at a later time point of infection (24h), HKII levels were reduced at the mitochondria of infected J774.2 Mϕ, suggesting a dissociation of HKII into the cytosol (**Fig. 16B**). Interestingly, treatment of the Mϕ with dexamethasone or doramapimod

resulted in prolonged accumulation of HKII at the mitochondria. While the treatment of TB-infected Mϕ with the p38 MAPK inhibitor BMS-582949 had no effect on HKII expression.

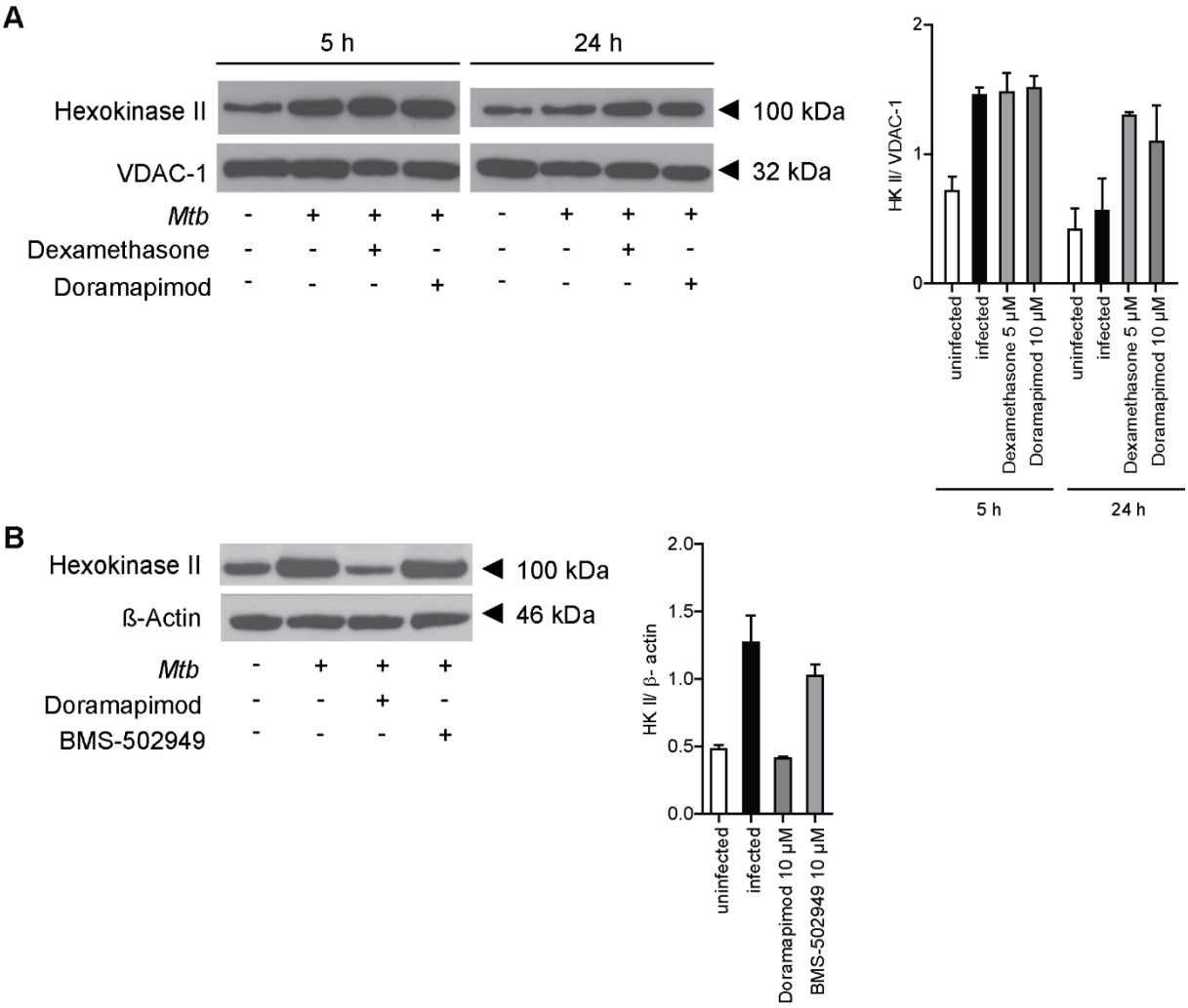

Figure 16. *Mtb* triggers mPTP opening by dissociation of hexokinase II (HKII) from the mitochondrium. Quantification of mitochondrial HKII following *Mtb* infection (MOI 5) at indicated time points. J774.2 Mϕ were treated with dexamethasone (5 µM) or doramapimod (10 µM) and subjected to Western blot analysis. VDAC-1 was used as a loading control (**A**). Quantification of HKII expression in whole cell lysates of *Mtb*-infected MRC-5 lung fibroblasts (MOI 10) 48 h post infection. Lysates were obtained from untreated cells as well as from cells treated with the p38 MAPK inhibitors doramapimod (10 µM) or BMS-582949 (10 µM). HKII was quantified by Western blot analysis using β-Actin as a loading control. Representative data from two experiments are shown. Results are expressed as mean ± SEM.

Additionally, HKII expression was significantly increased in *Mtb*-infected MRC-5 lung fibroblasts (**Fig. 17A**). HKII can be inhibited by 3-bromopyruvate (3BP). Co-treatment of J774.2 Mϕ with dexamethasone and 3BP or doramapimod and 3BP reduced the protective effect of dexamethasone and doramapimod, detected by decreased levels

of intracellular ATP (**Fig. 17B**). Therefore, HKII is not only important in glucose phosphorylation and ATP generation (Biasutto et al., 2016), but also in p38 MAPK-mediated host cell death.

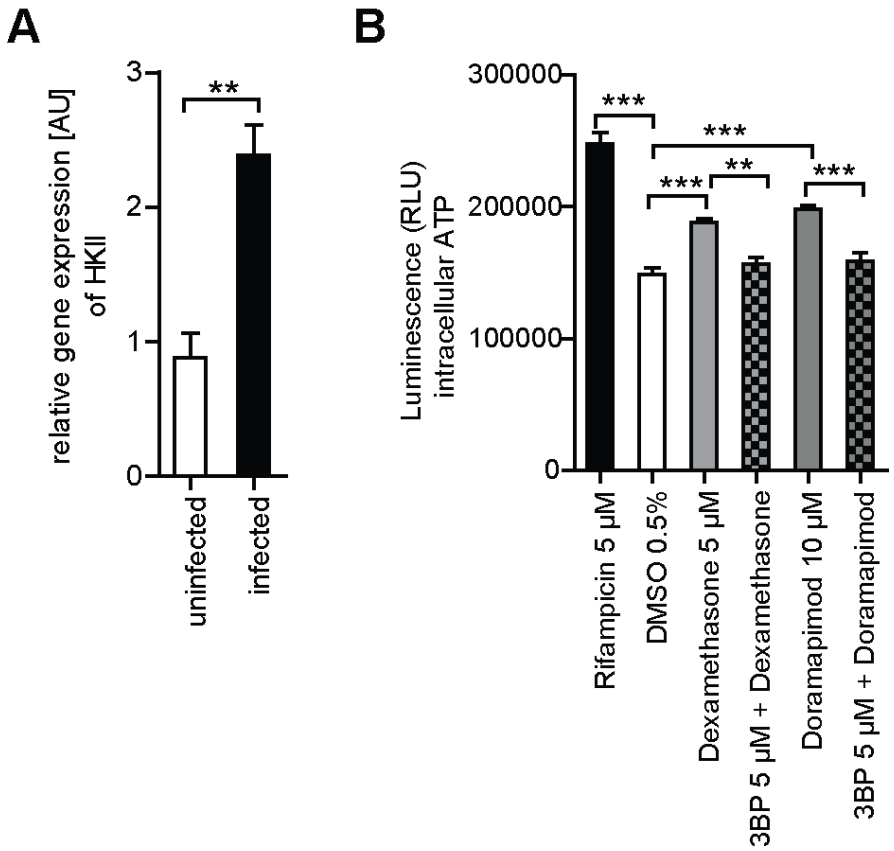

Figure 17. HKII as a regulator of mPTP opening. Expression of hexokinase II (HKII) in MRC-5 lung fibroblasts 24 h after infection (MOI 10) measured by qRT-PCR (**A**). Intracellular ATP levels in *Mtb*-infected J774.2 Mϕ in the presence or absence of dexamethasone (5 µM), doramapimod (10 µM) and bromopyruvic acid (3BP; 5 µM) following 24 h of infection. (**B**). Representative data from at least two experiments with multiple replicates are shown. Results are expressed as mean ± SEM and experiments were analyzed using unpaired t test (**A**) and One-Way ANOVA (**B**) (**, p≤ 0.01; ***, p≤ 0.001).

Another potential regulator of mPTP opening is the tumor protein p53, which can either directly interact with the mitochondrial membrane or modulate the interaction of HKII with the mPTP (Marchenko and Moll, 2014). Additionally, the transcription factor p53 is a target of p38 MAPK. Accumulation of p53 in the nucleus upon cell stress, initiates host cell death by activation of pro-apoptotic and suppression of anti-apoptotic Bcl-2 family proteins. Thereafter, pro-apoptotic proteins migrate to the mitochondria and cause permeabilization of the OMM, resulting in mPTP opening (Perfettini et al., 2005;

Stramucci et al., 2018). p53 might be another protein involved in *Mtb*-mediated host cell death and a potential link between p38 MAPK and the mPTP.

Mtb-infected human Mϕ were treated with the p53 inhibitor pifithrin-α, which resulted in increased viability of the cells (**Fig. 18A**). To further clarify the role of p53 in *Mtb*-mediated cell death, the expression of p53 in J774A.1 Mϕ was downregulated (p53 KD) by siRNA. Suppression of p53 expression significantly increased the viability of J774A.1 Mϕ post infection (**Fig. 18B**). These data show that the role of p53 in *Mtb*-driven host cell death is of similar importance as that of p38 MAPK.

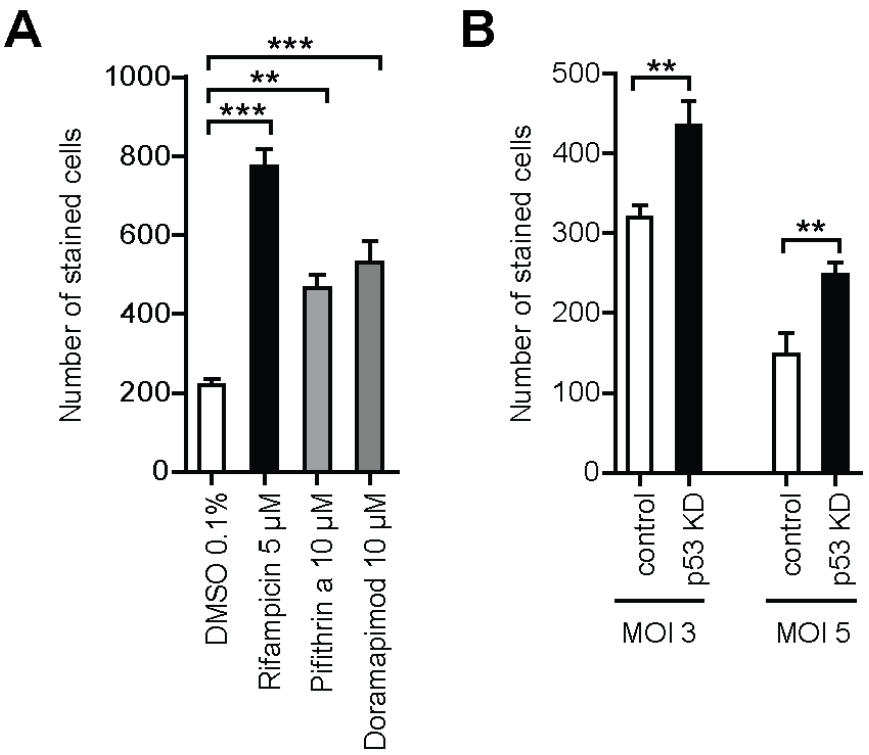

Figure 18. Chemical inhibition and knockdown of p53 is cytoprotective. Viability of *Mtb*-infected human Mϕ (MOI 1) in the presence or absence of the p53 inhibitor pifithrin α (10 µM; **A**) and viability of J774A.1 p53 KD Mϕ (**B**) quantified by DAPI staining 48 h post infection. Data were obtained from three (**A**) or two (**B**) experiments with multiple replicates and are shown as mean ± SEM. Analysis was done using One-Way ANOVA (*, p≤ 0.05; **, p≤ 0.01; ***, p≤ 0.001).

5.5.3 Overexpression of Bcl-2 prevents mitochondrial damage

The Bcl-2 family of proteins is mainly associated with apoptosis and consists of pro- and anti-apoptotic proteins. Pro-apoptotic proteins include, Bak and Bax, and anti-apoptotic proteins include Bcl-2 and Bcl-xL. The pro-apoptotic Bak and Bax can cause MOMP by oligomerizing and the formation of pores at the OMM. Hence, the anti-

apoptotic proteins are responsible for the inhibition of pro-apoptotic proteins to prevent MOMP (Lindsay et al., 2011). An overexpression of the anti-apoptotic protein Bcl-2 should thereby inhibit cell death by directly suppressing pro-apoptotic Bcl-2 proteins. Moreover, it has been reported that Bcl-2 overexpression reduces p53 accumulation and therefore also indirectly inhibits pro-apoptotic Bcl-2 proteins (Marchenko and Moll, 2014).

Since *Mtb* induces host cell death in a p53 and MOMP dependent manner, the overexpression of Bcl-2 should promote host cell survival. To verify this, mouse BMDM overexpressing Bcl-2 upon stimulation with Cre were infected with *Mtb*. Figure **19A** depicts the increased survival rate of Bcl-2 overexpressing BMDM compared to the unstimulated control (w/o Cre). To definitely clarify whether the increased survival rate of the mouse BMDM was due to reduced mitochondrial damage and not decreased phagocytosis of the bacteria, the bacterial load was determined. There was no significant difference in the intracellular mycobacterial load of mouse BMDM with Cre treatment compared to the untreated control (**Fig. 19B**). This illustrates that neither phagocytosis nor bacterial replication is impaired upon Bcl-2 overexpression. Furthermore, the overexpression of Bcl-2 is especially important in the protection of mitochondria from MOMP. Changes in the $\Delta\Psi m$ were detected by TMRM. Mouse BMDM without Cre failed to maintain the membrane potential and thereby showed a loss of TMRM. Simultaneously, mouse BMDM with Cre displayed a high accumulation of TMRM in the mitochondria, indicating that Bcl-2 overexpression suppressed MOMP (**Fig. 19C**).

Thus, the protection of mitochondria by Bcl-2 overexpression prevents *Mtb*-mediated host cell death as efficiently as the inhibition of CypD by CsA or the suppression of p38 MAPK by dexamethasone or doramapimod.

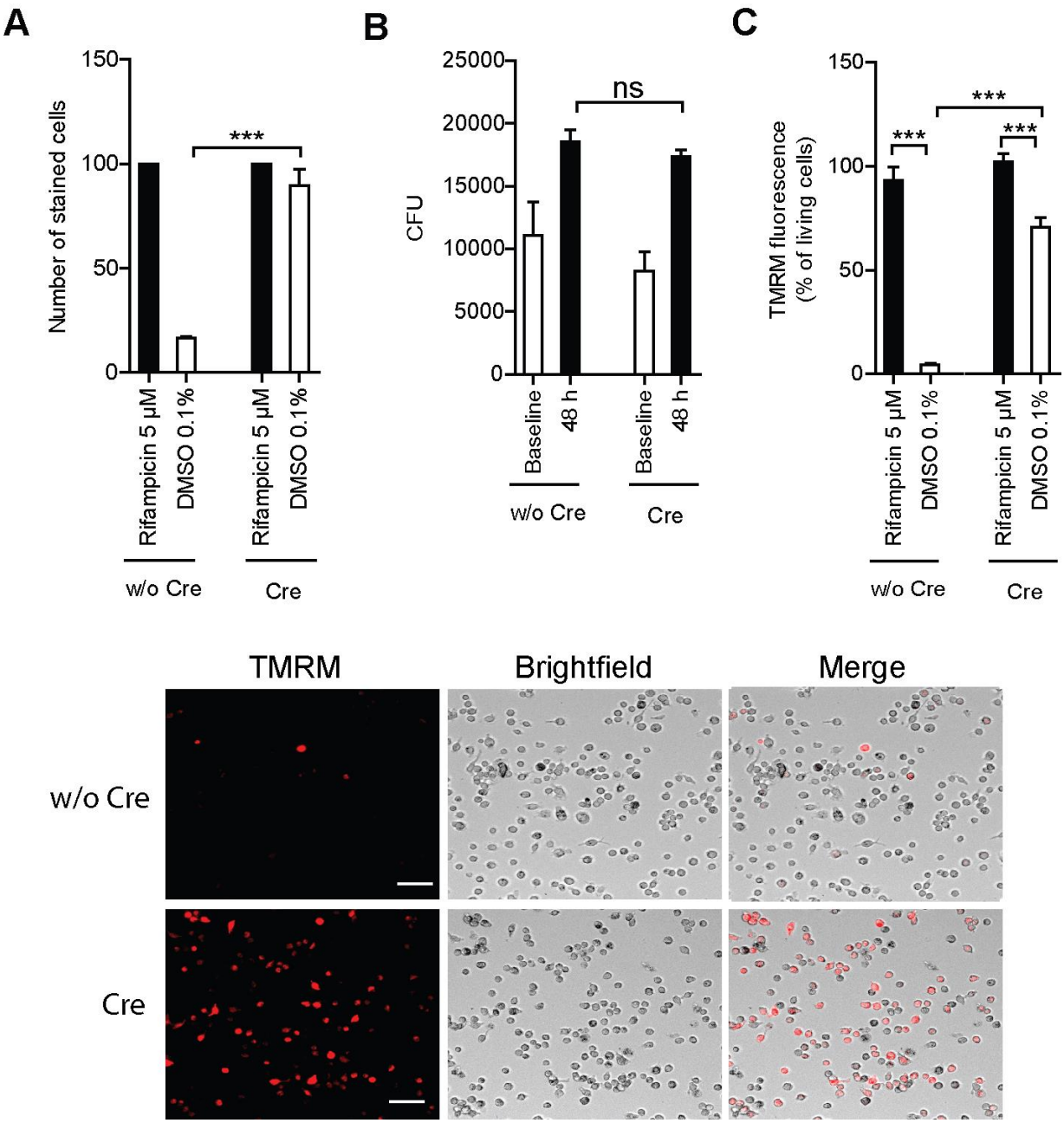

Figure 19. Overexpression of B cell lymphoma 2 (Bcl-2) promotes host cell survival in *Mtb*-infected BMDM. BMDM from Bcl-2 overexpressing mice were treated with Cre to induce Bcl-2 overexpression *ex vivo*. Viability of BMDM 24 h after infection (MOI 3) was quantified using DAPI staining (**A**). Determination of the CFU of *Mtb*-infected BMDM treated with or without (w/o) Cre prior to infection (**B**). Fluorescence microscopy of Bcl-2 BMDM infected with *Mtb* (MOI 3) and stained with TMRM 24 h post infection (scale bar: 100 µm). Images are representative of two independent experiments (**C**). Representative data from at least two experiments with multiple replicates are shown. Results are expressed as mean ± SEM. Analysis was done using One-Way ANOVA (ns, not significant; **, p≤ 0.01; ***, p≤ 0.001).

5.6 Model: A p38 MAPK dependent pathway is responsible for necrotic cell death induced by *Mtb*

Based on the data generated in this thesis, the following model for *Mtb*-mediated necrotic host cell death is proposed (**Fig. 20**). The phagocytosis of *Mtb* by Mϕ triggers the phosphorylation and activation of p38 MAPK. Thereafter, p53 promotes the dissociation of mitochondrial HKII and allows the opening of the mPTP induced by increasing levels of mitochondrial ROS and Ca^{2+}. The opening of the mPTP leads to MPT and depletion of intracellular ATP. Finally, the cell enters necrosis, releasing the nuclear protein HMGB1 into the extracellular milieu. The pathway can be prevented using different inhibitors. The corticosteroid dexamethasone and the GR agonist BI653048 activate MKP-1 to indirectly deactivate p38 MAPK. Similarly, p38 MAPK can be directly inhibited by the p38 MAPK inhibitor doramapimod. The opening of the mPTP can be prevented by two different mechanisms. Either by chemical inhibition with CsA, an inhibitor of the mPTP regulator CypD, or by overexpression of Bcl-2.

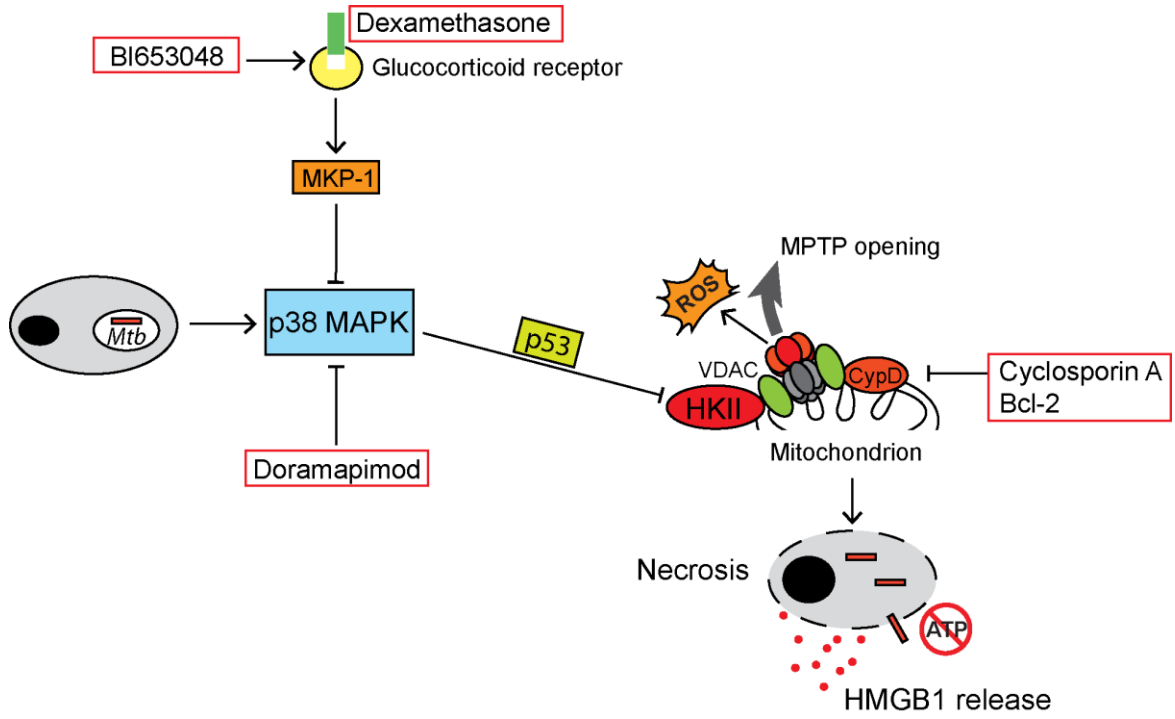

Figure 20. Model depicting *Mtb*-induced host cell death. Following phagocytosis of *Mtb*, p38 MAPK is phosphorylated and mediates the dissociation of HKII possibly via p53, resulting in mPTP opening. Necrosis of the host cell is characterized by an increase of mitochondrial ROS, a loss of intracellular ATP, and the release of HMGB1. Several compounds interfere with this pathway to promote host cell survival. Dexamethasone and BI653048 prevent p38 MAPK phosphorylation via the glucocorticoid receptor (GR) and MKP-1 activation, while doramapimod directly inhibits p38 MAPK. Further downstream cyclosporin A blocks mPTP opening by inhibition of cyclophillin D, a regulator of the mPTP. Opening of the mPTP can also be blocked by an overexpression of the protein Bcl-2 (adapted from (Gräb et al., 2019)).

6. Discussion

Mtb is responsible for the highest mortality among single infectious agents worldwide (Ferraris et al., 2018; Seddon et al., 2019). The rapid emergence and prevalence of drug resistant *Mtb* strains, especially in Asia and Eastern Europe, as well as the difficulties in identifying and developing new antibiotics has led to a global health crisis (Köser et al., 2015). In addition, the limited amounts of putative drug targets have become a challenge in TB drug discovery. These challenges highlight the need to not only develop alternative therapeutic approaches, like HDT, in addition to antibiotic treatment (Tsenova and Singhal, 2020), but also to intensify the development of novel and highly potent antibiotics. To find a suitable drug for a HDT, further understanding of the host-pathogen interaction is necessary. One of the major mechanisms of pathogenesis in TB infection is the induction of host cell death. However, so far host cell death has not been exploited as a drug target due to limited knowledge on the type of cell death promoted by *Mtb*. Thus, different forms of cell death have to be studied in *Mtb*-infected cells, in order to identify a potential target for the development of future therapies.

6.1 Identification and characterization of *Mtb*-mediated host cell death

Mtb is a highly adaptable pathogen that relies on the human as a host. After the infection, the bacteria are phagocytosed by immune cells and contained within the granuloma, which represents a close environment for *Mtb*. The induction of host cell death allows the escape from granulomas and dissemination of the disease, often resulting in hyperinflammation and tissue damage (Zhai et al., 2019). Therefore, host cell death could be exploited for therapeutic approaches. However, the type of cell death induced by *Mtb* remains a matter of debate. In order to overcome this lack of knowledge, I analyzed the different paths of cell death in phagocytes infected with virulent *Mtb*.

I first performed a high-throughput drug screening of FDA-approved drugs to identify a compound which inhibits *Mtb*-mediated host cell death. One of the compounds that prevented host cell death of non-professional and professional phagocytes, such as lung fibroblasts and Mϕ, was the corticosteroid dexamethasone. Dexamethasone exhibited no bactericidal or bacteriostatic effects, demonstrating that the drug only impacts on the host cell. This shows a so far undescribed effect of dexamethasone on

host cell death. Thus, I further characterized the protective effect of dexamethasone and analyzed the type of cell death triggered by virulent *Mtb* to identify new therapeutic targets.

My detailed analysis identified a cell death pathway involving p38 MAPK as a key regulator in *Mtb*-mediated host cell death. Corticosteroids can inhibit MAPK phosphorylation by activating MKP-1 (Abraham et al., 2006). Using chemical inhibition and knock-down cells, I identified a highly druggable pathway involving the glucocorticoid receptor, MKP-1, and MAPK. MAPK, including p38 MAPK, JNK and ERK play a major role in many cellular processes, such as proliferation and cell survival (Johnson and Lapadat, 2002). I demonstrated that only p38 MAPK was activated in response to the TB infection in phagocytes. This observation was confirmed by Rand et al., who showed in histopathology of human biopsies activation of p38 MAPK in Mϕ adjacent to granulomas (Rand et al., 2009). Hence, p38 MAPK activation represents a potential target for a HDT. Notably, p38 MAPK is of major interest in many inflammatory and autoimmune diseases, such as rheumatoid arthritis (RA). RA and the connection to p38 MAPK led to the development of several chemical p38 MAPK inhibitors (Arthur and Ley, 2013). I tested a series of commercially available p38 MAPK inhibitors in *Mtb*-infected phagocytes and was surprised to see distinctive activity of each inhibitor. While all p38 MAPK inhibitors are active in the nanomolar range, they differ in their ability to inhibit the four isotypes of p38 MAPK (Cuenda and Rousseau, 2007). I analyzed the activity of BMS-582949 and doramapimod among other p38 MAPK inhibitors. BMS-582949 specifically blocks the α isotype of p38 MAPK, which was not sufficient to inhibit *Mtb*-induced host cell death. In contrast, the broad-spectrum inhibitor doramapimod (Pargellis et al., 2002), was able to inhibit p38 MAPK phosphorylation even at later time points of infection. Since both dexamethasone and doramapimod interfere with the activation of p38 MAPK to increase host cell survival, I wanted to further confirm the role of p38 MAPK by using Mϕ with an introduced p38 MAPK knockdown. The data obtained during the experiments verified the importance of p38 MAPK phosphorylation in *Mtb*-induced host cell death. Therefore, p38 MAPK inhibitors may present a therapeutic approach with less adverse and off-target effects compared to corticosteroids (Strambu et al., 2019).

Since p38 MAPK is highly involved in different cell death pathways, such as apoptosis and necrosis, I continued to dissect the pathway downstream of p38 MAPK. Especially,

stress-induced activation of p38 MAPK is mainly associated with apoptotic cell death (Cuenda and Rousseau, 2007). Thus, I first studied the role of apoptosis in my infection model. Notably, evidence for the activation (Aporta et al., 2012) and inhibition (Divangahi et al., 2009) of apoptosis in TB infection has been provided. Aguiló et al. suggested a key role of p38 MAPK in ER-stress-mediated intrinsic apoptosis by *Mtb* (Aguilo et al., 2013). In this model, *Mtb* triggers ER stress via the secretion of EsxA, leading to increasing levels of mitochondrial ROS and Ca^{2+} (Tajeddine, 2016; Zorov et al., 2014). One of the downstream targets of ER-stress is the ASK1-p38 MAPK pathway, which promotes the activation of pro-apoptotic Bcl-2 family proteins and p53. The accumulation of pro-apoptotic Bcl-2 proteins at the mitochondria causes MOMP and results in intrinsic apoptosis (Lindsay et al., 2011). In line with several publications, I detected increasing amounts of the ER-stress activators mitochondrial ROS and Ca^{2+} in *Mtb*-infected Mϕ leading to the activation of the effector caspases 3 and 7 following the infection. Therefore, ER-stress-induced p38 MAPK activation may lead to apoptosis via the proteolytic cleavage of caspase 3 in my experimental setup. However, inhibition of caspases with the pan-caspase inhibitor Z-VAD-FMK had no effect on host cell survival, indicating that apoptosis is not utilized by *Mtb* to escape the host cell. Therefore, my data contradict those of Aguiló et al. who have shown that apoptosis is reduced in *Mtb*-infected J774 cells in the absence of caspases 3 and 7 (Aguilo et al., 2014). These discrepancies might be due to different *Mtb* strains (virulent or avirulent), and different MOI used in the experimental setup. For instance, a varying MOI can lead to either apoptosis or necrosis in the same experimental setup (Aporta et al., 2012). In addition, the absence of standardized procedures and protocols have made it increasingly difficult to define specific cell death phenotypes *in vitro* (Aporta et al., 2012). Especially data obtained from virulent (Erdman, H37Rv) and avirulent (BCG) *Mtb* strains need to be distinguished from each other. Moreover, a clear definition of early and late phases of infection might help establish a better definition of *Mtb*-induced cell death *in vitro*.

In line with my results, other research groups have indicated that apoptosis is induced by attenuated *Mtb* strains, whereas virulent *Mtb* strains rather suppress this form of cell death (Danelishvili et al., 2003; Martin et al., 2014). It has been reported that apoptotic cell death is more beneficial for the host cell than for *Mtb* by limiting bacterial viability and spread. Therefore, Mϕ induce caspase-mediated apoptosis in response to attenuated *Mtb* strains, such as H37Ra, to control the infection (Martin et al., 2014)

However, virulent *Mtb* strains suppress apoptosis to maintain their replication niche and subsequently escape the Mϕ by inducing necrosis (Lee et al., 2011). Inhibition of apoptosis by virulent *Mtb* is mediated via a reduced Fas expression on the surface of infected Mϕ, preventing FasL-induced apoptosis (Oddo et al., 1998). In addition, a study of the expression profile of Mϕ infected with H37Ra and H37Rv revealed that several pro-apoptotic genes involved in the TNFR1 signaling cascade are downregulated in H37Rv infected cells (Spira et al., 2003). In line with my results, these data demonstrate that apoptosis is only an incidental event rather than the major form of cell death induced by virulent *Mtb*.

Taken together, these studies suggest that both apoptosis and necrosis can mutually occur during *Mtb* infection. The critical factor might be the *Mtb* strain, the stage of infection and the bacterial burden. At early phases of infection *Mtb* favors apoptotic cell death. The delayed adaptive immune response allows *Mtb* to colonize the host without resistance. During this stage of infection, *Mtb* reaches a high bacterial burden without being exposed to the immune system of the host (Cooper, 2009). However, at later stages of infection *Mtb* promotes necrotic cell death to escape the granulomas, allowing transmission of the disease to new hosts (Aguilo et al., 2013).

6.2 Induction of necrosis in *Mtb*-infected cells

Necrosis is a pro-inflammatory process which leads to the release of cellular debris, such as DAMP, into the extracellular space and results in tissue inflammation (D'Arcy, 2019). Unlike the well-defined pathways of apoptosis, necrosis can be instigated by several stimuli triggering different pathways of necrotic cell death. Common features displayed by cells undergoing necrosis are mitochondrial membrane rupture, ATP depletion, increased ROS production and a loss of Ca^{2+} homeostasis as well as a loss of plasma membrane integrity. Contrary to the initial description of necrosis as an unregulated process, it is now well-known that necrosis can also be a programmed type of cell death (Vanden Berghe et al., 2014).

Following my observation that apoptosis is not induced as the major type of cell death by virulent *Mtb in vitro*, it was important to further mechanistically dissect necrosis as a potential cell death pathway. Necrosis is highly beneficial for *Mtb* since it allows the pathogen to enter the extracellular space and to infect newly recruited cells.

So far, only a few biomarkers have been established to identify necrosis. These include the secretion of HMGB1 and release of LDH (Yang et al., 2014). Infection of fibroblasts and Mϕ lead to an increased release of both HMGB1 and LDH, a process that could be prevented by treatment of the cells with the corticosteroid dexamethasone or the p38 MAPK inhibitor doramapimod. With this experiment, I was able to link p38 MAPK activation to necrotic cell death induced by virulent *Mtb* for the first time. Interestingly, HMGB1 also acts as a DAMP responsible for recruiting neutrophils to the site of inflammation (Berthelot et al., 2012). Therefore, HMGB1 could be a potential diagnostic marker for necrotic damage in TB patients (Chen et al., 2016).

Following the verification of necrosis in *Mtb*-infected cells, I analyzed different necrotic pathways to further decipher the molecular pathway triggered in response to the infection. One of the best described necrotic pathways is that of necroptosis. Since TNF plays an important role for both *Mtb* and necroptosis, it has previously been associated with *Mtb*-induced cell death. The binding of TNF to its receptor activates a signaling cascade involving RIPK1, RIPK3 and MLKL, which in the presence of inactivated caspase 8 results in necroptosis of the cell (Vandenabeele et al., 2010). Therefore, the role of TNF and necroptosis in TB infection has been studied extensively. It has been shown that a deficiency of TNF leads to increased bacterial growth and results in death of the host cell and release of *Mtb* (Clay et al., 2008). The use of TNF inhibitors such as infliximab and etanercept in the clinic, has led to a reactivation of LTBI and disseminated TB. Furthermore, Wallis et al. showed that the conversion of sputum cultures of TB patients treated with etanercept as an adjuvant immunotherapy in addition to antibiotics was not as rapid as in patients treated with the corticosteroid prednisolone (Wallis, 2005). In comparison, increasing TNF production by the host cell has been reported to induce necroptotic cell death. An excess of TNF may activate RIPK1 and RIPK3, which stimulates mitochondrial ROS production and allows *Mtb* to escape from the Mϕ (Roca and Ramakrishnan, 2013). This hypothesis was supported by Tobin et al., who have shown that a dysregulation of the leukotriene A4 hydrolase (LTA4H) induces an overproduction of leukotriene B4 and finally an overproduction of TNF to promote necroptosis (Tobin et al., 2012). Contrary to these data, it has been shown that the deletion of MLKL and the inhibition of RIPK1 has no effect on *Mtb*-induced host cell death (Stutz et al., 2018). Furthermore, the main necroptosis-inducing factor of *Mtb*, the tuberculosis necrotizing toxin (TNT), has been reported to act independently of TNF and RIPK1 (Pajuelo et al., 2018). I was

able to confirm these data by using chemical as well as genetic targeting of TNF, RIPK1 and MLKL to provide further evidence that necroptosis does not play a role in p38 MAPK-mediated necrosis. Interestingly, these data show that the protective effect of dexamethasone is independent of TNF inhibition and further demonstrate that corticosteroid treatment is more beneficial than TNF inhibitors for TB patients (Wallis, 2005). However, Newton et al. showed that RIPK3-induced necrosis only takes place in the absence of caspase 8 activation (Newton et al., 2014). To further clarify that RIPK3 signaling is not involved in *Mtb*-mediated host cell death I created a pro-necroptotic environment by inhibiting caspase activation with the pan-caspase inhibitor Z-VAD-FMK. However, even in the absence of caspase activity, the inhibition of RIPK3 had no cytoprotective effect on *Mtb*-infected cells. Therefore, I concluded that RIPK3 signaling and necroptosis is not promoted by *Mtb*.

Since necroptosis, a mitochondria independent form of cell death, is primed but not executed in *Mtb*-infected cells, other possible pathways were analyzed. As previously mentioned, one of the most commonly present cellular events in necrosis is damage to the mitochondrial membrane. This could also be shown in *Mtb*-infected cells. Chen et al. demonstrated that the infection of human Mϕ with H37Rv caused MOMP and irreversible MPT via the translocation of Bax to the mitochondria, leading to a loss in the ΔΨm and finally to necrosis (Chen et al., 2006). I first investigated the influence of virulent *Mtb* infection on mitochondrial function and integrity using a TMRM staining as an indicator for the ΔΨm. A loss of TMRM translates to a loss of the ΔΨm (Creed and McKenzie, 2019). The infection of Mϕ with virulent *Mtb* led to a decrease in the ΔΨm and thereby indicates a decrease in mitochondrial health. Furthermore, it has been reported that *Mtb* promotes the production of the eicosanoid LXA_4, which inhibits PGE2 and thereby inhibits membrane repair. However, the molecular mechanisms how *Mtb* influences mitochondrial function and integrity remain unclear. Therefore, I investigated the role of mitochondria in *Mtb*-mediated host cell death.

6.3 Role of mitochondria in *Mtb*-induced necrosis

Although I have provided evidence that *Mtb* triggers necrosis via p38 MAPK signaling and causes mitochondrial damage, the molecular mechanism remains elusive. Hence, I wondered whether there is a link between p38 MAPK and mitochondria dysregulation. I extended my studies to decipher the role of mitochondria in TB infection and possible regulatory proteins downstream of p38 MAPK.

Mitochondria are responsible for energy production and lipid synthesis among other functions. In recent years mitochondria have become the focus of many studies, especially in relation to aging and infectious diseases (Ramond et al., 2019). Many intracellular bacteria, including *L. monocytogenes* (Stavru et al., 2011) and *Shigella flexneri* (Lum and Morona, 2014), have developed strategies to manipulate mitochondrial function and integrity by disrupting the mitochondrial morphology. *L. monocytogenes* causes rapid mitochondrial fission by the release of the pore-forming toxin listeriolysin O, which results in the fragmentation of the mitochondrial network (Stavru et al., 2011). These bacteria target mitochondria as an important part of the immune response. Mitochondria take part in antibacterial defense by producing ROS, which results in the death of some bacteria (West et al., 2011). Moreover, mitochondria perform oxidative phosphorylation (OXPHOS) to generate ATP via the tricarboxylic acid (TCA) cycle and the electron transport chain (ETC) (Bratic and Trifunovic, 2010). Therefore, bacteria can also modulate the metabolism of their host cell by targeting these organelles. One such bacterium is *Mtb*. *Mtb* induces aerobic glycolysis in a TLR2 and protein kinase B (PKB/ AKT)- mammalian target of rapamycin (mTOR) dependent pathway (Gleeson et al., 2016). It has been reported that the infection of Mϕ with *Mtb* leads to an increase in glycolytic enzymes and a decrease in OXPHOS enzymes, resulting in an increased production of lactate. In addition, aerobic glycolysis increases the proliferation of host cells while reducing the ATP production in a process called the Warburg effect that was previously observed in cancer cells. Gillmaier et al. showed that *L. monocytogenes* had a higher replication rate in cancer cell lines compared to BMDM (Gillmaier et al., 2012). Thus, *Mtb* uses aerobic glycolysis to reduce pro-inflammatory responses of the host cell and to increase its own growth (Gleeson et al., 2016). This process might be of major importance at early stages of TB infection in which *Mtb* is mainly focused on reaching a critical bacterial burden. I also observed a low ATP production in *Mtb*-infected Mϕ compared to the uninfected controls, indicating a shift to aerobic glycolysis in the host cell. Furthermore, previous studies have demonstrated that MPT triggers the release of pyridine nucleotides from mitochondria to further decrease the amount of ATP and mitochondrial respiration, resulting in necrotic cell death (Batandier et al., 2004). Therefore, intracellular bacteria modulate the metabolism of the host cell to their own advantage. Intriguingly, treatment of cells with doramapimod and dexamethasone restored the generation of ATP in Mϕ and lung fibroblasts. Although, these data collectively indicate that the infection with *Mtb* highly

impacts OXPHOS and glycolysis of the host cell, further characterization is necessary to fully understand the influence of bacterial infection on mitochondrial function.

Another reason why I was highly interested in the role of mitochondria in *Mtb* infection was that in my original high-throughput drug screening CsA was identified as a hit compound. CsA is an inhibitor of CypD, an essential regulatory component of the mPTP. Other components of mPTP include the voltage-dependent anion channel (VDAC), the adenosine translocase (ANT) and the ATP synthase (Biasutto et al., 2016). Notably, CypD inhibition by CsA has already been established as a mechanism to inhibit *Mtb*-mediated cell death and mPTP opening (Roca and Ramakrishnan, 2013; Zhao et al., 2017). However, CsA as a non-selective inhibitor also blocks calcineurin activity in T cells. I excluded the potential protective effect of calcineurin inhibition in TB infection by treating cells with FK-506, a selective calcineurin inhibitor. As expected, the inhibition of CypD by CsA was responsible for preventing host cell death in *Mtb*-infected cells. Nevertheless, the dual effect of calcineurin and CypD inhibition makes CsA not suitable for a HDT. Therefore, an alternative, more specific compound is required. To determine whether doramapimod and dexamethasone impact on mitochondrial CypD expression, I evaluated the effect of both compounds on *Mtb*-infected Mϕ. Surprisingly, neither p38 MAPK inhibition by doramapimod nor activation of the glucocorticoid receptor by dexamethasone had any effect on mitochondrial CypD expression. Thus, I wondered how doramapimod and dexamethasone prevent mitochondrial damage.

Although, CypD is not a target of doramapimod and dexamethasone, both interfere with mitochondrial HKII expression. HKII is involved in glucose metabolism by phosphorylating glucose and acts as a signaling molecule (Roberts and Miyamoto, 2015). Moreover, increased levels of HKII are cytoprotective, while low amounts of HKII sensitize cells to necrosis (Ahmad et al., 2002). The protective effect of HKII is dependent on the enzyme binding directly to CypD and VDAC on the mitochondrial membrane (Sun et al., 2008). However, the exact molecular mechanism by which HKII protects mitochondria from damage is not yet fully understood. For instance, it has been reported that the accumulation of HKII at the mitochondria protects the cells from ROS exposure by increasing the pentose phosphate pathway activity to prevent opening of the mPTP (McCommis et al., 2013). Consistent with these studies I found that both doramapimod and dexamethasone increase mitochondrial HKII levels and

simultaneously decrease mitochondrial ROS production. I next inhibited HKII with 3BP and thereby decreased the cytoprotective effect of doramapimod and dexamethasone. Hence, I provide indirect evidence that the inhibition of p38 MAPK blocks mitochondrial dissociation of HKII and thereby prevents MPT and ATP depletion to promote host cell survival. Surprisingly, HKII dissociation is a common target for intracellular pathogens, such as *S. flexneri*, and might represent a method of detecting bacterial peptidoglycan (Wolf et al., 2016). Collectively, my data represent a link between p38 MAPK and HKII, which I further evaluated.

Since HKII has no p38 MAPK response element, it is unlikely that they directly interact with each other. Therefore, I next investigated a possible mediator between these two proteins. One such a candidate is the regulatory protein p53. p53 is not only a target of p38 MAPK but also directly interacts with the mitochondrial membrane (Marchenko and Moll, 2014). Upon bacterial infection, p53 ubiquitylation is blocked and p53 accumulates in the nucleus. Subsequently, p53 promotes the expression of death receptors to activate pro-apoptotic Bcl-2 proteins, resulting in cell death (Perfettini et al., 2005). I have generated data showing that the chemical inhibition or knockdown of p53 has similar effects on host cell survival as p38 MAPK inhibition. In recent years, the role of p53 regarding bacterial infections, especially host-pathogen interactions, has become of high interest. During bacterial infection, p53 is responsible for the downregulation of the metabolism of the infected cell in order to limit bacterial growth, as well as initiating apoptosis. However, Galietti et al. demonstrated that the upregulation of p53 is not only beneficial for the host cell, but is also beneficial for *Mtb* to inhibit host cell death at early stages of infection (Galietti et al., 2001). In line with these results, it has been shown that the inhibition of p53 in *Mtb*-infected Mϕ triggers an increase in Bcl2 levels, which prevents mitochondrial damage and thereby prevents host cell death (Cruz et al., 2015). Furthermore, p53 is able to translocate to the mitochondria and directly interact with HKII since HKII contains a p53 response element (Mathupala et al., 1997). These results indicate a possible connection of p38 MAPK and mitochondrial HKII. Nevertheless, the exact link between p38 MAPK and opening of the mPTP as well as the role of the potential regulators HKII and p53 requires further analysis in the future.

Since modulation of the mitochondrial metabolism is important in *Mtb* infection, one could investigate the metabolic function in *Mtb*-infected Mϕ by analyzing the OXPHOS

of mitochondria. This would provide further insight into the role of HKII and mitochondria in TB infection. In addition, one could analyze the influence of a p53 knockdown on necrosis, using the necrotic marker LDH, and mitochondrial integrity by TMRM. Another possible target connecting immunity, inflammation and glycolysis is the NLRP3 inflammasome. Since HKII is involved in glycolysis, it was reported that HKII interacts with NLRP3 to activate caspase 1, resulting in the production of IL-1β and pyroptosis (Eisenreich et al., 2019). I have generated preliminary data showing that *Mtb* induces the secretion of the pyroptotic cytokines IL-1β and IL18. Additionally, I observed that the knockout of caspase 1 and ASC reduces *Mtb*-mediated host cell death. Thus, it would be interesting to decipher the molecular pathway of pyroptosis downstream of p38 MAPK activation.

Another approach to confirm mitochondrial damage as a main driver of necrosis, is the evaluation of cells overexpressing the anti-apoptotic protein Bcl-2. Thus, I wondered whether Bcl-2 overexpression could protect the host cell from *Mtb*-induced cell death. When infecting Bcl-2 overexpressing cells, they displayed an increased survival rate without showing an altered phagocytotic ability. In addition, I could verify the data by Lindsay et al. that Bcl-2 is important for maintaining the $\Delta\Psi m$ (Lindsay et al., 2011). Therefore, the overexpression of Bcl-2 is as protective as the inhibition of p38 MAPK or the inhibition of p53.

Bcl-2 is localized at the OMM, the nuclear membrane and the ER. Pro-apoptotic Bcl-2 family proteins, like Bax and Bak, are majorly responsible for the mitochondria-mediated cell death pathway. Following activation, both Bax and Bak induce pore formation at the OMM, which allows the release of cell death factors, such as CytoC to induce host cell death (Tait and Green, 2013). Therefore, the anti-apoptotic protein Bcl-2 prevents cell death by inhibiting Bax and Bak. Surprisingly, it has been shown that mitochondrial HKII also protects the cells by antagonizing the pro-apoptotic Bcl-2 proteins Bak and Bax (Lindsay et al., 2011). However, not much is known about the function of Bcl-2 except for the inhibition of pro-apoptotic Bcl-2 family proteins. Interestingly, Bcl-2 is regulated by post-translational modifications and a direct target of p38 MAPK. The phosphorylation of Bcl-2 by p38 MAPK at serine 87 and threonine 56 leads to a conformational change in the protein, which decreases the anti-apoptotic activity of Bcl-2. Thereafter, mitochondrial damage is caused by Bax and Bak inducing the release of CytoC into the cytoplasm and finally causing host cell death. The

conformational changes in Bcl-2 might also compromise its ability to interact with the mPTP. The inhibition of p38 MAPK thereby restores the function of Bcl-2 (De Chiara et al., 2006). Similarly, overexpression of Bcl-2 reduces the activation of p38 MAPK to prevent host cell death (Cheng et al., 2001). Moreover, Bcl-2 also interacts with p53 by limiting p53 accumulation at the mitochondria to prevent host cell death (Marchenko and Moll, 2014). Thus, Bcl-2 is an important regulator in mitochondrial damage and *Mtb*-mediated host cell death, which has to be further investigated.

In summary, I was able to identify a novel cell death pathway of *Mtb*, which involves the activation of p38 MAPK and p53, leading to the mitochondrial dissociation of HKII and subsequently opening of the mPTP and ATP depletion. This pathway can be inhibited by the activation of MKP-1 by dexamethasone and BI653048 or by inhibition of p38 MAPK by doramapimod. Furthermore, mitochondrial damage and the opening of the mPTP can be prevented either by Bcl-2 overexpression or CsA. Therefore, I provide several novel targets for HDT in TB treatment.

In a next step, research should focus on additional host cell death pathways induced by *Mtb* such as pyroptosis and the NLRP3 inflammasome. I have generated preliminary data indicating that the inflammasome is activated in response to the infection. There is increasing evidence linking NLRP3 activation to mitochondrial damage and pyroptotic cell death (Liu et al., 2018; Yu et al., 2014). These findings will provide further starting points for host directed therapies in TB.

7. References

Abe, J., and Morrell, C. (2016). Pyroptosis as a Regulated Form of Necrosis: PI+/Annexin V-/High Caspase 1/Low Caspase 9 Activity in Cells = Pyroptosis? Circulation research *118*, 1457-1460.

Abraham, S. M., Lawrence, T., Kleiman, A., Warden, P., Medghalchi, M., Tuckermann, J., Saklatvala, J., and Clark, A. R. (2006). Antiinflammatory effects of dexamethasone are partly dependent on induction of dual specificity phosphatase 1. The Journal of experimental medicine *203*, 1883-1889.

Aguilo, N., Marinova, D., Martin, C., and Pardo, J. (2013). ESX-1-induced apoptosis during mycobacterial infection: to be or not to be, that is the question. Frontiers in cellular and infection microbiology *3*, 88.

Aguilo, N., Uranga, S., Marinova, D., Martin, C., and Pardo, J. (2014). Bim is a crucial regulator of apoptosis induced by Mycobacterium tuberculosis. Cell death & disease *5*, e1343.

Ahmad, A., Ahmad, S., Schneider, B. K., Allen, C. B., Chang, L. Y., and White, C. W. (2002). Elevated expression of hexokinase II protects human lung epithelial-like A549 cells against oxidative injury. American journal of physiology Lung cellular and molecular physiology *283*, L573-584.

Alderwick, L. J., Harrison, J., Lloyd, G. S., and Birch, H. L. (2015). The Mycobacterial Cell Wall--Peptidoglycan and Arabinogalactan. Cold Spring Harbor perspectives in medicine *5*, a021113.

Aporta, A., Arbues, A., Aguilo, J. I., Monzon, M., Badiola, J. J., de Martino, A., Ferrer, N., Marinova, D., Anel, A., Martin, C., and Pardo, J. (2012). Attenuated Mycobacterium tuberculosis SO2 vaccine candidate is unable to induce cell death. PloS one *7*, e45213.

Arthur, J. S., and Ley, S. C. (2013). Mitogen-activated protein kinases in innate immunity. Nature reviews Immunology *13*, 679-692.

Batandier, C., Leverve, X., and Fontaine, E. (2004). Opening of the mitochondrial permeability transition pore induces reactive oxygen species production at the level of the respiratory chain complex I. The Journal of biological chemistry *279*, 17197-17204.

Beatty, W. L., Rhoades, E. R., Ullrich, H. J., Chatterjee, D., Heuser, J. E., and Russell, D. G. (2000). Trafficking and release of mycobacterial lipids from infected macrophages. Traffic (Copenhagen, Denmark) *1*, 235-247.

Berthelot, F., Fattoum, L., Casulli, S., Gozlan, J., Marechal, V., and Elbim, C. (2012). The effect of HMGB1, a damage-associated molecular pattern molecule, on polymorphonuclear neutrophil migration depends on its concentration. J Innate Immun *4*, 41-58.

Biasutto, L., Azzolini, M., Szabo, I., and Zoratti, M. (2016). The mitochondrial permeability transition pore in AD 2016: An update. Biochimica et biophysica acta *1863*, 2515-2530.

Blackburn, D., Hux, J., and Mamdani, M. (2002). Quantification of the Risk of Corticosteroid-induced Diabetes Mellitus Among the Elderly. Journal of general internal medicine *17*, 717-720.

Bold, T. D., and Ernst, J. D. (2009). Who benefits from granulomas, mycobacteria or host? Cell *136*, 17-19.

Bratic, I., and Trifunovic, A. (2010). Mitochondrial energy metabolism and ageing. Biochimica et biophysica acta *1797*, 961-967.

Brennan, P. J., and Nikaido, H. (1995). The envelope of mycobacteria. Annual review of biochemistry *64*, 29-63.

Cambier, C. J., Falkow, S., and Ramakrishnan, L. (2014). Host evasion and exploitation schemes of Mycobacterium tuberculosis. Cell *159*, 1497-1509.

Chambers, H. F., Moreau, D., Yajko, D., Miick, C., Wagner, C., Hackbarth, C., Kocagoz, S., Rosenberg, E., Hadley, W. K., and Nikaido, H. (1995). Can penicillins and other beta-lactam antibiotics be used to treat tuberculosis? Antimicrobial agents and chemotherapy *39*, 2620-2624.

Chen, M., Gan, H., and Remold, H. G. (2006). A mechanism of virulence: virulent Mycobacterium tuberculosis strain H37Rv, but not attenuated H37Ra, causes significant mitochondrial inner membrane disruption in macrophages leading to necrosis. Journal of immunology (Baltimore, Md : 1950) *176*, 3707-3716.

Chen, Y., Zhang, J., Wang, X., Wu, Y., Zhu, L., Lu, L., Shen, Q., and Qin, Y. (2016). HMGB1 level in cerebrospinal fluid as a complimentary biomarker for the diagnosis of tuberculous meningitis. SpringerPlus *5*, 1775.

Cheng, A., Chan, S. L., Milhavet, O., Wang, S., and Mattson, M. P. (2001). p38 MAP kinase mediates nitric oxide-induced apoptosis of neural progenitor cells. The Journal of biological chemistry *276*, 43320-43327.

Clay, H., Volkman, H. E., and Ramakrishnan, L. (2008). Tumor necrosis factor signaling mediates resistance to mycobacteria by inhibiting bacterial growth and macrophage death. Immunity *29*, 283-294.

Conrad, M., Angeli, J. P., Vandenabeele, P., and Stockwell, B. R. (2016). Regulated necrosis: disease relevance and therapeutic opportunities. Nature reviews Drug discovery *15*, 348-366.

Cooper, A. M. (2009). Cell-mediated immune responses in tuberculosis. Annual review of immunology *27*, 393-422.

Creed, S., and McKenzie, M. (2019). Measurement of Mitochondrial Membrane Potential with the Fluorescent Dye Tetramethylrhodamine Methyl Ester (TMRM). Methods in molecular biology (Clifton, NJ) *1928*, 69-76.

Cruz, A., Ludovico, P., Torrado, E., Gama, J. B., Sousa, J., Gaifem, J., Appelberg, R., Rodrigues, F., Cooper, A. M., Pedrosa, J.*, et al.* (2015). IL-17A Promotes Intracellular Growth of Mycobacterium by Inhibiting Apoptosis of Infected Macrophages. Frontiers in immunology *6*, 498.

Cuenda, A., and Rousseau, S. (2007). p38 MAP-kinases pathway regulation, function and role in human diseases. Biochimica et biophysica acta *1773*, 1358-1375.

D'Arcy, M. S. (2019). Cell death: a review of the major forms of apoptosis, necrosis and autophagy. Cell biology international *43*, 582-592.

Danelishvili, L., McGarvey, J., Li, Y. J., and Bermudez, L. E. (2003). Mycobacterium tuberculosis infection causes different levels of apoptosis and necrosis in human macrophages and alveolar epithelial cells. Cellular microbiology *5*, 649-660.

Davis, J. M., and Ramakrishnan, L. (2009). The role of the granuloma in expansion and dissemination of early tuberculous infection. Cell *136*, 37-49.

De Chiara, G., Marcocci, M. E., Torcia, M., Lucibello, M., Rosini, P., Bonini, P., Higashimoto, Y., Damonte, G., Armirotti, A., Amodei, S.*, et al.* (2006). Bcl-2 Phosphorylation by p38 MAPK: identification of target sites and biologic consequences. The Journal of biological chemistry *281*, 21353-21361.

Deretic, V., Singh, S., Master, S., Harris, J., Roberts, E., Kyei, G., Davis, A., de Haro, S., Naylor, J., Lee, H. H., and Vergne, I. (2006). Mycobacterium tuberculosis inhibition of phagolysosome biogenesis and autophagy as a host defence mechanism. Cellular microbiology *8*, 719-727.

Divangahi, M., Chen, M., Gan, H., Desjardins, D., Hickman, T. T., Lee, D. M., Fortune, S., Behar, S. M., and Remold, H. G. (2009). Mycobacterium tuberculosis evades macrophage defenses by inhibiting plasma membrane repair. Nature immunology *10*, 899-906.

Duan, W., Li, X., Ge, Y., Yu, Z., Li, P., Li, J., Qin, L., and Xie, J. (2019). Mycobacterium tuberculosis Rv1473 is a novel macrolides ABC Efflux Pump regulated by WhiB7. Future microbiology *14*, 47-59.

Eisenreich, W., Rudel, T., Heesemann, J., and Goebel, W. (2019). How Viral and Intracellular Bacterial Pathogens Reprogram the Metabolism of Host Cells to Allow Their Intracellular Replication. Frontiers in cellular and infection microbiology *9*, 42.

Elmore, S. (2007). Apoptosis: a review of programmed cell death. Toxicologic pathology *35*, 495-516.

Ferraris, D. M., Miggiano, R., Rossi, F., and Rizzi, M. (2018). Mycobacterium tuberculosis Molecular Determinants of Infection, Survival Strategies, and Vulnerable Targets. Pathogens (Basel, Switzerland) *7*.

Ferri, K. F., and Kroemer, G. (2001). Organelle-specific initiation of cell death pathways. Nature cell biology *3*, E255-263.

Galietti, F., Bollo, E., Cappia, S., Dondo, A., Pregel, P., Nicali, R., and Pozzi, E. (2001). p53 expression in cultured blood human monocytes infected with mycobacterial strains. Panminerva Med *43*, 249-255.

Gao, L. Y., Laval, F., Lawson, E. H., Groger, R. K., Woodruff, A., Morisaki, J. H., Cox, J. S., Daffe, M., and Brown, E. J. (2003). Requirement for kasB in Mycobacterium mycolic acid biosynthesis, cell wall impermeability and intracellular survival: implications for therapy. Molecular microbiology *49*, 1547-1563.

Gillmaier, N., Gotz, A., Schulz, A., Eisenreich, W., and Goebel, W. (2012). Metabolic responses of primary and transformed cells to intracellular Listeria monocytogenes. PloS one *7*, e52378.

Gleeson, L. E., Sheedy, F. J., Palsson-McDermott, E. M., Triglia, D., O'Leary, S. M., O'Sullivan, M. P., O'Neill, L. A., and Keane, J. (2016). Cutting Edge: Mycobacterium tuberculosis Induces Aerobic Glycolysis in Human Alveolar Macrophages That Is Required for Control of Intracellular Bacillary Replication. Journal of immunology (Baltimore, Md : 1950) *196*, 2444-2449.

Gräb, J., and Rybniker, J. (2019). The Expanding Role of p38 Mitogen-Activated Protein Kinase in Programmed Host Cell Death. Microbiology insights *12*, 1178636119864594.

Gräb, J., Suarez, I., van Gumpel, E., Winter, S., Schreiber, F., Esser, A., Holscher, C., Fritsch, M., Herb, M., Schramm, M.*, et al.* (2019). Corticosteroids inhibit Mycobacterium tuberculosis-induced necrotic host cell death by abrogating mitochondrial membrane permeability transition. Nature communications *10*, 688.

Hasselgren, P. O., Alamdari, N., Aversa, Z., Gonnella, P., Smith, I. J., and Tizio, S. (2010). Corticosteroids and muscle wasting: role of transcription factors, nuclear cofactors, and hyperacetylation. Current opinion in clinical nutrition and metabolic care *13*, 423-428.

Herdman, A. V., and Steele, J. C., Jr. (2004). The new mycobacterial species--emerging or newly distinguished pathogens. Clinics in laboratory medicine *24*, 651-690, vi.

Hotchkiss, R. S., and Nicholson, D. W. (2006). Apoptosis and caspases regulate death and inflammation in sepsis. Nature reviews Immunology *6*, 813-822.

Johnson, G. L., and Lapadat, R. (2002). Mitogen-activated protein kinase pathways mediated by ERK, JNK, and p38 protein kinases. Science (New York, NY) *298*, 1911-1912.

Kaufmann, S. H. (2001). How can immunology contribute to the control of tuberculosis? Nature reviews Immunology *1*, 20-30.

Köser, C. U., Javid, B., Liddell, K., Ellington, M. J., Feuerriegel, S., Niemann, S., Brown, N. M., Burman, W. J., Abubakar, I., Ismail, N. A.*, et al.* (2015). Drug-resistance mechanisms and tuberculosis drugs. Lancet (London, England) *385*, 305-307.

Lee, J., Repasy, T., Papavinasasundaram, K., Sassetti, C., and Kornfeld, H. (2011). Mycobacterium tuberculosis induces an atypical cell death mode to escape from infected macrophages. PloS one *6*, e18367.

Lindsay, J., Esposti, M. D., and Gilmore, A. P. (2011). Bcl-2 proteins and mitochondria--specificity in membrane targeting for death. Biochimica et biophysica acta *1813*, 532-539.

Liu, Q., Zhang, D., Hu, D., Zhou, X., and Zhou, Y. (2018). The role of mitochondria in NLRP3 inflammasome activation. Molecular immunology *103*, 115-124.

Liu, X., Zhang, Z., Ruan, J., Pan, Y., Magupalli, V. G., Wu, H., and Lieberman, J. (2016). Inflammasome-activated gasdermin D causes pyroptosis by forming membrane pores. Nature *535*, 153-158.

Lum, M., and Morona, R. (2014). Dynamin-related protein Drp1 and mitochondria are important for Shigella flexneri infection. International journal of medical microbiology : IJMM *304*, 530-541.

Mack, U., Migliori, G. B., Sester, M., Rieder, H. L., Ehlers, S., Goletti, D., Bossink, A., Magdorf, K., Holscher, C., Kampmann, B.*, et al.* (2009). LTBI: latent tuberculosis infection or lasting immune responses to M. tuberculosis? A TBNET consensus statement. The European respiratory journal *33*, 956-973.

Marchenko, N. D., and Moll, U. M. (2014). Mitochondrial death functions of p53. Molecular & cellular oncology *1*, e955995.

Martin, C. J., Peters, K. N., and Behar, S. M. (2014). Macrophages clean up: efferocytosis and microbial control. Curr Opin Microbiol *17*, 17-23.

Mathupala, S. P., Heese, C., and Pedersen, P. L. (1997). Glucose catabolism in cancer cells. The type II hexokinase promoter contains functionally active response elements for the tumor suppressor p53. The Journal of biological chemistry *272*, 22776-22780.

Maus, C. E., Plikaytis, B. B., and Shinnick, T. M. (2005). Mutation of tlyA confers capreomycin resistance in Mycobacterium tuberculosis. Antimicrobial agents and chemotherapy *49*, 571-577.

McCommis, K. S., Douglas, D. L., Krenz, M., and Baines, C. P. (2013). Cardiac-specific hexokinase 2 overexpression attenuates hypertrophy by increasing pentose phosphate pathway flux. Journal of the American Heart Association *2*, e000355.

Miller, J. L., Velmurugan, K., Cowan, M. J., and Briken, V. (2010). The type I NADH dehydrogenase of Mycobacterium tuberculosis counters phagosomal NOX2 activity to inhibit TNF-alpha-mediated host cell apoptosis. PLoS pathogens *6*, e1000864.

Mukhopadhyay, P., Rajesh, M., Hasko, G., Hawkins, B. J., Madesh, M., and Pacher, P. (2007). Simultaneous detection of apoptosis and mitochondrial superoxide production in live cells by flow cytometry and confocal microscopy. Nature protocols *2*, 2295-2301.

Napier, R. J., Rafi, W., Cheruvu, M., Powell, K. R., Zaunbrecher, M. A., Bornmann, W., Salgame, P., Shinnick, T. M., and Kalman, D. (2011). Imatinib-sensitive tyrosine kinases regulate mycobacterial pathogenesis and represent therapeutic targets against tuberculosis. Cell host & microbe *10*, 475-485.

Newton, K., Dugger, D. L., Wickliffe, K. E., Kapoor, N., de Almagro, M. C., Vucic, D., Komuves, L., Ferrando, R. E., French, D. M., Webster, J.*, et al.* (2014). Activity of protein kinase RIPK3 determines whether cells die by necroptosis or apoptosis. Science (New York, NY) *343*, 1357-1360.

Nguyen, L. (2016). Antibiotic resistance mechanisms in M. tuberculosis: an update. Archives of toxicology *90*, 1585-1604.

Oddo, M., Renno, T., Attinger, A., Bakker, T., MacDonald, H. R., and Meylan, P. R. (1998). Fas ligand-induced apoptosis of infected human macrophages reduces the viability of intracellular Mycobacterium tuberculosis. Journal of immunology (Baltimore, Md : 1950) *160*, 5448-5454.

Oglesby, W., Kara, A. M., Granados, H., and Cervantes, J. L. (2019). Metformin in tuberculosis: beyond control of hyperglycemia. Infection *47*, 697-702.

Pagan, A. J., and Ramakrishnan, L. (2014). Immunity and Immunopathology in the Tuberculous Granuloma. Cold Spring Harbor perspectives in medicine *5*.

Pajuelo, D., Gonzalez-Juarbe, N., Tak, U., Sun, J., Orihuela, C. J., and Niederweis, M. (2018). NAD(+) Depletion Triggers Macrophage Necroptosis, a Cell Death Pathway Exploited by Mycobacterium tuberculosis. Cell reports *24*, 429-440.

Pargellis, C., Tong, L., Churchill, L., Cirillo, P. F., Gilmore, T., Graham, A. G., Grob, P. M., Hickey, E. R., Moss, N., Pav, S., and Regan, J. (2002). Inhibition of p38 MAP kinase by utilizing a novel allosteric binding site. Nature structural biology *9*, 268-272.

Perfettini, J. L., Castedo, M., Nardacci, R., Ciccosanti, F., Boya, P., Roumier, T., Larochette, N., Piacentini, M., and Kroemer, G. (2005). Essential role of p53 phosphorylation by p38 MAPK in apoptosis induction by the HIV-1 envelope. The Journal of experimental medicine *201*, 279-289.

Porvaznik, I., Solovic, I., and Mokry, J. (2017). Non-Tuberculous Mycobacteria: Classification, Diagnostics, and Therapy. Advances in experimental medicine and biology *944*, 19-25.

Pym, A. S., Brodin, P., Brosch, R., Huerre, M., and Cole, S. T. (2002). Loss of RD1 contributed to the attenuation of the live tuberculosis vaccines Mycobacterium bovis BCG and Mycobacterium microti. Molecular microbiology *46*, 709-717.

Ramakrishnan, L. (2012). Revisiting the role of the granuloma in tuberculosis. Nature reviews Immunology *12*, 352-366.

Ramond, E., Jamet, A., Coureuil, M., and Charbit, A. (2019). Pivotal Role of Mitochondria in Macrophage Response to Bacterial Pathogens. Frontiers in immunology *10*, 2461.

Rand, L., Green, J. A., Saraiva, L., Friedland, J. S., and Elkington, P. T. (2009). Matrix metalloproteinase-1 is regulated in tuberculosis by a p38 MAPK-dependent, p-aminosalicylic acid-sensitive signaling cascade. Journal of immunology (Baltimore, Md : 1950) *182*, 5865-5872.

Roberts, D. J., and Miyamoto, S. (2015). Hexokinase II integrates energy metabolism and cellular protection: Akting on mitochondria and TORCing to autophagy. Cell death and differentiation *22*, 364.

Roca, F. J., and Ramakrishnan, L. (2013). TNF dually mediates resistance and susceptibility to mycobacteria via mitochondrial reactive oxygen species. Cell *153*, 521-534.

Romagnoli, A., Etna, M. P., Giacomini, E., Pardini, M., Remoli, M. E., Corazzari, M., Falasca, L., Goletti, D., Gafa, V., Simeone, R.*, et al.* (2012). ESX-1 dependent impairment of autophagic flux by Mycobacterium tuberculosis in human dendritic cells. Autophagy *8*, 1357-1370.

Russell, D. G. (2007). Who puts the tubercle in tuberculosis? Nature reviews Microbiology *5*, 39-47.

Schaible, U. E., Collins, H. L., Priem, F., and Kaufmann, S. H. (2002). Correction of the iron overload defect in beta-2-microglobulin knockout mice by lactoferrin abolishes their increased susceptibility to tuberculosis. The Journal of experimental medicine *196*, 1507-1513.

Schaible, U. E., Sturgill-Koszycki, S., Schlesinger, P. H., and Russell, D. G. (1998). Cytokine activation leads to acidification and increases maturation of Mycobacterium avium-containing phagosomes in murine macrophages. Journal of immunology (Baltimore, Md : 1950) *160*, 1290-1296.

Schutz, C., Davis, A. G., Sossen, B., Lai, R. P., Ntsekhe, M., Harley, Y. X., and Wilkinson, R. J. (2018). Corticosteroids as an adjunct to tuberculosis therapy. Expert review of respiratory medicine *12*, 881-891.

Seddon, J. A., Tugume, L., Solomons, R., Prasad, K., and Bahr, N. C. (2019). The current global situation for tuberculous meningitis: epidemiology, diagnostics, treatment and outcomes. Wellcome open research *4*, 167.

Shah, S., and Briken, V. (2016). Modular Organization of the ESX-5 Secretion System in Mycobacterium tuberculosis. Frontiers in cellular and infection microbiology *6*, 49.

Shaw, M. H., Reimer, T., Kim, Y. G., and Nunez, G. (2008). NOD-like receptors (NLRs): bona fide intracellular microbial sensors. Current opinion in immunology *20*, 377-382.

Shiloh, M. U., Manzanillo, P., and Cox, J. S. (2008). Mycobacterium tuberculosis senses host-derived carbon monoxide during macrophage infection. Cell host & microbe *3*, 323-330.

Shimada, K., Skouta, R., Kaplan, A., Yang, W. S., Hayano, M., Dixon, S. J., Brown, L. M., Valenzuela, C. A., Wolpaw, A. J., and Stockwell, B. R. (2016). Global survey of cell death mechanisms reveals metabolic regulation of ferroptosis. Nature chemical biology *12*, 497-503.

Spira, A., Carroll, J. D., Liu, G., Aziz, Z., Shah, V., Kornfeld, H., and Keane, J. (2003). Apoptosis genes in human alveolar macrophages infected with virulent or attenuated Mycobacterium tuberculosis: a pivotal role for tumor necrosis factor. Am J Respir Cell Mol Biol *29*, 545-551.

Stavru, F., Bouillaud, F., Sartori, A., Ricquier, D., and Cossart, P. (2011). Listeria monocytogenes transiently alters mitochondrial dynamics during infection. Proceedings of the National Academy of Sciences of the United States of America *108*, 3612-3617.

Stockwell, B. R., Friedmann Angeli, J. P., Bayir, H., Bush, A. I., Conrad, M., Dixon, S. J., Fulda, S., Gascon, S., Hatzios, S. K., Kagan, V. E.*, et al.* (2017). Ferroptosis: A Regulated Cell Death Nexus Linking Metabolism, Redox Biology, and Disease. Cell *171*, 273-285.

Strambu, I. R., Kobalava, Z. D., Magnusson, B. P., MacKinnon, A., and Parkin, J. M. (2019). Phase II Study of Single/Repeated Doses of Acumapimod (BCT197) to Treat Acute Exacerbations of COPD. Copd *16*, 344-353.

Stramucci, L., Pranteda, A., and Bossi, G. (2018). Insights of Crosstalk between p53 Protein and the MKK3/MKK6/p38 MAPK Signaling Pathway in Cancer. Cancers *10*.

Stutz, M. D., Ojaimi, S., Allison, C., Preston, S., Arandjelovic, P., Hildebrand, J. M., Sandow, J. J., Webb, A. I., Silke, J., Alexander, W. S., and Pellegrini, M. (2018). Necroptotic signaling is primed in Mycobacterium tuberculosis-infected macrophages, but its pathophysiological consequence in disease is restricted. Cell death and differentiation *25*, 951-965.

Sun, L., Shukair, S., Naik, T. J., Moazed, F., and Ardehali, H. (2008). Glucose phosphorylation and mitochondrial binding are required for the protective effects of hexokinases I and II. Molecular and cellular biology *28*, 1007-1017.

Tait, S. W., and Green, D. R. (2013). Mitochondrial regulation of cell death. Cold Spring Harbor perspectives in biology *5*.

Tajeddine, N. (2016). How do reactive oxygen species and calcium trigger mitochondrial membrane permeabilisation? Biochimica et biophysica acta *1860*, 1079-1088.

Tobin, D. M., Roca, F. J., Oh, S. F., McFarland, R., Vickery, T. W., Ray, J. P., Ko, D. C., Zou, Y., Bang, N. D., Chau, T. T.*, et al.* (2012). Host genotype-specific therapies

can optimize the inflammatory response to mycobacterial infections. Cell *148*, 434-446.

Tsenova, L., and Singhal, A. (2020). Effects of host-directed therapies on the pathology of tuberculosis. The Journal of pathology.

Vanden Berghe, T., Linkermann, A., Jouan-Lanhouet, S., Walczak, H., and Vandenabeele, P. (2014). Regulated necrosis: the expanding network of non-apoptotic cell death pathways. Nature reviews Molecular cell biology *15*, 135-147.

Vandenabeele, P., Galluzzi, L., Vanden Berghe, T., and Kroemer, G. (2010). Molecular mechanisms of necroptosis: an ordered cellular explosion. Nature reviews Molecular cell biology *11*, 700-714.

Wallis, R. S. (2005). Reconsidering adjuvant immunotherapy for tuberculosis. Clinical infectious diseases : an official publication of the Infectious Diseases Society of America *41*, 201-208.

Wallis, R. S., and Hafner, R. (2015). Advancing host-directed therapy for tuberculosis. Nature reviews Immunology *15*, 255-263.

Wawrocki, S., and Druszczynska, M. (2017). Inflammasomes in Mycobacterium tuberculosis-Driven Immunity. The Canadian journal of infectious diseases & medical microbiology = Journal canadien des maladies infectieuses et de la microbiologie medicale *2017*, 2309478.

West, A. P., Brodsky, I. E., Rahner, C., Woo, D. K., Erdjument-Bromage, H., Tempst, P., Walsh, M. C., Choi, Y., Shadel, G. S., and Ghosh, S. (2011). TLR signalling augments macrophage bactericidal activity through mitochondrial ROS. Nature *472*, 476-480.

WHO (2019). Global tuberculosis report 2018. World Health Organization (2019).

Wolf, A. J., Reyes, C. N., Liang, W., Becker, C., Shimada, K., Wheeler, M. L., Cho, H. C., Popescu, N. I., Coggeshall, K. M., Arditi, M., and Underhill, D. M. (2016). Hexokinase Is an Innate Immune Receptor for the Detection of Bacterial Peptidoglycan. Cell *166*, 624-636.

Wong, K. W. (2017). The Role of ESX-1 in Mycobacterium tuberculosis Pathogenesis. Microbiology spectrum *5*.

Yang, M., Antoine, D. J., Weemhoff, J. L., Jenkins, R. E., Farhood, A., Park, B. K., and Jaeschke, H. (2014). Biomarkers distinguish apoptotic and necrotic cell death during hepatic ischemia/reperfusion injury in mice. Liver transplantation : official publication of the American Association for the Study of Liver Diseases and the International Liver Transplantation Society *20*, 1372-1382.

Yew, W. W., Lange, C., and Leung, C. C. (2011). Treatment of tuberculosis: update 2010. The European respiratory journal *37*, 441-462.

Ying, Y., and Padanilam, B. J. (2016). Regulation of necrotic cell death: p53, PARP1 and cyclophilin D-overlapping pathways of regulated necrosis? Cellular and molecular life sciences : CMLS *73*, 2309-2324.

Yu, J., Nagasu, H., Murakami, T., Hoang, H., Broderick, L., Hoffman, H. M., and Horng, T. (2014). Inflammasome activation leads to Caspase-1-dependent mitochondrial damage and block of mitophagy. Proceedings of the National Academy of Sciences of the United States of America *111*, 15514-15519.

Zarubin, T., and Han, J. (2005). Activation and signaling of the p38 MAP kinase pathway. Cell research *15*, 11-18.

Zhai, W., Wu, F., Zhang, Y., Fu, Y., and Liu, Z. (2019). The Immune Escape Mechanisms of Mycobacterium Tuberculosis. International journal of molecular sciences *20*.

Zhang, Y. J., Reddy, M. C., Ioerger, T. R., Rothchild, A. C., Dartois, V., Schuster, B. M., Trauner, A., Wallis, D., Galaviz, S., Huttenhower, C*., et al.* (2013). Tryptophan biosynthesis protects mycobacteria from CD4 T-cell-mediated killing. Cell *155*, 1296-1308.

Zhao, X., Khan, N., Gan, H., Tzelepis, F., Nishimura, T., Park, S. Y., Divangahi, M., and Remold, H. G. (2017). Bcl-xL mediates RIPK3-dependent necrosis in M. tuberculosis-infected macrophages. Mucosal immunology *10*, 1553-1568.

Zorov, D. B., Juhaszova, M., and Sollott, S. J. (2014). Mitochondrial reactive oxygen species (ROS) and ROS-induced ROS release. Physiological reviews *94*, 909-950.

8. Summary

The emergence and prevalence of *Mycobacterium tuberculosis* (*Mtb*) resistant strains requires the development of alternative therapeutic strategies, such as host-directed therapies (HDT), to treat tuberculosis (TB) infections. These HDT act on the host-response to a pathogen rather than directly on the pathogen itself. A HDT already applied to TB patients are corticosteroids, such as dexamethasone, which are combined with antibiotic treatment in a subset of patients. The exact mechanism of action of corticosteroids in TB remains elusive. *Mtb* is a highly adapted pathogen that continuously exploits the immune system of the host to ensure its own survival. A major mechanism of pathogenesis in TB is the induction of host cell death. Host cell death leads to the escape of *Mtb* from the phagocyte and results in dissemination of the disease. However, the exact cell death pathway induced by *Mtb* as well as the key regulators remain unknown. In-depth understanding of this cell death pathway and the protective mechanism of dexamethasone would provide valuable targets for HDT and may allow for a tailored therapy in patients with extensive tissue necrosis and inflammation.

In this thesis, I decipher a novel host cell death pathway triggered by *Mtb,* which can be inhibited by dexamethasone. Infection of macrophages (Mϕ) with *Mtb* induces the phosphorylation of p38 mitogen-activated protein kinase (MAPK). I show that p38 MAPK signaling triggers necrosis rather than apoptosis in *Mtb*-infected phagocytes. The activation of p38 MAPK promotes the dissociation of hexokinase II (HKII) from mitochondria and allows the opening of the mitochondrial permeability transition pore (mPTP). The opening of the mPTP results in adenosine triphosphate (ATP) depletion and finally in necrosis of the host cell. I can show that dexamethasone inhibits this pathway by activating MAPK phosphatase 1 (MKP-1) to downregulate p38 MAPK activity. Moreover, a direct inhibition of p38 MAPK by the specific p38 MAPK inhibitor doramapimod has similar effects on host cell survival. Since corticosteroids are anti-inflammatory drugs, which among others inhibit tumor necrosis factor (TNF) signaling, I further characterized TNF and necroptosis in *Mtb*-infected cells using mixed lineage kinase domain-like pseudokinase (MLKL) and TNF receptor 1 (TNFR1) knockout Mϕ. I could demonstrate that the underlying mechanism of dexamethasone is independent from TNF and necroptosis.

Thus, my results link p38 MAPK inhibition by corticosteroids or p38 MAPK inhibitors to the abrogation of mitochondria-mediated host cell death in TB infection and provides new opportunities for research on novel HDT concepts.

9. Zusammenfassung

Die Entstehung und Verbreitung von multiresistenten Stämmen des *Mycobaterium tuberculosis* (*Mtb*) erfordert die Entwicklung alternativer therapeutischer Strategien, wie zum Beispiel adjuvanter Therapieansätze (host-directed therapy, HDT), zur Behandlung von Infektionen mit Tuberkulose (TB). Diese HDT wirken auf die Immunantwort der Wirtszelle und nicht direkt auf den Krankheitserreger selbst. Eine bereits bei TB-Patienten angewandte HDT sind Kortikosteroide wie Dexamethason, die bei einer Untergruppe von Patienten mit einer Antibiotikabehandlung kombiniert werden. Der genaue Wirkmechanismus von Kortikosteroiden bei TB ist nach wie vor nicht bekannt. *Mtb* ist ein hochgradig angepasster Krankheitserreger, der das Immunsystem des Wirts kontinuierlich ausnutzt, um sein eigenes Überleben zu sichern. Ein Hauptmechanismus der Pathogenese bei TB ist die Induktion des Wirtszelltods. Der Tod der Wirtszelle führt zum Austritt von *Mtb* aus den Phagozyten und führt zur Verbreitung der Krankheit. Der genaue Zelltodweg, der durch *Mtb* induziert wird, sowie die wichtigsten Regulatoren bleiben jedoch unbekannt. Ein tiefgreifendes Verständnis dieses Zelltodweges und des Schutzmechanismus von Dexamethason würde wertvolle Angriffspunkte für HDT liefern und könnte eine maßgeschneiderte Therapie bei Patienten mit erheblichen Gewebeschäden und Entzündung ermöglichen.

In dieser Doktorarbeit identifiziere ich einen neuartigen, durch *Mtb* ausgelösten Wirtszelltodweg, der durch Dexamethason gehemmt werden kann. Die Infektion von Makrophagen (Mϕ) mit *Mtb* induziert die Phosphorylierung von p38-mitogenaktivierte Proteinkinase (MAPK). Ich zeige, dass der p38-MAPK-Signalweg in *Mtb*-infizierten Phagozyten eher eine Nekrose als eine Apoptose auslöst. Die Aktivierung von p38 MAPK fördert die Dissoziation von Hexokinase II (HKII) aus den Mitochondrien und ermöglicht die Öffnung der mitochondrialen Permeabilitäts-Transitionspore (mPTP). Die Öffnung der mPTP führt zur Depletion von Adenosintriphosphat (ATP) und schließlich zur Nekrose der Wirtszelle. Ich kann zeigen, dass Dexamethason diesen Signalweg hemmt, indem es MAPK Phosphatase 1 (MKP-1) aktiviert, um die Aktivität der p38 MAPK zu verringern. Darüber hinaus hat eine direkte Hemmung der p38 MAPK durch den spezifischen p38 MAPK Inhibitor Doramapimod ähnliche Auswirkungen auf das Überleben der Wirtszelle. Da Kortikosteroide entzündungshemmende Medikamente sind, die unter anderem den Signalweg des

Tumornekrosefaktors (TNF) blockieren, habe ich TNF und Nekroptose in *Mtb*-infizierten Zellen weiter charakterisiert, indem ich MLKL (mixed lineage kinase domain-like pseudokinase) und TNF Rezeptor 1 (TNFR1) knockout Makrophagen verwendet habe. Ich konnte zeigen, dass der zugrundeliegende Mechanismus von Dexamethason unabhängig von TNF und Nekroptose ist.

So verknüpfen meine Ergebnisse die p38 MAPK Inhibierung durch Dexamethason oder p38 MAPK Inhibitoren mit der Aufhebung des mitochondrial vermittelten Wirtszelltods bei der Tuberkuloseinfektion und bieten neue Möglichkeiten für die Erforschung neuer HDT-Konzepte.

10. List of figures

11. List of tables

12. Acknowledgements

An dieser Stelle möchte ich mich bei allen bedanken, die mich während der letzten 4 Jahre unterstützt haben. Ich danke,

Prof. Dr. Michael Hallek, für die Möglichkeit die Doktorarbeit in seiner Klinik anzufertigen.

Prof. Dr. Hamid Kashkar, für die Übernahme des Erstgutachtens meiner Arbeit, für seine hilfreichen Diskussionen und seine Unterstützung.

Prof. Dr. Karin Schnetz, für die freundliche Übernahme des Zweitgutachtens und stete Hilfsbereitschaft und Motivation während meiner Promotionszeit.

In besonderer Weise meinem Betreuer Dr. Jan Rybniker, der es mir ermöglichte meine Doktorarbeit anzufertigen. Für die herzliche Aufnahme in seiner Arbeitsgruppe und die hilfreichen Diskussionen, sowie sein stetiger Glauben an den Erfolg des Projekts.

Sandra Winter und Edeltraud van Gumpel für die wunderbaren Stunden die sie gemeinsam mit mir im Labor verbracht haben, sowie die aufmunternden Gespräche. Ohne sie wäre diese Arbeit nicht möglich gewesen.

An alle anderen ehemaligen und aktuellen Arbeitskollegen für die wunderschöne Arbeitsatmosphäre und die netten und unterhaltsamen Kaffeepausen.

Jan Rybniker und Sebastian Theobald für die Korrektur meiner Arbeit.

Von Herzen meinen Eltern und meinen Freunden die mich tatkräftig unterstützt und motiviert haben, auch wenn es schwierig wurde.

Ich widme diese Arbeit in liebevoller Erinnerung meinem verstorbenen Großvater Karl Gräb.

13. Declaration

Ich versichere, dass ich die von mir vorgelegte Dissertation selbständig angefertigt, die benutzten Quellen und Hilfsmittel vollständig angegeben und die Stellen der Arbeit − einschließlich Tabellen, Karten und Abbildungen −, die anderen Werken im Wortlaut oder dem Sinn nach entnommen sind, in jedem Einzelfall als Entlehnung kenntlich gemacht habe; dass diese Dissertation noch keiner anderen Fakultät oder Universität zur Prüfung vorgelegen hat; dass sie − abgesehen von unten angegebenen Teilpublikationen − noch nicht veröffentlicht worden ist, sowie, dass ich eine solche Veröffentlichung vor Abschluss des Promotionsverfahrens nicht vornehmen werde. Die Bestimmungen der Promotionsordnung sind mir bekannt. Die von mir vorgelegte Dissertation ist von Herrn Prof. Dr. Hamid Kashkar und Herrn Dr. Dr. Jan Rybniker betreut worden.

Teilpublikationen:

Gräb, J., Suarez, I., van Gumpel, E., Winter, S., Schreiber, F., Esser, A., Hölscher, C., Fritsch, M., Herb, M., Schramm, M., et al. (2019). Corticosteroids inhibit Mycobacterium tuberculosis-induced necrotic host cell death by abrogating mitochondrial membrane permeability transition. Nature communications 10, 688.

Köln, den 27.04.2020 Jessica Gräb

14. Curriculum vitae

Der Lebenslauf ist in der Online Version aus Gründen des Datenschutzes nicht enthalten.